Chapter 11: Geochemistry of the Solid Earth

11.1 Introduction

Having considered the Earth's formation in the last chapter, let's now use the tools of geochemistry we acquired in the first eight chapters to consider how the Earth works. The Earth, unlike many of its neighbors, has evolved over its long history and it remains geologically active. Four and a half billion years later, it is very different place than it was first formed. Certainly one of the main objectives of geochemistry is to understand this activity and unravel this history.

The solid Earth consists of 3 distinct layers: crust, mantle, and core. As Table 11.01 shows, these layers become progressively denser with depth, reflecting a stable density stratification of the planet (one shared by the other terrestrial planets). Unfortunately, only the shallowest of these layers, the crust, is accessible to direct study. The crust may well be the most interesting part of the planet, but it represents less than half a percent of its mass. Even most of the crust is out of reach; the deepest boreholes drilled in the continental crust, which is 35 km thick on average, are only 12 km deep; the deepest borehole in oceanic crust, which is on average 7 km thick, is only 1.5 km deep. Thus study of the solid Earth necessarily relies on indirect approaches and on rare samples of deeper material brought to the surface through geologic processes.

We'll begin by considering the geochemistry of the mantle because it represents the largest fraction of the Earth, both by mass (67%) and volume (88%). Although remote, the mantle is important for a number of reasons. For one, the crust has been formed from it. For another, convection within the Earth's mantle drives most tectonic activity that affects us on the surface, including plate motions, earthquakes, and volcanoes. We'll next consider the core. As we found in the previous chapter, the core formed quite early – more or less simultaneously with formation of the Earth itself. While we do have a few samples of the Earth's mantle, we have none at all from the core, so its composition and history must be inferred entirely indirectly. Lastly, we'll consider the Earth crust – the part of the Earth we inhabit and are most familiar with. The crust, particularly the continental crust, is the most varied, and arguably the most interesting, part of our planet. We'll find that the continental crust, unlike the core which is as old as the Earth itself, has grown through geologic time through magmatism. The crust, particularly the continental crust, is where the geologic history of the planet is preserved.

11.2 The Earth's Mantle

Parts of the mantle are occasionally thrust to the surface as so-called alpine peridotites; fracture zones in the oceanic crust also occasionally expose mantle rocks. And volcanic eruptions sometimes carry small pieces of the mantle to the surface as *xenoliths.* Nevertheless, much of what we know about the mantle has been deduced indirectly. Indirect methods of study include determination of geophysical properties such as heat flow, density, electrical conductivity, and seismic velocity. Another indirect method of study is examination of volcanic rocks produced by partial melting of the mantle. Finally, cosmochemistry provides an important constraint on the composition of the Earth.

Table 11.01. Volumes and Masses of the Earth's Shells

	Thickness (km)	Volume 10^{12} km^3	Mean Density kg/m^3	Mass 10^{24} kg	Mass Percent
Atmosphere				0.000005	0.00009
Hydrosphere	3.80	0.00137	1026	0.00141	0.024
Crust	17	0.0087	2750	0.024	0.4
Mantle	2883	0.899	4476	4.018	67.3
Core	3471	0.177	10915	1.932	32.3
Whole Earth	6371	1.083	5515	5.974	100.00

The mantle was once viewed as being homogeneous, but we now realize that the chemistry of the mantle is heterogeneous on all scales. On a large scale, the mantle appears to consist of a number of reservoirs that have complex histories. The best evidence for this large-scale heterogeneity comes from trace element and isotope ratio studies of volcanic rocks, but there is also evidence that the major element composition of the mantle varies. While trace elements may vary by an order of magnitude or more, the major element variations are much more subtle, just as they are in volcanic rocks and in the crust. Isotope studies have proven tremendously valuable in understanding the mantle for several reasons. First, unlike trace element and major element concentrations, isotope ratios do not change during the magma generation process (except by mixing of the magma with other components such as assimilated crust). Second, radiogenic isotope ratios provide *time-integrated* information about the parent/daughter ratios, and therefore allow inferences about the history of the mantle.

The crust has been created by extraction of partial melts from the mantle (i.e., volcanism), a process that has continued over the Earth's entire history. For the major elements, crust formation affects the composition of the mantle only slightly because the volume of the crust is so small. For example, if the SiO_2 concentration in the mantle were originally 45%, extraction of continental crust containing an average of 60% from that mantle would reduce the SiO_2 concentration in the mantle only to 44.6%. Of course, extraction of partial melt undoubtedly has changed the major element composition of the mantle *locally*, as we will see in subsequent sections of this chapter. Furthermore, the concentrations of highly incompatible elements in the mantle undoubtedly have changed significantly as a result of formation of the crust. The idea that the core and the mantle segregated very early and the crust formed subsequently gives rise to the notion of a *primitive mantle* composition. This composition is the composition of the mantle before the crust was extracted from it. It is identical to the composition of the crust plus the mantle. Thus, the terms *primitive mantle composition* and *bulk silicate Earth composition* (BSE) are synonymous. One of the objectives of this chapter will be to estimate this composition.

In attempting to assess this composition, we have essentially 3 kinds constraints. The first is *geophysical:* geophysical measurements of moment of inertia and seismic wave velocities allow us to constrain the density, compressibility, and rigidity of the mantle, which in turn constrains its composition. The second is *cosmochemical:* the Earth formed from the solar nebula which has a chondritic composition for condensable elements and therefore the composition of the Earth should relate in some rational way to the composition of chondrites. Finally, the mantle can be directly sampled locally where it is tectonically exposed or where small pieces are carried to the surface by volcanic eruptions and indirectly through volcanism. Most lavas erupted on the surface of the Earth are basalts and they are products of partial melting of the mantle. The composition of the mantle thus must be such that it yields basaltic magma upon melting. There is, however, a caveat: only the uppermost mantle sampled by volcanism and tectonism. Even the most deeply generated magmas, kimberlites, come from the upper few hundred km of the mantle, which is nearly 3000 km deep.

11.2.1 Structure of the Mantle & Geophysical Constraints on Mantle Composition

Geophysical measurements constrain the physical properties of the Earth and its interior, and therefore constrain it composition. One set of constraints comes from the velocities with which seismic waves travel through the Earth. There are two kinds of seismic body waves: *compressional* or p-waves, in which particle motion is parallel to wave motion, and *shear* or *s*-waves, in which particle motion is perpendicular to wave motion. P-waves can travel through all media, they are the familiar sound waves in air, but s-waves can only travel through solids. Indeed, the absence of s-waves arrivals in a zone between about 100° and 180° from an earthquake epicenter, the so-called s-wave shadow zone, provided the original and still most compelling evidence that the outer core is liquid. The velocity with which seismic waves travel depend on the square root of the ratio of the elastic modulus to density. For s-waves this is:

$$v_s = \sqrt{\frac{\mu}{\rho}} \qquad 11.01$$

where ρ is density and μ is the rigidity modulus, defined as the ratio of shear stress to shear strain. For p-waves the velocity is given by:

$$v_p = \sqrt{\frac{\kappa + \frac{4}{3}\mu}{\rho}} \qquad 11.02$$

where κ is the bulk modulus. κ is defined as:

$$\kappa = -V\left(\frac{\partial P}{\partial V}\right)_S \qquad 11.03$$

κ is very nearly the inverse of the compressibility, which we defined in equation 2.12. The only difference is that in equation 2.12 we specified constant temperature in the differential term and here we are specifying constant entropy. This makes things slightly easier for the present problem because the temperature of the Earth would continually increase downward as a result of adiabatic compression, even if there were no other sources of heat in the Earth's interior. Here, we allow for that adiabatic temperature increase. Density, rigidity modulus, and compressibility all depend on the phases constituting a material rather than just composition. However, assuming equilibrium conditions prevail, only one phase assemblage will be possible for a given composition, pressure, and temperature.

We can independently constrain density, and its variation through the Earth, in another way. The density of the Earth is, of course, simply its mass divided by its volume. The latter has been known since the Greek mathematician Eratosthenes determined the Earth's radius in third century BC. The mass of the Earth was first estimated from the strength of it gravitational field by Issac Newton in the 17th century and refined by Henry Cavendish in the 18th century. Using the most recent determinations of these parameters, we can calculate a mean density for the Earth of 5515 kg/m^3. Comparing this value with the value of typical crustal rocks, which are in the range of 2000-3000 kg/m^3, immediately leads to the conclusion that density must be greater in the Earth's interior.

Let's now see how we can combine density and seismic wave velocity variations to provide further constraints. First, we know that density is inversely related to volume:

$$\frac{d\rho}{\rho} = -\frac{dV}{V} \qquad 11.06$$

We can now rewrite equation 11.3 in terms of density rather than volume as:

$$\kappa = -\rho\left(\frac{\partial P}{\partial \rho}\right)_S \qquad 11.07$$

Then we note that pressure will vary with radial distance from the center of the Earth as:

$$\frac{dP}{dr} = -\rho(r)g(r) \qquad 11.08$$

where $g(r)$ is the gravitational acceleration at radial distance r. We can combine these equations to write:

$$\left(\frac{\kappa}{\rho}\right) = g(r)\rho(r)\frac{dr}{d\rho} \qquad 11.09$$

Interestingly, it is readily shown that the term on the left can be derived from the seismic wave velocities:

$$\left(\frac{\kappa}{\rho}\right) = V_P^2 - \frac{4}{3}V_s^2 \qquad 11.10$$

The acceleration of gravity at radial distance r is given by:

$$g(r) = \frac{G}{r^2}\int 4\pi\rho(r)r^2 dr \qquad 11.11$$

Combining 11.09 through 11.11, we have:

$$\frac{d\rho(r)}{dr} = \frac{G}{r^2}\frac{\rho(r)}{V_P^2 - \frac{4}{3}V_s^2}\int 4\pi\rho(r)r^2 dr \qquad 11.12$$

Equation 11.12 describes how density changes in a self-compressing, but otherwise uniform sphere and is known as the *Adams-Williamson Equation*. It allows us to predict the density of an infinitesimally small layer at distance r_1 from seismic velocities provided we know the density at an adjacent layer, r_2. Since we can directly measure density at the surface, we can began there and work our way through the Earth calculating density variation.

Yet another parameter, the Earth's *moment of inertia*, also allows us to constrain how density changes with depth. The moment of inertia for a rotating sphere of uniform density is simply:

$$I = \frac{2}{5}mr^2 \qquad 11.13$$

where m is mass and r is radius. For a spherical body whose density is a function of depth, the moment of inertia is:

$$I = \int \frac{4}{3}\pi r^4 \rho(r) dr \qquad 11.14$$

The situation for the Earth is slightly more complex since it is not strictly spherical. Rather, as a consequence of centrifugal force, it is an oblate spheroid with its equatorial radius slightly greater than polar radius. The gravitational interaction between the slightly flattened Earth and the Moon results in a gravitational torque which causes the Earth's rotational vector to itself slowly rotate, or *precess*. From the rate of this precession, about one rotation per 25,000 years, a moment of inertia of 8.07 x 10^{37} kg/m^2 can be calculated.

Any density distribution we obtain using seismic velocities and the Adams-Williamson equation can also be used to calculate a moment of inertia, which should agree with that measured from precession. The two do not agree if we take the Earth to be a self-compressing sphere for the simple reason that there are density discontinuities in the Earth that result from compositional changes, such as at the core-mantle boundary, as well as phase changes. The problem then is to produce a density model for the Earth that accounts for both observed seismic wave velocities and moment of inertia. The generally accepted model that accomplishes this is called the *Preliminary Reference Earth Model* or *PREM* (Dziewonski & Anderson, 1981). PREM is based on many decades of seismic records. The term *preliminary* clearly implies further refinements are expected, but

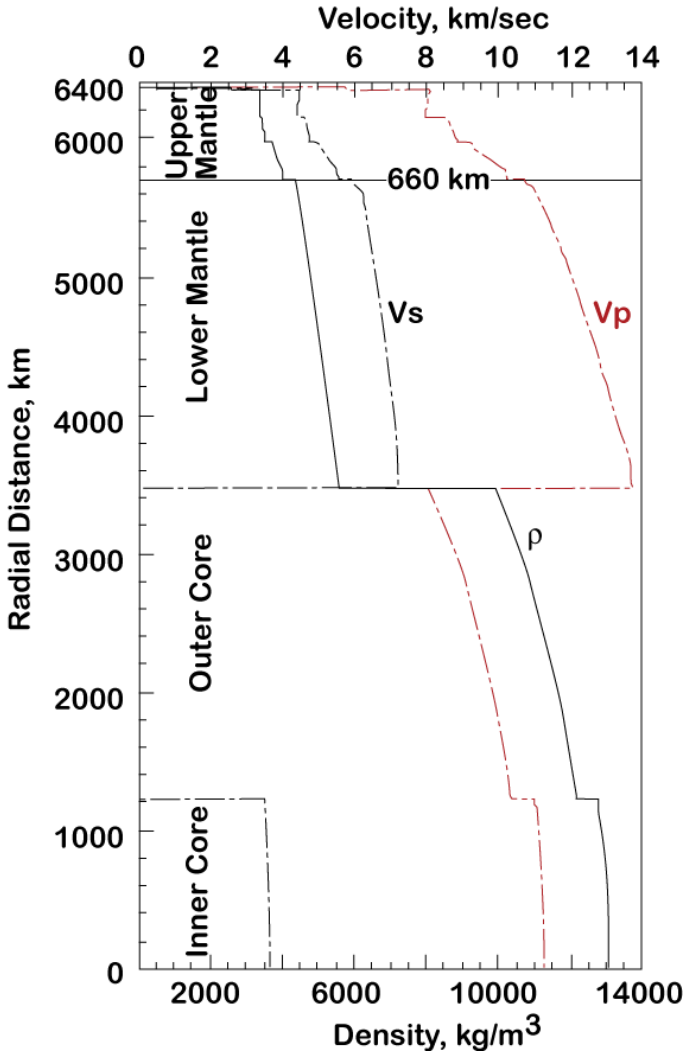

Figure 11.01. The PREM model of seismic velocities and density variation through the Earth.

no revisions have been made since the model was agreed upon in 1981. In part, this is because geophysicists have tended to focus on local deviations from PREM rather than further refine the spherically symmetric model, but it also means that the PREM model is actually reasonably mature. Density and seismic wave velocities of the PREM model are shown in Figure 11.01.

11.2.2 Cosmochemical Constraints on Mantle Composition

In Chapter 10 we considered the composition of that part of our cosmic environment accessible to sampling: meteorites, the solar surface (deduced from optical spectra and solar wind particles), Mars, and the Moon. The meteorite data provide first order constraints on the formation and composition of the Earth. Since the mantle comprises roughly 99% of the silicate part of the Earth, these constraints also apply to the mantle. Two important cosmochemical assumptions guide our thinking about the composition of the Earth: *(1) the entire solar system formed at one time from a nebula of gas and dust, (2) the composition of this nebula was similar to that of CI chondrite for the condensable elements.* The last statement should not be construed to mean that all bodies that formed from this nebula are necessarily of chondritic composition. Indeed, we will see that the Earth's composition differs from chondritic in significant ways.

Thus far there is essentially no evidence to contradict the first assumption (provided we interpret "simultaneous" in a geologic sense; i.e., this process may have lasted 10^8 or more years); the second assumption certainly holds to a first approximation, beyond that there is some uncertainty. In defense of it, however, we should emphasize the isotopic homogeneity of the solar system. The isotopic anomalies we have discussed previously are very much the exception to the rule and serve to emphasize the general homogeneity of the solar system (except, of course, for oxygen). *The implication is that the presolar nebula was well mixed.* We can reasonably conclude that it was *initially* chemically homogeneous as a result. Processes occurring within the nebula resulted in chemical variation that in turn produced a range of composition of chondritic parent bodies.

In summary, we can draw the following conclusions relevant to the formation and composition of the Earth from cosmochemistry:

1. The material from which the solar system formed was of CI chondritic composition (plus gases).
2. Despite (1), the composition of bodies formed from this nebula is variable. This is apparent from the composition of chondrites as well as from density variations of the planets.
3. Formation of planets and asteroids occurred within roughly 10^8 years of the beginning of the solar system (which we take to be the formation of its oldest objects, the CAI's found in chondrites).
4. Asteroids and the terrestrial planets underwent differentiation in which iron metal and silicate segregated. Based on the age of differentiated meteorites, and on W isotope ratios of iron meteorites in particular, the process began very early – with a few 10^6 years at most of the beginning of the solar system.
5. The final stages of the formation of planetary assembly involved energetic collisions of large bodies. In the case of the Earth-Moon system, this culminated in a collision s that released vast amounts of energy. A consequence of this was a magma ocean on the Moon and, most likely, the Earth as well.

11.2.3 Observational Constraints on Mantle Composition

Figure 11.01 implies that the uppermost mantle should consist of rock having a density of around 3400 kg/m^3 and p-wave velocities of about 8 km/sec. Rocks having these properties are occasionally exposed at the surface in alpine massifs of collision zones, in fracture zones along mid-ocean ridges, and in sections of obducted oceanic crust called ophiolites. These rocks are invariably Mg- and Fe-rich silicates. In addition, rocks having these properties are sometimes found as xenoliths in lavas; they are also Mg- and Fe-rich silicate rocks that consist dominantly of olivine and pyroxenes. Chondrites, of course, are also Mg- and Fe-rich and consist dominantly of olivine and pyroxenes, so it would seem that such rocks meet both geophysical and cosmochemical constraints for mantle composition. The term *ultramafic* is applied to silicate rocks rich in magnesium and iron, which typically consist of olivine and pyroxenes (but hydrated ultramafic rocks can be dominated by minerals such as serpentine or talc). *Peridotite* is a rock dominated by olivine (*peridot* is the gem name for olivine). If the olivine exceeds 90%

of the rock, it is termed a *dunite* (Figure 11.02). Rocks with substantial amounts of both pyroxenes as well as olivine are *lherzolites*. This can be prefaced by the name of the Al-bearing phase, e.g., spinel lherzolite, whose nature depends on pressure. Figure 11.03 shows the compositions of ultramafic xenoliths found in the volcanics of Kilbourne Hole, New Mexico. The most common types are lherzolites. This suggests we should be focusing our attention on lherzolite as mantle material. Lherzolite also has appropriate density and seismic velocities to be mantle material. Furthermore, upon partial melting at high pressures it produces basaltic magma. Ringwood (1975) coined the term "pyrolite", meaning pyroxene-olivine rock, for the lherzolitic composition matching geophysical and cosmochemical constraints.

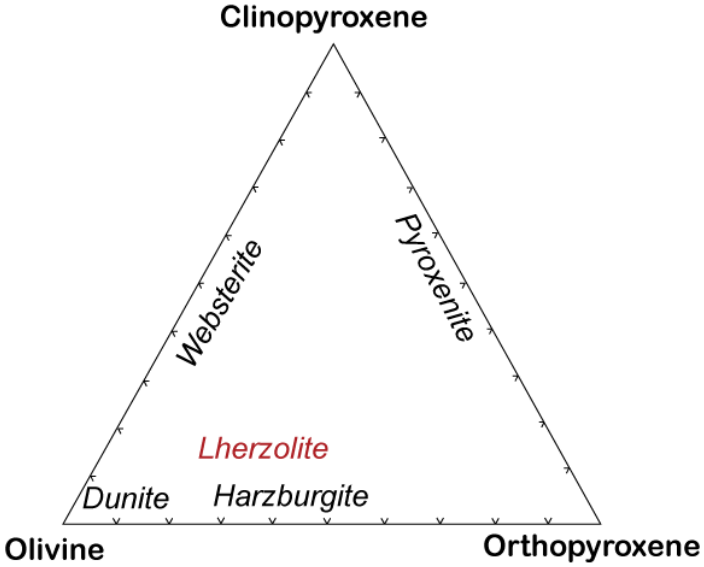

Figure 11.02. Ternary diagram illustrating ultramafic rock nomenclature based on minerals present.

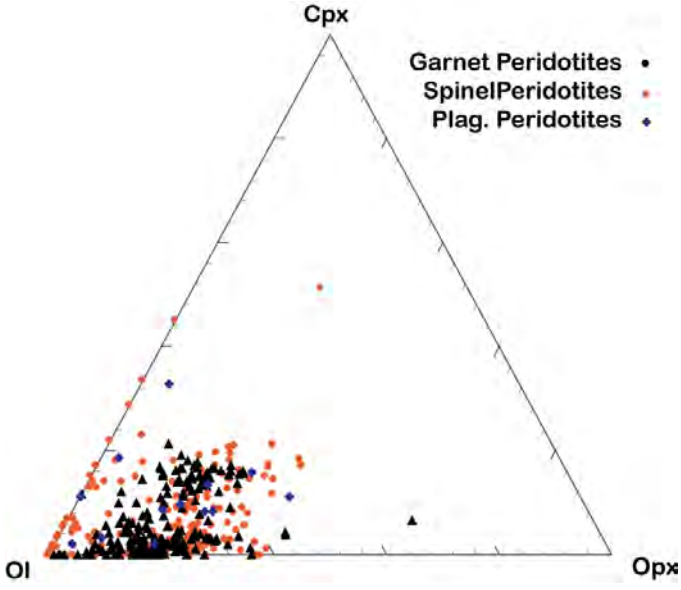

Figure 11.03. Modal mineralogy of peridotite xenoliths in the Deep Lithosphere Database of EarthChem (www.earthchem.org) projected onto the Ol-Opx-Cpx plane.

Pyrolite is not unique as a mantle candidate, and some had argued that the mantle, or at least the upper mantle, consists dominantly of *eclogite.* Eclogite consists of garnet and an Na- and Al-rich pyroxene called omphacite and is the mineralogy of basalt at high pressure. It can produce basaltic magma upon partial melting, but must melt much more extensively than lherzolite to do so. Eclogite does not match the chondritic composition sufficiently well, and is considerably rarer as xenoliths than peridotites. Furthermore, seismic anisotropy* observed in some parts of the upper mantle suggests the mantle is olivine-rich. However, Anderson (e.g., Anderson, 1989) has argued for an upper mantle consisting of olivine-bearing eclogite, for which he coined the term *piclogite* an olivine-rich basalt is called a picrite; piclogite would be the high pressure equivalent of picrite). The eclogite, which he argues was produced by crystal accumulation in a primordial magma ocean, is the source of MORB in his model. This idea has not been particularly well received by geochemists, perhaps even less so by petrologists. We'll adopt Ringwood's term, *pyrolite,* as the rock

* Seismic anisotropy refers to seismic waves traveling faster in one direction than another and is related to crystal properties. Anisotropy occurs in orthorhombic olivine, but since garnet has a cubic (isotropic) structure, seismic velocity is equal in all crystallographic directions. Seismic anisotropy only occurs when crystallographic axes of individual grains tend to align, as can arise from flow associated with convection.

that constitutes the mantle. In a subsequent section, we'll consider various estimates of its chemical composition.

11.2.4 Mantle Mineralogy and Phase Transitions

11.2.4.1 Upper Mantle Phase Changes

Figure 11.01 shows that a number of discontinuities exist in the density and seismic velocity profiles of the Earth. Some of these are clearly compositional changes, such as the shallowest discontinuity, which is the crust-mantle boundary, and the core-mantle boundary. Others represent phase changes that are isochemical, or nearly so. The most prominent is the inner core—outer core boundary, which is principally a solid–liquid phase change. The discontinuities within the mantle now all appear to be *primarily* phase changes, but some still argue they may be compositional boundaries as well.

In the upper 200 km or so of the mantle, the only important phase changes are the nature of the aluminous phase (Figure 11.04), which changes from plagioclase to spinel ($MgAl_2O_4$) and then to garnet with increasing pressure.

The garnet lherzolite assemblage remains stable to depths of about 300 km. At this depth, appreciable amounts of pyroxenes begin to dissolve in garnet, forming a solid solution with the general composition $M_2(MSi,Al_2)Si_3O_{12}$ where M is Mg, Fe, or Ca. This garnet, called *majorite*, differs from those found at lower pressure in that up to a quarter of the silicon atoms are in octahedral coordination (i.e., surrounded by 6 oxygens rather than 4). The octahedral coordination is favored because anions such as oxygen are more compressible than are cations such as silicon. When compressed, more oxygens can be packed around each silicon atom. This phase change is a gradual one, with complete conversion of pyroxenes to majorite at about 460 km depth (Figure 11.05). The phase change results in a roughly 10% increase in density of the "pyroxene" component.

11.2.4.2 The Transition Zone

Between 400 and 670 km depth seismic velocities increase more rapidly than elsewhere (Figure 11.01); this depth interval is called the transition zone. At about 400 km, or 14 GPa, olivine undergoes a structural change from the low pressure, or α form, to the β form, also known as *wadsleyite*. In contrast to the pyroxene-to majorite phase change, this phase boundary is relatively sharp, with a transition interval of 9-17 km. It results in an 8% increase in density.

At about 500 km depth or so, olivine undergoes a further structural change to the γ-form. The structure is similar to that of $MgAl_2O_4$ spinel, and this phase is sometimes, somewhat confusingly, referred to simply as spinel. More properly it has been given the name *ringwoodite*, which occurs naturally in shocked meteorites. The change from β to γ-olivine is thought to be more gradual than the α-β transition, occurring over a depth interval of 30 km, and involves only a 2% increase in den-

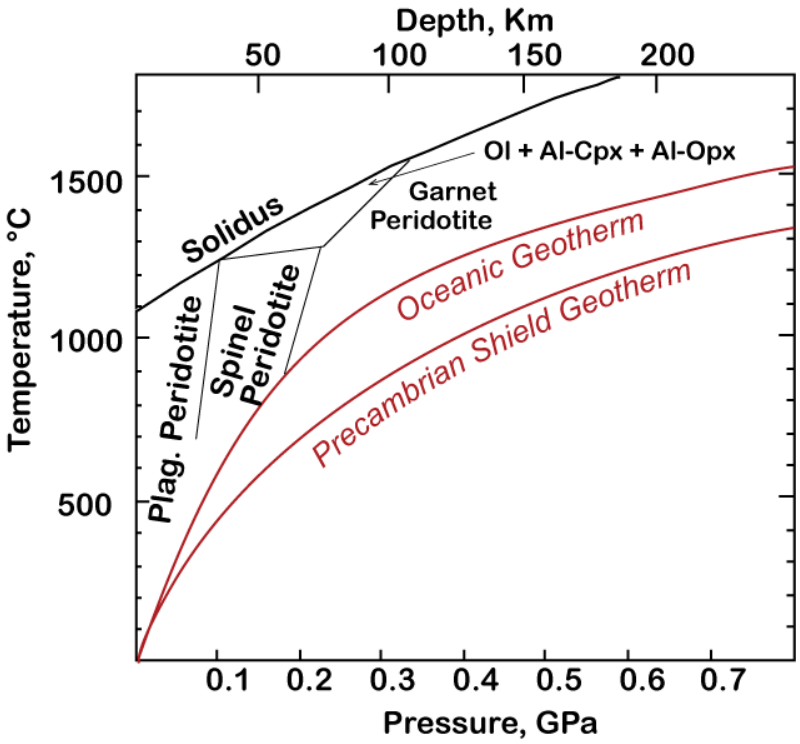

Figure 11.04. Upper mantle phase diagram.

sity. In both the β and γ phases silicon remains in tetrahedral coordination.

Within the transition zone, some of the Mg and Ca in majorite begin to exsolve to form $CaSiO_3$ in the perovskite structure and $MgSiO_3$ in the ilmenite structure. The proportion of $CaSiO_3$ perovskite increases with depth until majorite disappears at about 720 km. $MgSiO_3$ ilmenite persists only to 660 km.

As Figure 11.01 shows, a sharp and large increase in seismic velocity occurs at around 660 km depth or roughly 24 GPa; this is called the *660 seismic discontinuity*. This depth marks the beginning of the lower mantle. In the past, there was debate as to whether this discontinuity is a chemical boundary or a phase change. There is now complete agreement that it is *primarily* a phase change. At this depth γ-olivine disproportionates to form $(Mg,Fe)SiO_3$ in the perovskite structure and (Mg,Fe)O *magnesiowüstite* (perhaps more properly called ferripericlase), with the Fe going preferentially in the magnesiowüstite. This phase change results in a density increase of about 11%. The $(Mg,Fe)SiO_3$ perovskite†, has the chemical stoichiometry of pyroxene, but the silicons are in octahedral coordination. The structure, illustrated in Figure 11.06, is similar to that of the "high-temperature" cuprate superconductors discovered in the 1980's.

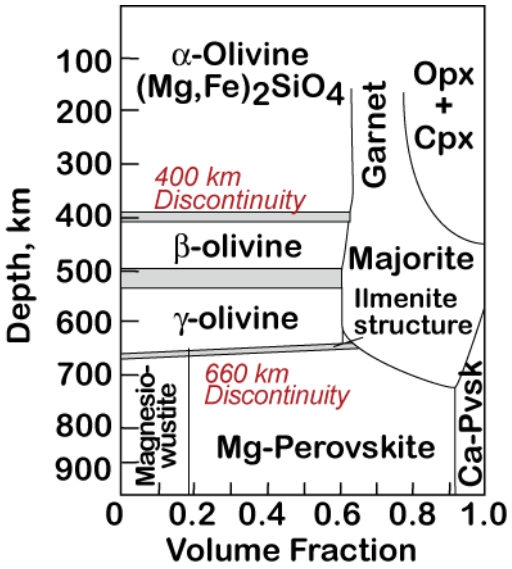

Figure 11.05. Mineral assemblages in the upper 1000 km of the mantle. After Ringwood (1991).

High pressure experiments carried out with the diamond anvil show that the transition is quite sharp, occurring within a pressure interval of 0.15 GPa at 1600° C. The transition has a negative Clapeyron slope (P (GPa) = 27.6 – 0.0025 T (°C); e.g., Chopelas, et al., 1994), so that it will occur at somewhat shallower depth in hot regions, such areas of mantle upwelling, and at greater depth in cooler regions, such as subducted lithosphere, though since the Clapeyron slope is shallow, the effect is small. The effect of these differences is to oppose motion across the boundary, and therefore to stabilize any chemical differences that might exist between the upper and lower mantle. The negative Clapeyron slope is probably not sufficient to prevent motion across this boundary, however. Indeed, this is just what seismic tomographic images show: slabs seem to encounter resistance at 660 Km, but most ultimately manage to sink through the boundary.

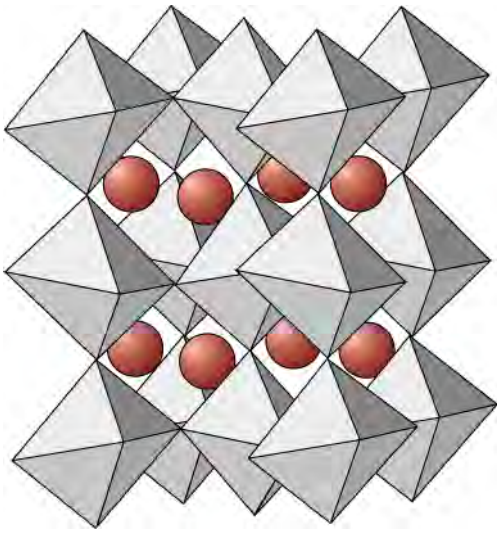

Figure 11.06. The structure of $MgSiO_3$ perovskite. The structure consists of corner-sharing SiO_6 octahedra with Mg^{2+} in dodecahedral sites.

11.2.4.3 The Lower Mantle

The lower mantle, the region between the 660 km seismic discontinuity and the core-mantle boundary at 2900 km, is substantially less accessible to study than is the upper mantle. Although a few small inclusions in diamond containing lower mantle assemblages have been found,

† We will refer to this phase as Mg-perovskite. This mineral does not have a formal name since it have not been *found* in nature, although it can be synthesized in the lab. $(Mg,Fe)SiO_3$ accompanied by (MgFe)O phases have been found in inclusions in diamond. Since this is the expected lower mantle phase assemblage, these diamonds probably originated at or below 660 km. However, the actual $(MgFe)SiO_3$ phase now present in the inclusion is pyroxene. The interpretation is that the original Mg-perovskite has retrograded to pyroxene as a consequence of pressure reduction.

these do not provide significant compositional constraints; so the nature of the lower mantle and its composition must be inferred indirectly. The principal constraint on its composition is seismic velocities and density. The assumption that the Earth is approximately chondritic forms another constraint. It is generally agreed that the lower mantle is similar in compositional to the upper mantle, i.e., composed dominantly of SiO_2, MgO, and FeO with lesser amounts of CaO, Al_2O_3, TiO_2, etc., but some disagreement remains as to whether it might be slightly richer in FeO and SiO_2 than the upper mantle. For example, Lee et al. (2004) concluded a molar Mg/(Mg+Fe) ratio of about 0.85 for the lower mantle better fit seismic observations than did the upper mantle value of 0.9. However, Mattern et al. (2005) have concluded that the density and elastic properties of lower mantle phases are not sufficiently well known to distinguish between these alternatives, as the predicted densities of the pyrolite and chondritic models of the lower mantle differ by less than 0.06 g/cc. Uncertainties about the temperature of the lower mantle and the coefficient of thermal expansion of lower mantle materials compound the problem. If chemical layering exists in the mantle, it cannot presently be detected with confidence.

Mg-perovskite and magnesiowüstite remain the principal phases to depths of 2700 km or so. There had been some debate about how Al_2O_3 is accommodated in lower mantle minerals. The most recent experiments however, suggest that while a separate aluminous phase may form at relatively low pressure (25-30 GPa, corresponding to the region of 600-800 km), Mg-perovskite apparently accepts all available Al_2O_3 in its structure at pressures above about 35 GPa (e.g., Kesson et al., 1994). On the other hand, the solid solution between Mg-perovskite and Ca-perovskite appears to be quite limited, so that Ca-perovskite is probably present as a separate phase, and probably accepts all the Na_2O. For a 'pyrolite' mantle, the phase assemblage will be 65-80% Mg-perovskite, 15-30% magnesiowüstite, and about 5% Ca-perovskite. Mg-perovskite is thus the most abundant mineral in the Earth. The magnesiowüstite/perovskite partition coefficient for Fe decreases with increasing pressure, so that the proportion of Fe in perovskite should increase somewhat with depth down to about 30 GPa (~900 km), and then is constant at greater pressure. At this depth, the mole fractions of Mg (Mg/(Mg+Fe)) in Mg–perovskite and magnesiowüstite ((Mg,Fe)O) for a pyrolite composition are about 0.94 and 0.80 respectively.

The deepest layers of the mantle are particularly interesting. The core-mantle boundary represents a profound change in physical state (solid to liquid), density, composition, oxygen fugacity, seismic velocity, and probably temperature. From a geochemical perspective, it is a fascinating region. Seismic investigations show that the lowermost 200 km or so of the mantle, called the D" layer (pronounced "dee-double prime"), is a region of unusual and highly variable properties. There appears to be a roughly 1% increase in density at the top of this layer, and seismic wave velocities within this layer are notably anisotropic. The unusual properties of this layer have led to considerable speculation as to its nature.

Reproducing the temperature and pressure conditions of the deep mantle in the laboratory is challenging to say the least. Pressures reach 135 GPa and temperatures exceed 3000 K. However, these conditions can be reproduced using the diamond anvil high-pressure cell, albeit only on a scale of less than a millimeter. They can also be simulated using an *ab initio* approach, in which materials are simulated at the atomic level using computers. Recent experiments and *ab initio* simulations show that the structure of $MgSiO_3$ should transform from that of perovskite to a $CaIrO_3$-like one is which the silica octahedral are organized into sheets as in Figure 11.07 (Murakami, et al, 2004; Oganov and Ono, 2004). This transformation should occur at about 125 GPa and 2500-3000 K, corresponding to a depth of about 2700 km, or close to the top of the D"

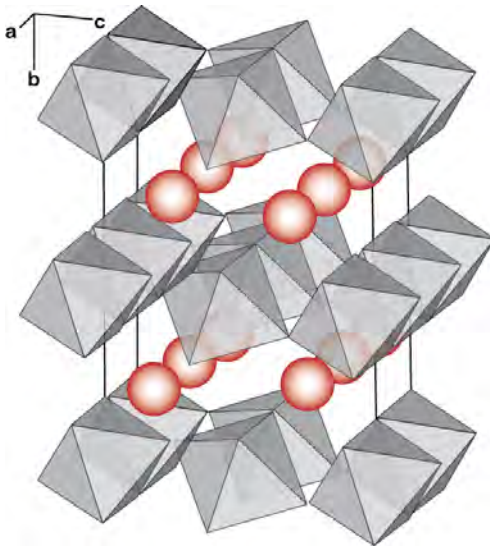

Figure 11.07. The post-perovskite structure of $MgSiO_3$. The Si-octahedra are organized into sheets, with Mg atoms (spheres) located between the sheets. After Oganov and Ono (2004).

layer. The density increase in this phase transition is close to predicted from seismic velocities: about 1%. The layered structure strongly suggests that this mineral should be seismically anisotropic. Thus the discovery of this phase seems to go a long way towards explaining the mystery of D".

11.3 ESTIMATING MANTLE AND BULK EARTH COMPOSITION

11.3.1 Major Element Composition

We can draw several important conclusions from the geophysical properties of the mantle when we combine them with the laboratory experiments of mineral physicists and petrologists. The first of these is that the material that best meets combined cosmochemical, geophysical, and mineral physics has the composition of *pyrolite*. Second, it appears that all seismic discontinuities can be explained by phase changes. Thus there is no compelling geophysical evidence that the mantle is compositionally layered (although we can also not rule it out). This does not, however, rule out the possibility of compositional heterogeneity in the mantle that is more randomly distributed. Consequently, we will assume that the composition of the upper mantle is also the composition of the whole mantle. As we noted at the beginning of section 11.2, this composition will be the same as the *primitive mantle* and bulk silicate Earth compositions for major elements.

Table 11.02 compares several estimates for the major and minor element composition of the bulk silicate Earth with the composition of CI chondrites. Clearly, chondrites are much richer in siderophile elements (e.g., Fe, Ni) than all these estimated mantle compositions. The chondritic composition matches the upper mantle composition much better after a sufficient amount of the siderophile elements has been removed to form the Earth's core. However, even after removing the siderophile and highly volatile elements, there are significant differences between the apparent composition of the mantle and chondrites.

First, the mantle is depleted in the alkali elements (e.g., K and Na in Table 11.02). The depletion in alkalis is also apparent by comparing Sr isotope ratios of the mantle and chondrites, as Gast demonstrated in 1960. Some of the Rb depletion of the mantle may be explained by extraction of the Rb into

Table 11.02. Comparison of Bulk Silicate Earth Compositions

	CI Chondrites	CI Chondritic Mantle[1]	Hart & Zindler[2]	McDonough & Sun[3]	Palme & O'Neill[4]	Lyubetskaya & Korenga[5]	O'Neill & Palme[6]
SiO_2	22.89	49.77	45.96	45.0	45.4	44.95	45.40
Al_2O_3	1.60	3.48	4.06	4.45	4.49	3.52	4.29
FeO	23.71	6.91	7.54	8.05	8.10	7.97	8.10
MgO	15.94	34.65	37.78	37.8	36.77	39.95	36.77
CaO	1.30	2.83	3.21	3.55	3.65	2.79	3.52
Na_2O	0.671	0.293	0.332	0.36	0.33	0.30	0.281
K_2O	0.067	0.028	0.032	0.029	0.031	0.023	0.019
Cr_2O_3	0.387	0.409	0.468	0.384	0.368	0.385	0.368
MnO	0.250	0.112	0.130	0.135	0.136	0.131	0.136
TiO_2	0.076	0.166	0.181	0.20	0.21	0.158	0.183
NiO	1.371	0.241	0.277	0.25	0.24	0.252	0.237
CoO	0.064	0.012	0.013	0.013	0.013	0.013	0.013
P_2O_5	0.212	0.014	0.019	0.021	0.20	0.15	0.015
Sum	69.79	100.0	100.0	100.2	99.8	100.0	

[1]After removing volatiles and siderophile elements and some oxygen from mantle to form core. Hart and Zindler (1986)
[2]Hart and Zindler (1986)
[3] McDonough and Sun (1995)
[4]Palme & O'Neill (2003)
[5]Lyubetskaya & Korenga (2007)
[6] calculated from the equations of O'Neill & Palme (2008).

the crust. Indeed more than half the Earth's Rb may be in the crust. However, the terrestrial Rb/Sr ratio appears to be nearly an order of magnitude lower than chondritic (0.03 vs. 0.25) even when crustal Rb is considered. Independent of Sr isotope considerations, a number of other studies have demonstrated depletion of K, Rb, and Cs in the Earth. This depletion is thought to encompass all the moderately volatile elements. Many of the moderately volatile elements are siderophile or chalcophile, so their depletion in the mantle may also reflect extraction into the core.

The Earth's depletion in moderately volatile elements is not entirely surprising, given that it, along with the other terrestrial planets, is obviously depleted in the atmophile elements. Since the depletion in the highly volatile elements is a feature shared by all the terrestrial planets, it is probably due to temperatures in the inner solar system being too high for these elements to condense completely during the period that the planetesimals that ultimately formed the terrestrial planets were accreting. High temperatures achieved during formation of the Earth (due to release of gravitational energy during collisions), particularly as a result of the giant impact, may have also contributed to volatile loss.

Table 11.02 reflects a general agreement that at least the upper mantle is depleted in silicon relative to a 'chondritic' mantle (whether this is true of the entire mantle is a question we will return to). The silicon depletion can be demonstrated in several ways. For example, Hart and Zindler (1986) showed that Mg/Si and Al/Si ratios of chondritic and terrestrial samples plot along separate arrays that intersect at the low-Si end of the chondritic range (Figure 11.04). Hart and Zindler argued that the "meteorite array" reflects fractionation during processes occurring in the solar nebula or during planet formation (e.g., evaporation, condensation), whereas the "terrestrial array" reflects processes occurring in the Earth's mantle such as partial melting and crystallization.

Table 11.02 also shows that there is broad agreement among the most recent compositional estimates on the FeO concentration in the upper mantle. This reflects the observation that mantle peridotites have uniform concentrations of FeO of about 8±1%.

Let's consider how other elemental concentrations are estimated in one of the more recent studies, that of Palme & O'Neill (2003). They begin by adopting a FeO concentration of 8.1%. According to them, the least modified peridotites have an MgO/(MgO+FeO) molar ratio (this ratio is referred to as the Mg-number, often written Mg#) of 0.89. Using that value and FeO of 8.1%, they calculate an MgO concentration for the mantle of 36.77%. They then examined the relationship of other oxides, such as SiO_2, CaO, and Al_2O_3 to MgO in peridotites. As Figure 11.05 shows, there is an inverse correlation, which is thought to result largely from melt extraction from these peridotites. Melt extraction leaves the residual peridotite richer in MgO, but poorer in SiO_2, Al_2O_3, and CaO. If the MgO concentration of the undepleted mantle is known, the concentrations of these other oxides can be estimated from these correlations. Values deduced in this way correspond to Mg/Si and Ca/Al molar ratios of 0.94 and 1.1 respectively. The Mg/Si ratio is quite difference from the CI chondrite ratio of 0.83, but in good agreement with the values of 0.95 and 0.94 estimated by Hart and Zindler (1986) and McDonough and Sun (1995), respectively, who used similar approaches.

The Ca/Al ratio agrees well with all other estimates for the Earth as well as with the CI chondrite value. The 50% condensation temperatures of these elements in a gas of solar composition at 10 Pa are: Al: 1650 K, Ca: 1518 K, Mg: 1340 K, and Si: 1311 K (Larimer, 1988). Lithophile elements with 50%

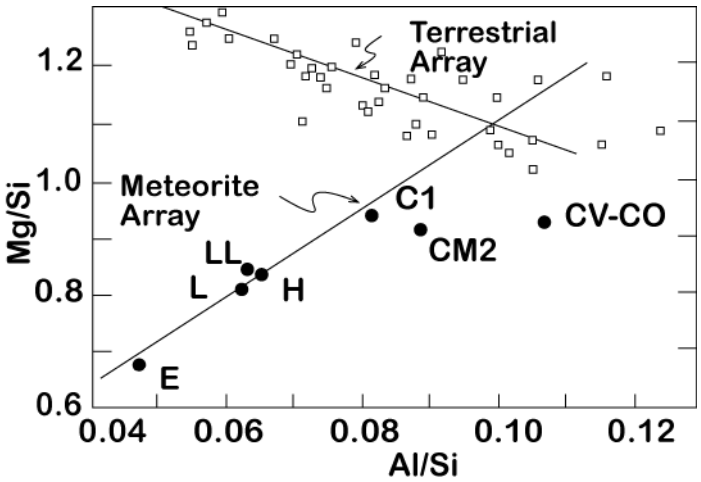

Figure 11.08. Variation of Mg/Si as a function of Nd/Si in terrestrial mantle xenoliths and meteorites. The data suggest the Earth is depleted in Mg and Si relative to chondrites. After Hart and Zindler (1986).

condensation temperatures above that of Mg are generally present in constant proportions in chondritic meteorites. It would seem that temperatures in the solar nebula were never hot enough to fractionate these elements. Consequently, a widely held assumption is that these elements, referred to as *refractory lithophile elements*, should be present in the Earth and other planetary bodies in chondritic proportions. One of these elements is Ti, so using this logic, the Ti concentration can be estimated from the Ti/Al ratio in chondrites and the Al concentration deduced above. The remaining elements in Table 11.02 are either to varying degrees volatile (Na, K, Mn) and/or siderophile (Ni, Co, Cr), meaning they are concentrated in the Earth's core. Palme & O'Neill (2003) estimated concentrations of these elements from the correlations with MgO in peridotites. One exception is K. The K/U and K/La ratios in the mantle and crust show only limited variation. U and La are refractory lithophile elements, so Palme and O'Neill used these ratios to estimate K.

The approach used by Lyubetskaya and Korenga (2007) was similar to that of earlier studies in that they relied on correlations between elements in peridotites. However, they employed more sophisticated statistical techniques including principal component analysis and Monte Carlo simulations. Principal component analysis is based on correlations among variables (concentrations in this case) and attempts to extra secondary variables, the 'components', that predict the behavior of the primary variables. They found that a single such component could predict 82% of the compositional variance. They interpreted this component as the effects of melt extraction, an interpretation consistent with earlier studies. As did earlier studstudies, they adopted the asassumption that refractory lithophile elements are present in the Earth in chondritic relative proportions, but rather than adopt strict ratios, they incorporate that assumption in their statistical analysis as a "cost function". As Table 11.02 shows, their results are broadly similar to earlier studies, but there are a few important differences. Their estimate of MgO is significantly higher than earlier ones and their estimated concentrations of refractory lithophile elements (Al, Ca, Ti) significantly lower. They also found that the Earth had lower concentrations of the incompatible elements Na, K, and P than estimated in earlier studies. This apparent depletion of incompatible elements in their study is intriguing and suggests some of the assumptions of earlier estimates of bulk Earth composition might be flawed. Another indication that this might be the case comes from an entirely dif-

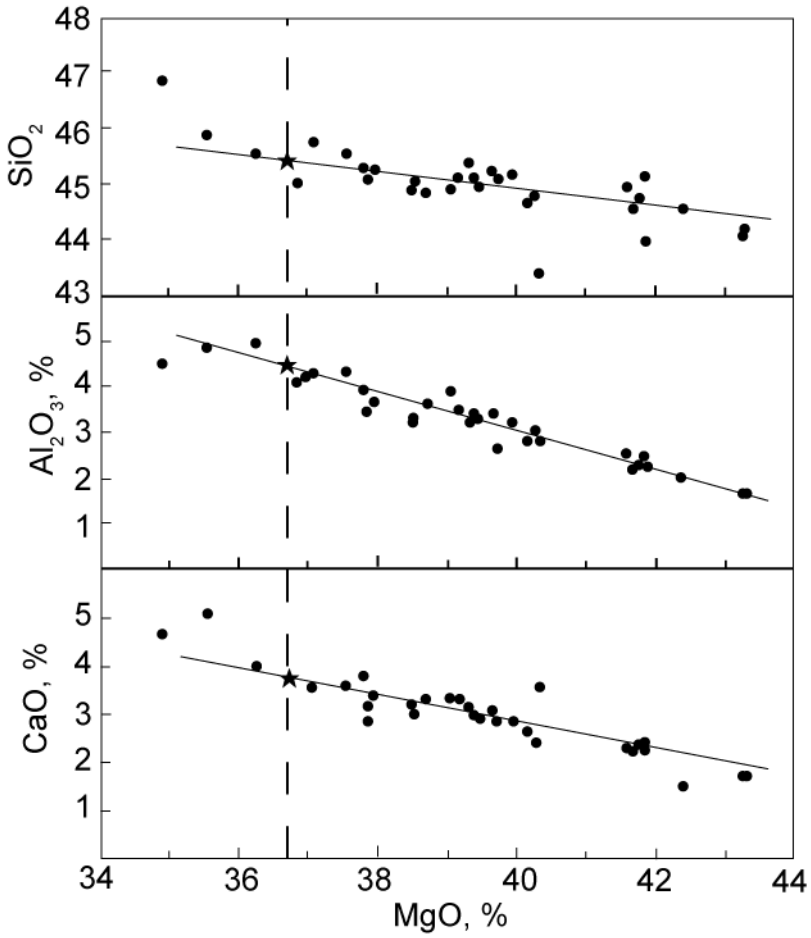

Figure 11.09. Correlation of SiO_2, Al_2O_3, and CaO with MgO in peridotites from the central Dinarides (Balkans). Stars indicate estimated mantle primitive compositions. After Palme & O'Neill (2003).

ferent kind of evidence: Nd isotopic composition.

11.3.2 The ^{142}Nd Conundrum

In Chapter 8 (8.5.4), we noted that recent studies of the $^{142}Nd/^{144}Nd$ ratio in chondrites and terrestrial materials provide evidence that the Sm/Nd ratio of the Earth, or at least the part of accessible to sampling, is not be chondritic. (Recall that ^{142}Nd is produced by α-decay of ^{146}Sm, which has a half-life of 103 Ma.) This is surprising to say the least because it had been widely assumed that refractory lithophile elements are present in the Earth in chondritic relative proportions. For Sm and Nd, this appears to be a good assumption indeed. These two elements are very similar to each other, having identical configurations of bonding electrons orbitals, and are both refractory lithophile elements. Indeed, Nd and Sm have 50% condensation temperatures of 1602 and 1590 K, respectively. It is difficult to see how processes operating in the solar nebula could have fractionated these elements significantly. The total range of high precision Sm/Nd ratio measurements in chondrites varies by only 3%, which would seem to confirm that these elements were not fractionated in the solar nebula. Yet the $^{142}Nd/^{144}Nd$ ratio of all modern terrestrial materials is different from that of chondrites (Figure 8.27), implying differences in $^{146}Sm/^{144}Nd$ ratios.

How might these isotopic differences come about? Three possible answers have been proposed. First, it is possible that the early solar system was isotopically heterogeneous. As we learned in Chapter 10, some isotopic heterogeneity existed in the early solar system, most notably for oxygen. More significantly, small variations in the isotopic composition of Nd and Sm have been found in chondrites (Andreasen and Sharma, 2006; Carlson et al.; 2007; Gannoun et al., 2011; Qin et al.,, in press). Indeed, carbonaceous, ordinary, and enstatite chondrites each appear to have different $^{142}Nd/^{144}Nd$ despite identical Sm/Nd. Both ^{146}Sm and ^{144}Sm are p-process-only nuclide produced exclusively in supernova explosions while ^{142}Nd is primarily an s-process nuclide produced in red giants, with a small fraction (<5%) produced by the p-process. Incomplete mixing of material from different stars thus could result in variations in $^{142}Nd/^{144}Nd$ in the early solar system. However, Andreasen and Sharma (2006) and Qin et al. (in press) concluded that while the observed isotopic heterogeneity could explain $^{142}Nd/^{144}Nd$ variations observed among chondrites, it could not entirely explain the difference between the Earth and chondrites.

A second possibility was suggested by Boyet and Carlson (2005). They suggested that Earth underwent early differentiation forming an *early enriched reservoir*, such as a primordial crust that sank into the deep mantle and has not been sampled since. This differentiation might have occurred as a consequence of crystallization of a terrestrial magma ocean analogous to the lunar magma ocean. Alternatively, crystallization of the terrestrial magma ocean might have left a layer of residual melt, similar to the KREEP source on the Moon. Boyet and Carlson (2005) noted that if it were rich in Fe and Ti, as is the lunar KREEP reservoir is, once crystallized, the EER could have sunk into the deep mantle, where it remains because if its high density. As Boyet and Carlson (2005) point out, this early enriched reservoir must have formed in the upper mantle. Below the 660 km discontinuity, Mg- and Ca-perovskite would crystallize and fractionate incompatible elements in a manner much different than observed.

A third possibility, "collisional erosion", has been suggested by Caro et al. (2008) and O'Neill and Palme (2008). As we discussed in Chapter 10, planetary bodies are thought to form through the process of "oligarchic growth". The initial stages of this process involve aggregations of dust-sized particles to form sand-sized particles, which in turn aggregate to form pebble-sized particles, etc. The later stages of this process involve infrequent, energetic collisions between large bodies. Sufficient energy is released in these collisions that the growing planet extensively melts. Between collisions, one might reasonably expect a primitive basaltic crust to form through crystallization at the surface. Caro et al. (2008), O'Neill and Palme (2008), and Caro and Bourdon (2010) suggest that a substantial fraction of this crust was blasted away in these collisions, leaving the Earth depleted in elements that were concentrated in that crust: incompatible elements.

Common to both the second and third hypotheses is the idea that planetary melting and consequent differentiation begins during, rather than after, planetary accretion. Both hypotheses rely on the idea of formation, through melting and fractional crystallization, of a primitive crust enriched in incompatible elements. Such a crust would have a low Sm/Nd ratio, leaving the remainder of the planet with a

higher Sm/Nd ratio than the material from which it accreted. In the Boyet and Carlson (2005) hypothesis, this early crust sinks into the deep mantle where it remains as an isolated reservoir. In collisional erosion hypothesis, this early crust is lost from the Earth. Several observations suggest the latter hypothesis is preferable.

The first of these observations is that both the Moon appears to have $^{142}Nd/^{144}Nd$ ratios higher than chondritic. All lunar rocks are ancient, and consequently they have variable $^{142}Nd/^{144}Nd$ ratios. When these ratios are plotted against $^{147}Sm/^{144}Nd$ they display a correlation indicating the bulk Moon has $^{142}Nd/^{144}Nd$ about 17 ppm higher than the chondritic value, identical, within uncertainty, to the modern terrestrial value (Boyet and Carlson, 2007). The similarity of $^{142}Nd/^{144}Nd$ in the Earth and Moon implies that the Sm/Nd fractionation must have occurred before the giant impact that formed the Moon. One reaches the same conclusion when one considers the timing of the Moon forming event. Once corrected for the effects of cosmic rays, tungsten isotope ratios on the Moon are uniform and indistinguishable from those of the Earth, indicating the Moon-forming event occurred at least 50 and as much as 150 million years after the start of the solar system (Figure 10.41; Touboul et al., 2009). A fractionation event increasing the Sm/Nd ratio occurring this late would require unreasonably high Sm/Nd ratios to explain the $^{142}Nd/^{144}Nd$ of the Earth and Moon. Thus the early enriched reservoir hypothesized by Boyet and Carlson must predate the giant impact. It is unlikely it could have survived this event without being remixed into the mantle (Caro and Bourdon, 2010).

Mars may also have the same $^{142}Nd/^{144}Nd$ as the Earth (Caro et al., 2008), but this remains controversial. It is possible that higher than chondritic Sm/Nd ratios is a common feature of terrestrial planets.

Geophysical considerations also cast doubt on the existence of a highly incompatible element-enriched reservoir in the deep mantle. In order to explain the 6% increase in Sm/Nd ratio in the remaining mantle, this reservoir would have to contain at least 40% of the Earth's inventory of highly incompatible lithophile elements. This group of elements includes the heat-producing elements K, U, and Th. Thus the early enriched reservoir at the base of the mantle would be responsible for some 40% of the heat production in the Earth, and 70% or more of the heat production in the mantle. If this were the case, the mantle should be heated mainly from below. As Davies (2009) points out, this would produce a very different style of convention than actually occurs. Convective layers heated mainly from below are dominated by plumes that initiate as instabilities at the base of the layer. While some plumes do form at the base of the mantle and rise through it, the dominant form of convection in the Earth's mantle is plate tectonics, which is the kind of convection expected in systems heated from within (lava lakes, for example, convect in a way similar to plate tectonics).

We conclude then that the through the process of collisional erosion, the Earth lost a fraction of a primitive crust of roughly basaltic composition. For most of the major elements such as Si, Al, and Ca, this does not have a discernable effect on mantle or bulk Earth composition. For those elements listed in Table 11.02, only K is affected significantly. The effect on incompatible trace elements is more significant, as we shall see in the following section.

11.3.3 Composition of the Bulk Silicate Earth

All previous effects to estimate bulk Earth composition rely on the assumption that refractory lithophile elements are present in the Earth in chondritic relative proportions. However, the Earth's non-chondritic $^{142}Nd/^{144}Nd$ ratio implies a Sm/Nd ratio higher than chondritic, meaning this assumption must be discarded or modified. O'Neil and Palme (2008) suggest a way to modify the chondritic assumption to account for erosional loss of a primitive crust and we will follow their approach here. O'Neil and Palme (2008) begin by assuming that the growing proto-earth partially melted to produce a proto-crust of mass fraction f^1_{p-c}. The concentration of an element, *i*, in the proto-crust is given by the batch melting equation (equation 7.42):

$$\frac{c_i^{pc}}{c_i^o} = \frac{1}{D_i + f^1_{p-c}(1 - D_i)} \qquad 11.15$$

where D_i is the bulk partition coefficient of *i*. They assume that some of this crust corresponding to a mass fraction f^2_{p-c} is removed by erosion, along with a fraction of the residue of crust formation, f^2_{res}. The depletion of element *i* in the bulk silicate Earth is then:

$$\frac{c_i^{BSE}}{c_i^o} = \frac{f^1_{p-c}(1-D_i) + D_i(1-f^2_{res}) - f^2_{p-c}}{(D_i + f^1_{p-c}(1-D_i))(1-f^2_{res} - f^2_{p-c})} \qquad 11.16$$

The unknowns in this equation are the three mass fraction terms and the partition coefficients. For the latter, O'Neil and Palme adopt the bulk partition coefficients for formation of the basaltic oceanic crust of Workman and Hart (2005). The other unknowns can be constrained by geochemical considerations.

First, O'Neil and Palme (2008) note that the bulk Earth (including the core) Fe/Mg ratio is about 2.1, compared to the solar and chondritic value, which is about 1.9. Since Fe and Mg have similar volatiles, one would expect the terrestrial ratio to be close to the solar one. Collisional erosion would increase the Fe/Mg ratio because the material eroded would come from the mantle and proto-crust, and not from the core, which they assume had already formed). On this basis, O'Neil and Palme estimate the mass fraction lost, $f^2_{p-c} + f^2_{res}$, to be about 10%. A second constraint comes from the amount of ^{40}Ar in the atmosphere. Essentially all atmospheric ^{40}Ar has been produced by the decay of ^{40}K. The amount of K necessary to produce this Ar corresponds to a K concentration of 120 ppm, which is about half that estimated from K/U and K/La ratios under the assumption of chondritic refractory lithophile relative abundances. The maximum computed K loss occurs if the partition coefficient is 0, so provides a lower limit on c_K^{BSE}/c_K^o of 0.5 when $D_K = 0$. The third constraint comes from the observed difference in ^{142}Nd/^{144}Nd between the Earth and chondrites, implying a Sm/Nd ratio greater than chondritic. The difference in ^{142}Nd/^{144}Nd between the Earth an ordinary chondrites implies a terrestrial Sm/Nd 6% greater than chondritic. Based on this, O'Neill and Palme (2008) concluded that $f^1_{p-c} = 0.026$ and $f^2_{p-c} = 0.014$. In other words, the proto-crust was about 2.6% of the mass of the Earth and about 0.014/0.026 = 54% of this crust was lost. However, the difference in ^{142}Nd/^{144}Nd between the Earth and enstatite chondrites implies a terrestrial Sm/Nd ratio only 3% greater than chondritic. The enstatite chondrites are unique having the same O isotopic composition as the Earth (Chapter 10); they thus may represent a better compositional model for the Earth. This Sm/Nd ratio can be matched with a slightly larger crust fraction, 3% and a slightly smaller fraction of it lost, 33%, i.e., $f^1_{p-c} = 0.03$ and $f^2_{p-c} = 0.01$ ($f_{res} = 0.09$). Nd isotopes ratios correlate with Sr and Hf isotope ratios in mantle material. One can reasonable expect that the Nd, Sr and Hf isotopic compositions should fall within these "mantle arrays" (Chapter 8). Consequently, appropriate parameters for eroded Earth model should also predict the Rb/Sr and Lu/Hf ratios of the bulk silicate Earth as deduced from the Sr and Hf isotope ratios. The model does predict a Lu/Hf ratio that would produce a terrestrial ^{176}Hf/^{177}Hf ratios falling within the mantle array, but predicts a Rb/Sr ratio that is too low. The Rb concentration and Rb/Sr can adjusted upward, however, by adding 1% of CI chondritic material to the calculated eroded Earth composition. As we discuss in section 11.4.3 below, just such an addition of a "late accretionary veneer" has be widely viewed as the explanation for the nearly chondritic relative abundances of highly siderophile elements (Kimura et al. 1974; Palme and O'Neill, 2003). Adding 1% chondritic material to the eroded Earth composition calculated above raises concentrations of moderately volatile elements such as Rb but has a negligible effect on refractory lithophile elements.

Table 11.03 compares the composition of the silicate Earth using the approach described above where the c^o values are taken from Palme and O'Neil (2003) with bulk silicate Earth compositions of McDonough and Sun (1995) and Lyubestskaya and Korenaga (2007). For those elements that Workman and Hart (2005) do not give *D* values, bulk *D* values were estimated (e.g., Li, Na), or concentrations were adjusted appropriately based on Palme and O'Neill's original estimate. As an example of the latter, Palme and O'Neill estimated the As concentration from the observation that the As/Ce ratio in the Earth is 0.37. Using the revised Ce concentration of 1.53 ppm, which is 14% lower than Palme and O'Neill's (2003) value, the As concentration is calculated as 0.05 ppm, also 14% lower. Other concentrations, such as Cu and Zn were derived by Palme and O'Neill (2003) by correlation with MgO and as such are independent of the assumption of chondritic abundances of refractory lithophile elements and are taken unmodified from Palme and O'Neill (2003). K in Table 11.03 (and K_2O in Table 11.02) has

been estimated using a revised estimate of the K/U ratio of the Earth of Arevalo et al. (2009) of 13,800, based largely on an upwardly revised K/U in MORB. The Pb concentration is constrained from Pb isotope systematics such that the U/Pb ratio should be 0.133.

The data in Table 11.03 correspond to $^{147}Sm/^{144}Nd$, $^{87}Rb/^{86}Sr$, and $^{176}Lu/^{177}Hf$ ratios of 0.2024, 0.0764, and 0.03565, respectively, which in turn correspond to present-day $^{143}Nd/^{144}Nd$, $^{87}Sr/^{86}Sr$, and

Table 11.03. Bulk Silicate Earth Composition

	McDonough & Sun (1995)	Lyubetskaya & Korenga (2007)	"Eroded Earth"		McDonough & Sun (1995)	Lyubetskaya & Korenga (2007)	"Eroded Earth"
Li	1.60	1.60	1.52	Ag	0.008	0.004	0.004
Be	0.07	0.05	0.06	Cd	0.040	0.050	0.064
B	0.30	0.17	0.23	In	0.011	0.010	0.012
C	120.00	—	100.00	Sn	0.130	0.103	0.125
F	25.00	18.00	22.88	Sb	0.0055	0.0070	0.0089
Na	2670	2220	2590	Te	0.012	0.008	0.008
Mg	228000	234100	221700	I	0.010	0.010	0.001
Al	23500	18700	23500	Cs	0.021	0.016	0.015
Si	210000	210900	212200	Ba	6.60	5.08	5.03
P	90	66	76	La	0.648	0.508	0.555
S	250	230	200	Ce	1.68	1.34	1.53
Cl	17	1.4	8.5	Pr	0.254	0.203	0.235
K	240	190	226	Nd	1.25	0.99	1.16
Ca	25300	20000	25541	Sm	0.406	0.324	0.389
Sc	16	13	16	Eu	0.154	0.123	0.147
Ti	1205	950	1176	Gd	0.544	0.432	0.523
V	82	74	86	Tb	0.099	0.080	0.097
Cr	2625	2645	2520	Dy	0.674	0.540	0.666
Mn	1045	1020	1050	Ho	0.149	0.121	0.149
Fe	62600	62000	63000	Er	0.438	0.346	0.440
Co	105	105	102	Tm	0.068	0.054	0.068
Ni	1960	1985	1860	Yb	0.441	0.346	0.440
Cu	30	25	20	Lu	0.068	0.054	0.068
Zn	55	58	54	Hf	0.283	0.227	0.269
Ga	4.0	4.2	4.4	Ta	0.037	0.030	0.031
Ge	1.1	1.2	1.2	W	0.029	0.012	0.012
As	0.050	0.050	0.057	Re	0.0003	0.0003	0.0003
Se	0.075	0.075	0.079	Os	0.0034	0.0034	0.0034
Br	0.05	0.004	0.022	Ir	0.0032	0.0032	0.0032
Rb	0.60	0.46	0.47	Pt	0.0071	0.0066	0.0066
Sr	19.90	15.80	17.48	Au	0.0010	0.0009	0.0009
Y	4.30	3.37	4.12	Hg	0.0100	0.0060	0.0060
Zr	10.50	8.42	9.64	Tl	0.0035	0.0002	0.0024
Nb	0.66	0.46	0.45	Pb	0.150	0.144	0.120
Mo	0.050	0.030	0.034	Bi	0.0025	0.0040	0.0044
Ru	0.005	0.005	0.005	Th	0.080	0.063	0.063
Rh	0.0009	0.0009	0.0009	U	0.02	0.0173	0.0164
Pd	0.0039	0.0036	0.0033				

All concentrations in ppm. "Eroded Earth" is modified from Palme & O'Neill (2003) as described in the text.

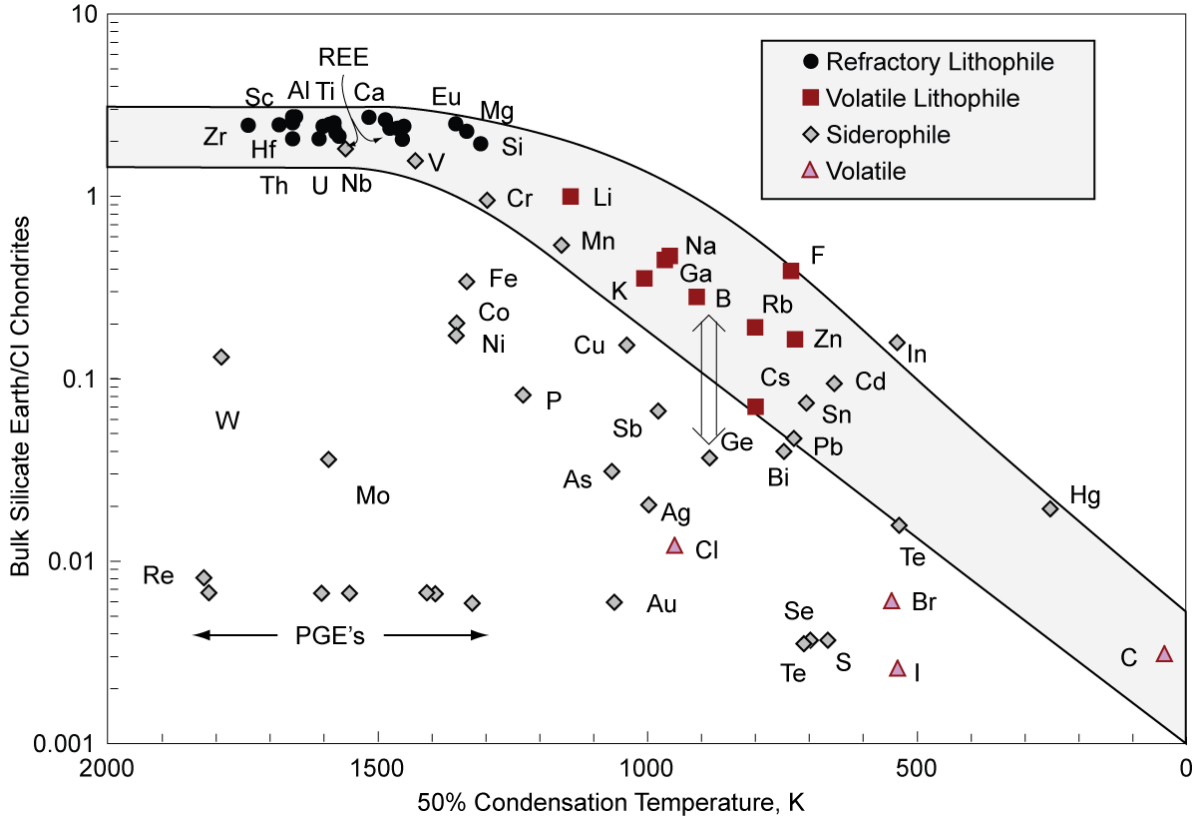

Figure 11.10. Abundances of the elements in the bulk silicate Earth (Table 11.3) relative to CI chondrite abundances as a function of 50% nebular condensation temperature (Lodders, 2003). Primary controlling factors are volatility and the siderophile or chalcophile nature of the element.

$^{176}Hf/^{177}Hf$ ratios of 0.51282, 0.70404, and 0.28287, respectively. This implies $\varepsilon_{Nd} = +3.6$ and $\varepsilon_{Hf} = +6.4$ for the bulk silicate Earth. Exact values, however, must be viewed as uncertain. For example, Caro and Bourdon (2010) use the $^{142Nd}/^{144}Nd$ difference between the Earth and *ordinary* chondrites to infer that the terrestrial Sm/Nd ratio is 6% higher than chondritic. This implies $^{147}Sm/^{144}Nd$, $^{87}Rb/^{86}Sr$, and $^{176}Lu/^{177}Hf$ ratios of 0.2082, 0.065, and 0.0375, respectively, corresponding to present-day $^{143}Nd/^{144}Nd$, $^{87}Sr/^{86}Sr$, and $^{176}Hf/^{177}Hf$ ratios of 0.51299, 0.7030, and 0.28313, respectively ($\varepsilon_{Nd} = +6.9$ and $\varepsilon_{Hf} = +12$).

It is worth emphasizing that if the Boyet and Carlson (2005) hypothesis that an 'early enriched reservoir' is present as an isolated layer at the base of the mantle is correct, then the composition listed in Table 11.03 becomes the composition of the geochemically 'observable Earth', namely continental crust that has formed after 3.5 Ga and that part of the mantle that has contributed to volcanism after that time.

The revised composition of the Earth (or the observable part of it) listed in Table 11.03, particularly the lower incompatible element abundances, has profound implications for the mantle structure and convection. Higher incompatible element concentrations derived from the assumption of chondritic refractory lithophile element abundances led to the conclusion that only a fraction, half or less, of the mantle had been involved in continental crust creation, and that half or more of the mantle retained their original inventory of volatile elements such as Ar. These observations were used as an argument in favor of "primitive" lower mantle and for layered mantle convection. The revised estimates remove geochemical objections to whole mantle convection. The concentrations of the heat producing elements K, U, and Th listed in Table 11.03 are substantially lower than previous estimates, meaning there is much less energy being generated in the mantle than previously believed. We'll explore these implications further in a subsequent section.

Figure 11.10 shows the abundances of the elements in the silicate Earth relative to CI chondritic (i.e., solar system) concentrations as a function of their 50% condensation temperatures under conditions relevant to the solar nebula. The refractory lithophile elements are enriched in the Earth by factors ranging from 1.5 to 2.8. Other elements show more variable enrichments. In general, the concentrations of volatile lithophile elements are a rough function of their 50% condensation temperatures, consistent with inferences made by Paul Gast and others a half a century ago. We also see that many elements are more depleted in the silicate Earth than we would predict from their volatility. We can infer from this that these elements are concentrated in the core, whose composition we consider in the following section.

11.4 The Earth's Core and Its Composition

11.4.1 Geophysical Constraints

That the Earth has an iron core is known even to schoolchildren. But how do we know this, since no one has ever seen or touched the core? Here again we turn to geophysics. Perhaps the first hint came when 17th century physicist William Gilbert observed that the Earth's magnetic field was similar to a bar magnet. The plot thickened in 1634, so to speak, when Henry Gellibrand demonstrated temporal changes in the Earth's magnetic field. Further evidence emerged when measurement of the mass of the Earth indicated a high-density interior (section 11.2.1). Unequivocal evidence of this, however, did not emerge until two centuries later. As seismology advanced in the early 20th century, Inga Lehmann found that the Earth had a core consisting of an outer layer that did not transmit s-waves, and therefore must be liquid, and an inner core that did, and therefore must be solid. Both the inner and outer core have lower seismic velocities than silicate, suggesting the core has higher density. Comparison of density solutions to the Adams-Williamson equation (Eq. 11.12) with the Earth's moment of inertia provided evidence that the Earth's high density interior could not be simply a consequence of self-compression: the material in the core must have intrinsically higher density. At this point, we can turn to cosmochemistry to ask what heavy element is abundant enough to make up the core, which makes up 16% of the volume and 32% of the mass of the Earth. Looking at Table 10.02, one answer immediately emerges: iron. Iron has a lower melting point than peridotite, making it easy to explain the transition from solid mantle to liquid iron outer core. Iron is also a conductor, and can, when placed in motion, generate a magnetic field. Looking further at cosmic abundances and at Table 11.02, we see that nickel is a cosmically abundant element, yet depleted in the silicate Earth. It seems likely then that the core contains substantial Ni as well.

Geophysical measurements can take us a bit further in deducing the composition of the core. Any combination of iron and nickel alone would produce a core that is 5 to 10% denser that the actual core (Birch, 1964; Anderson and Issak, 2002). Consequently, the core must contain a significant concentration of some lighter element or elements; how much depends on which element. If we again glance at cosmic abundances, and also consider which elements are underabundant in the silicate Earth and which could possibly alloy with iron, the main possibilities are H, C, O, Si and S. At one time or another, a case has been made for each of these. To further constraint the composition of the core, however, we need to look to meteorites.

11.4.2 Cosmochemical Constraints

Iron meteorites are now understood to represent pieces of asteroidal cores. In this sense, they may provide a good analogy for the Earth's core. Indeed, Emil Wiechert's 1897 proposal that the Earth had an iron core was inspired in part by the existence of iron meteorites. Iron meteorites are not pure iron, but rather are typically iron-nickel alloy with additional components. These include sulfides and phosphides. Iron meteorites also have high concentrations of siderophile and chalcophile trace elements. However, the analogy between the Earth's core and iron meteorites must be approached with caution because iron meteorites come from relatively small bodies whose core formed under relatively low-pressure conditions. The Earth's core may have formed under much higher-pressure conditions.

Table 11.04. Estimated Composition of the Earth's Core

Element	Conc.	Element	Conc.	Element	Conc.
H	600	Cu	125	Te	0.85
C	2000	Ge	20	I	0.13
N	75	As	5	Cs	0.065
Si %	6.0	Se	8	W	0.47
P	2000	Br	0.7	Re	0.23
S %	1.9	Mo	5	Os	2.8
Cl	200	Ru	4	Ir	2.6
V	150	Rh	0.74	Pt	5.7
Cr %	0.9	Pd	3.1	Au	0.5
Mn	300	Ag	0.15	Hg	0.05
Fe %	85.5	Cd	0.15	Tl	0.03
Co	2500	Sn	0.5	Pb	0.4
Ni %	5.2	Sb	0.13	Bi	0.03

Concentrations in ppm, except % where noted. From McDonough (2003).

Cosmochemistry can nevertheless provide some constraints on core composition. We again make the assumption that the Earth formed within a nebula of chondritic composition. The Earth's composition should therefore be related in some way to that of chondrites. As Figure 11.10 shows, the mantle is depleted in many elements relative to chondrites. Many of these elements are siderophile and it seems reasonable to think they are concentrated in the core. However, the Earth is also depleted in volatile elements. If an element is both siderophile and volatile, how do we know if their depletion in the mantle reflects concentration in the core because of their siderophile character, or depletion in the Earth as a whole because of their volatile character? The approach taken by McDonough (2003) has been to plot an element's bulk silicate Earth concentration against its 50% condensation temperature as in Figure 11.10. The 50% condensation temperature is the temperature at which 50% of the element condenses in a nebula of solar composition at 10 Pa (10^{-4} atm). When we do this a clear trend emerges (Figure 11.10). Lithophile elements with condensation temperatures above that of Mg (1336 K) are enriched in the silicate Earth. At lower condensation temperatures, a clear trend of decreasing concentration with decreasing condensation temperature emerges. A similar trend can be seen when carbonaceous chondrites are compared to CI chondrites (McDonough, 2003). Since the lithophile elements should not be concentrated in the core, this trend should be due to volatility alone. Most siderophile and chalcophile elements plot below this trend. Let's assume that when we consider the composition of the whole Earth, all elements plot along this volatility trend. That allows us to estimate the concentrations of all elements, and the concentration of elements in the core can be estimated by subtracting the mantle concentration from the whole Earth concentration. This is illustrated for Ge in Figure 11.10. Ge has only about 14% of the mantle concentration we would expect based on its condensation temperature of 883 K. Presumably then, 86% of the Earth's Ge inventory is in the core. From this, we can calculate that the concentration of Ge in the core should be about 20 ppm. In contrast, Ga, which is partly siderophile, is not depleted in the mantle beyond what would be expected from its volatility alone, hence its concentration in the core must be close to 0. Working through the periodic table in this way, McDonough (2003) derived the estimated core composition listed in Table 11.04.

We should treat the values in Table 11.04 with considerable caution for several reasons. First, they are based on the assumption that the Earth differs from a CI chondritic composition only because of volatility. Second, they are based on estimated mantle compositions that are themselves uncertain, particularly in light of the observation that the Earth does not have chondritic relative concentrations of the refractory lithophile elements. Third, the volatility trend defined by the lithophile elements is a broad one and this produces considerable error in the estimate of the core concentration of any particular element. Finally, the most volatile lithophile elements have condensation temperatures around 700 K; beyond that, the trend must be extrapolated. We cannot be sure the slope of the trend remains constant at low temperatures.

Some of the results of this approach are a bit surprising. Most surprising is the apparent lack of Ga in the core, as it is concentrated in iron meteorites. McDonough (2003) suggests that either the condensation temperature for Ga is too high, or that Ga behaved solely as a lithophile element when the Earth's core formed. If so, he says, "then determining under what conditions gallium becomes wholly lithophile provides an important constraint on core formation." We'll consider that in the following

section. It is also surprising that the core would have significant concentrations of Cs and the halides, Cl, Br, and I as none of these elements are found in fresh iron meteorites. It is possible that the estimated condensation temperatures for these elements are too high or that the estimated concentrations of Cl, Br, and I in the bulk silicate Earth are too low.

In McDonough's model, the core contains significant concentrations of S and P and minor concentrations of C and H, but the low density of the core arises mainly from the high concentration of Si. If Si is indeed present in the core this could explain the deficiency of the mantle in Si relative to chondrites. On the other hand, the concentration of Si relative to more refractory elements such as Mg, Al and Ca does vary even within carbonaceous chondrites, so it is clear that Si was fractionated from these elements within the solar nebula. Furthermore, such high Si concentrations in the core imply that the core formed under surprisingly reducing conditions. The explanation of the Si depletion may lie in Si's lower condensation temperature rather than it concentration in the core. It is perhaps best to state that cosmochemical considerations allow a significant concentration of Si in the core, but they do not require it.

In contrast, cosmochemical considerations would seem to preclude sulfur being the main light element in the core. Relative to CI chondrites, sulfur is depleted in almost all other classes of chondrites. Ahrens and Jeanloz (1987) found that a core with about 11% S would match the observed seismic properties of the core reasonably well. For the core to contain 11% S would require the Earth to have an S concentration that is 65% of the CI chondrite concentration. Given the low condensation temperature of S (664 K), this seems improbable.

11.4.3 Experimental Constraints

Experiments on the partitioning of elements between iron and silicate phases provide potential constraints both on the composition of the core and on how it formed. The idea that O might be the light element in the core is based on the observation that at high pressure FeO is miscible in Fe liquid, although it is not at low pressure. The eutectic composition in the Fe-FeO system at 16 GPa (still well below core pressures) contains about 10% FeO (e.g., Ringwood and Hibbertson, 1990). Furthermore, the Earth's mantle is depleted in oxygen compared with CI chondrites. The relevance of this last observation, however, is questionable, since the oxidation state of chondrites, and therefore presumably the solar nebula, clearly varied widely. Significant in this respect is the observation that based on O isotope ratios, the Earth appears to be more closely related to the highly reduced enstatite chondrites (Figure 10.28 and 10.29), which are highly reduced, than to other chondrites, particularly CI chondrites. In addition, O'Neill et al. (1998) pointed out that higher pressure, oxygen solubility in iron liquids decreases with pressure. They argue that core could contain at most about 2% oxygen.

The problem of oxygen illustrates a fundamental dilemma with partitioning studies: partition behavior depends on temperature, pressure, and composition. This is just as true for metal-silicate partitioning as it is for the silicate mineral–liquid partitioning we considered in Chapter 7. Indeed, the problem of temperature and pressure dependence is considerably more severe when we consider planetary scale differentiation because the range of temperatures and pressures over which partitioning might have occurred is enormous. Today, the metal-silicate boundary, which is the core-mantle boundary, is at 135 GPa and 3000-4000 K. However, that need not be the environment in which metal and silicate phases equilibrated. Suppose that material was accreted incrementally to the surface of a growing Earth, separated into metal and silicate portions, with subsequent sinking of the metal without further equilibration. In that case, the pressure of equilibration is close to 0.1 MPa and temperatures are far lower. Yet another scenario is that metal and silicate last equilibrated at the base of a magma ocean at mid-mantle pressures. As we shall see, the may be the plausible scenario. Experiments have also demonstrated the role of composition in partitioning between metal and silicate melts. In particular, the concentrations nickel and sulfur in the metallic liquid, the degree of polymerization of the silicate liquid, and the oxygen fugacity are important. Despite this complexity, experimental determination of partition coefficients has elucidated aspects of core formation.

For example, experiments by Righter et al. (1997) demonstrated a strong dependence of the metal-silicate partitioning of Ni, Co, W, and Mo on oxygen fugacity, pressure, temperature, silicate liquid composition. The effect of oxygen fugacity and pressure is illustrated in Figure 11.11. In the graph,

oxygen fugacity is expressed as the difference between actual oxygen fugacity and that of the iron-wüstite buffer (see Chapter 3).

Given the strong T, P and composition dependence of metal/silicate partitions coefficients, it seems useful to consider the thermodynamics of metal-silicate partitioning in more detail. In general, it is assumed that the partitioning occurs between silicate and metal *liquids*. It is, of course, possible that equilibration occurs below the liquidus of either or both phases, implying solids are present as well. However, so long as the solids are in equilibrium with their respective liquids, they will also be in equilibrium with the other liquid. Hence, provided two liquids are present, we need only focus on the liquid-liquid partition coefficients. Righter et al. (1997) considered the following reaction:

$$M^{n+}O_{n/2\ sil\ liq} = M_{met\ liq} + \frac{n}{4}O_{2\ gas} \qquad 11.17$$

where n is the valence of element M. For this equation, we can write the following equilibrium constant expression:

$$-\frac{\Delta G^\circ}{RT} = \ln\left(\frac{a_M f_{O_2}^{n/4}}{a_{MO_{n/2}}}\right) \qquad 11.18$$

where, as usual, a denotes activity and f denotes fugacity. Rearranging this expression, we have:

$$\ln\left(\frac{a_M}{a_{MO_{n/2}}}\right) = -\frac{n}{4}\ln\left(f_{O_2}\right) - \frac{\Delta G^\circ}{RT} \qquad 11.19$$

The free energy change will, of course, be temperature and pressure dependent. To express that dependence, we can expand the ΔG term to:

$$\Delta G^\circ = \Delta H^\circ - T\,\Delta S^\circ + P\,\Delta V^\circ \qquad 11.20$$

Substituting this in equation 11.17, we have:

$$\ln\left(\frac{a_M}{a_{MO_{n/2}}}\right) = -\frac{n}{4}\ln\left(f_{O_2}\right) - \frac{\Delta H^\circ}{RT} + \frac{\Delta S^\circ}{R} - \frac{P\,\Delta V^\circ}{RT} \qquad 11.21$$

It is certainly more convenient to deal with the ratio of concentrations than the ratio of activities. The ratio of concentrations is in this case identical to the distribution coefficient. So we can again modify our equation to become:

$$\ln D_M^{met/sil} = -\frac{n}{4}\ln\left(f_{O_2}\right) - \frac{\Delta H^\circ}{RT} + \frac{\Delta S^\circ}{R} - \frac{P\,\Delta V^\circ}{RT} - \ln\gamma_M + \gamma_{MO_{n/2}} \qquad 11.22$$

where the gamma terms are the activity coefficients, which we expect will be functions of the compositions of the two liquids. We now have an expression for the temperature, pressure, and compositional dependence of the partition coefficient.

On this theoretical basis, Righter et al. (1997) expressed metal/silicate partition coefficients as follows:

$$\ln D_M^{met/sil} = a\ln\left(f_{O_2}\right) + \frac{b}{T} + \frac{cP}{T} + d(nbo/t) + e\ln(1 - X_S) + f \qquad 11.23$$

where *nbo*/*t* is the non-bridging oxygen/tetrahedral cation ratio (see Chapter 4) and X_S is the mole fraction of sulfur in the metallic liquid. Comparing equations 11.22 and 11.23, we see that the parameter a should relate to the valence of the metal, b to ΔH°, c to ΔV°, d and e to the compositions of the silicate and metal liquids respectively, and f to ΔS°.

Understanding how elements partition between metal and silicate can help us understand the conditions under which the core formed. As Figure 11.10 suggests, the two siderophile elements Ni and Co are about equally depleted in the Earth's mantle. Put another way, the ratio of concentrations of these elements is nearly chondritic, even if their concentrations are not. That suggests the metal-silicate partition coefficients for the 2 elements should be similar. Early experiments at 1 atmosphere and moderate temperature indicated the partition coefficient of Ni was more than an order of magnitude higher than

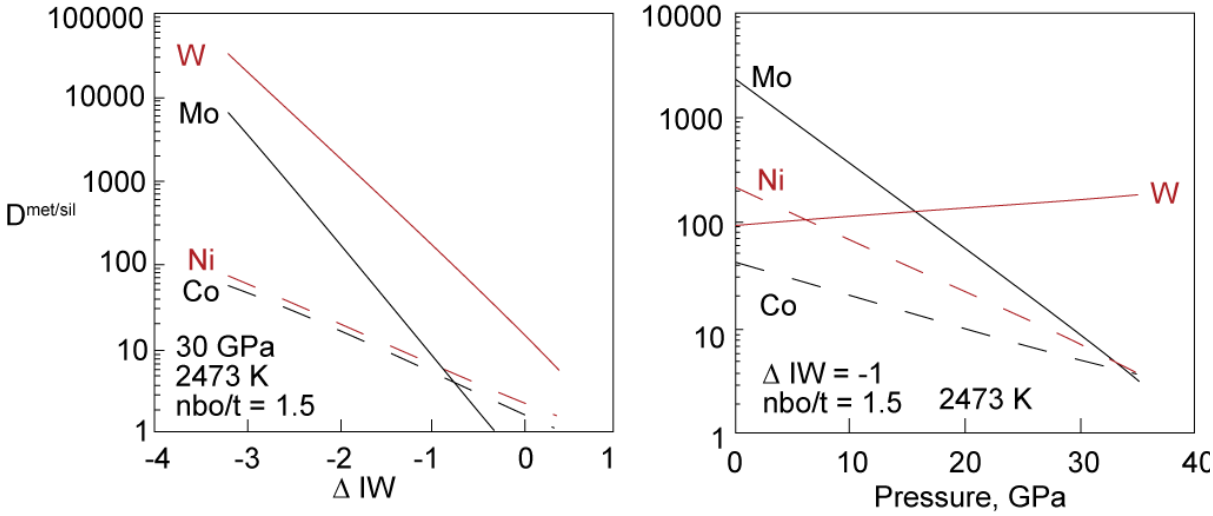

Figure 11.11. Dependence of experimentally determined liquid metal-liquid silicate partition coefficients of Ni, Co, W, and Mo on oxygen fugacity and pressure. ΔIW is the difference, in log units, between oxygen fugacity in the experiment and the oxygen fugacity of the iron-wüstite buffer. *nbo/t* is the ratio of non-bridging oxygens to tetrahedral cations in the silicate melt (Chapter 4). After Righter et al. (1997).

that of Co. As Figure 11.11 shows, however, the partition coefficients for these elements converge at higher pressure. Using equation 11.23, Righter et al. (1997) found that they could explain the concentrations of siderophile elements Ni, Co, Mo, W, and P in the Earth's mantle if metal-silicate equilibration last occurred at 27GPa and 2200 K with an oxygen fugacity 0.15 log units lower than the iron-wüstite buffer. Interestingly, this pressure corresponds to the top of the upper mantle, i.e., the depth where perovskite first becomes stable. Li and Agee (1996) reached a remarkably similar conclusion based on independently determined partition coefficients for Ni and Co. Righter et al. found that value of X_S necessary to fit the predicted and actual mantle abundances of these elements is about 0.15, which corresponds to a sulfur concentration in the core of about 6%. This is distinctly higher than the S content estimated from cosmochemical considerations.

We saw in the previous section that Ga is apparently not depleted in the mantle beyond what can be explained by its volatility, suggesting it is not concentrated in the core. Since Ga is concentrated in iron meteorites, this is surprising. However, Righter and Drake (2000) demonstrated that the Ga partition coefficient is strongly dependent on T, P, and composition. At low pressure, the Ga will partition about equally between metal and silicate, but the partition coefficient decreases with pressure, such that it is less than 0.1 at pressures above 20 GPa. This explains the apparent contradiction. Asteroids are small bodies and their cores segregated at low pressure, hence Ga in the metal is expected. But if the Earth's core segregated at pressures above 20 GPa, we would expect it to contain relatively little Ga.

Whether an element's metal/silicate partition coefficient is greater or less than 1 effectively determines whether that element is siderophile or lithophile. For most elements, the partition coefficient is either greater or less than one under all reasonable conditions. For a few elements, however, the partition coefficient may be greater or less than one depending on T, P, and composition. Thus some elements may be lithophile under some conditions and siderophile (or chalcophile) under others. Let's consider two examples. The first is the case of Nb, which has traditionally been considered a strictly lithophile element since it is not found in metal phases of meteorites. Nb is also highly refractory; being both refractory and lithophile, we would expect its ratio to other such elements, such as Ta and La, to be chondritic in the bulk silicate Earth. However, Nb/Ta and Nb/La ratios in both the continental crust and upper mantle are distinctly lower than chondritic. To explain this Nb deficit, Rudnick et al. (2001) suggested Nb was sequestered in the deep mantle in rutile-rich refractory eclogites, produced by subduction and subsequent dehydration of oceanic crust. Partitioning experiments suggest an altera-

tive and simpler explanation. Wade and Wood (2001) found that Nb becomes siderophile (i.e., $D^{met/sil} > 1$) at 25 GPa when f_{O_2} is more than about 2.5 log units below the iron-wüstite buffer. Indeed, they found Nb partition coefficients were similar to those of V and Cr. As Figure 11.10 shows, these two elements are depleted in the mantle and hence likely present in the core (Table 11.04). The also found that the partition coefficient for Nb was an order of magnitude or so greater than that of Si. Thus, they argued, if Si is present in the core, Nb should also be present. At f_{O_2} 2 log units below the iron-wüstite buffer, which is thought to be appropriate for core formation, they found the Nb partition coefficient was about 0.47. This would reduce the silicate Earth Nb concentration by about 20%, or enough to explain the apparent Nb deficit.

A second element of great interest is potassium. Potassium is, of course, radioactive and therefore a source of energy. If it is present in the core, it could supply some or all of the energy needed to drive the geodynamo that sustains the Earth's magnetic field. The dynamo certainly requires energy to be sustained, but how much is unclear. One source of energy is the latent heat of crystallization released as the solid inner core crystallizes from the outer core. In some models of the dynamo, this would provide sufficient energy to drive the dynamo, but not in others. This has raised the question of whether one or more radioactive elements could be present in the core. Attention has focused on K because an iron-potassium-sulfide phase (djerfisherite) has been found in enstatite chondrites. Several experimental partitioning studies have been carried out as a result. In experiments at 1.5 GPa, Chabot and Drake (1999) found that K partitions into the metal phase only when S is present. Gessmann and Wood (2002) found that K partitioning depended strongly on the oxygen concentration (or the activity of FeO) of the metal sulfide liquid. The partition coefficient decreased with increasing pressure, although only modestly. Under the range of conditions and compositions explored, K was never strongly siderophile, but Gessmann and Wood (2002) suggested that the core could contain up 250 ppm K under the very restricted condition where the core is rich in both O and S. At this concentration, K would presently supply about 2×10^{12} W of power to the core (for reference, energy loss from the core is thought to occur at a rate of 5×10^{12} W or less). K is depleted in the silicate Earth relative to chondrites. As Figure 11.10 shows, most of this depletion is likely due to its volatility. However, K plots on the low side of the lithophile volatility trend in Figure 11.10, which would allow for some K in the core. Indeed, the core could contain up to 400 ppm K and still plot within the gray band of the volatility trend in Figure 11.11. We may say that the cosmochemical and experimental constraints allow, but do not require, up to 250 ppm or so K in the core, but that is considerably less than some geophysicists have argued for.

Some siderophile concentrations in the silicate Earth are difficult to explain by metal/silicate partitioning alone. Most notably, the noble metals (Ru, Rh, Pd, Re, Os, Ir, Pt, Au) are strongly and uniformly depleted in the silicate Earth compared to chondrites (Figure 11.10). That they are strongly depleted is not surprising: experiments show these elements are highly siderophile with low-pressure metal/silicate partition coefficients in the range of 10^3 to 10^5. Given the large range of partition coefficients, it is surprising that these elements are so uniformly depleted in the mantle. The uniform nature of this depletion is emphasized by $^{187}Os/^{188}Os$ ratios in the mantle. The $^{187}Os/^{188}Os$ ratio of the modern mantle is effectively identical that of chondrites, suggesting the bulk silicate Earth has a Re/Os ratio that is within a few percent of chondritic. This requires that the partition coefficients of Re and Os be nearly identical. While some partition coefficients do tend to converge at high pressure, it seems improbable that the partition coefficients of these elements could be so similar.

One commonly invoked solution to this dilemma is the addition of a "late accretionary veneer" to the Earth after the core had segregated (Kimura et al. 1974). The idea is that after the core had completely segregated, a small amount of chondritic material continued to accrete to the Earth. To understand the effect of this, imagine that after core segregation, the noble metal concentrations in the mantle reflect metal/silicate equilibrium. This would leave concentrations that are 10^3 to 10^5 times lower than chondritic. Now image that 0.5% of chondritic material is added. This would raise the concentrations of all these elements in the mantle to just over 0.5% of chondritic. This readily explains why the abundances of these elements in the mantle range from 0.006 to 0.008 times chondrites.

In summary, there is very little we know with absolute certainty about the Earth's core. Nevertheless, it is possible to make a variety of inferences about its composition and formation through geophysical, cosmochemical, and experimental approaches. Our knowledge about the core is, however,

hardly static. Beyond the fundamental geophysical inferences of the late nineteenth and early twentieth century, much of what we have learned about the core has come in the few decades. Future studies will likely greatly refine our knowledge of the core.

11.5 Mantle Geochemical Reservoirs

Up to this point, we have considered the mantle as a uniform body of rock. There is, however, a very considerable body of evidence that the mantle is quite heterogeneous and that this heterogeneity has developed over geologic time, probably through geologic processes similar to those still occurring today. The *prima fascia* evidence of this is isotopic variations in oceanic basalts, first discovered in the 1960's (e.g., Hedge, 1966). The significance of radiogenic isotope ratios is that they are not changed by the processes of magma genesis. Thus isotopic variations in basalts implied isotopic variation in their mantle sources. Those isotopic variations in turn must result from long-standing variations in the ratios of radioactive parent to radiogenic daughter elements. Much of the present research in mantle geochemistry focuses on just what processes might have produced these chemical variations. Before we consider that questions, let's first review the evidence for heterogeneity in the mantle. We'll begin by considering evidence from oceanic basalts.

11.5.1 Evidence from Oceanic Basalts

Isotopic variations in basalts, which are partial melts of the mantle, provide clear evidence that the mantle is presently heterogeneous. Oceanic basalts provide better evidence of this than continental basalts because the possibility of the latter being contaminated by the crust through which they pass is much reduced. This is true for 3 reasons: oceanic crust is much thinner, it has a higher solidus, and it is compositionally similar to melts of the mantle (so that when assimilation does occur, its chemical affects are minimized). Of course, not all continental basalts are necessarily contaminated, nor is there a guarantee that all oceanic basalts have not been.

Let's first consider the isotopic evidence. The fundamental isotopic variation in oceanic basalts is between basalts erupted at mid-ocean ridge (mid-ocean ridge basalts or MORB) and those erupted on oceanic island volcanoes (oceanic island basalts or OIB). Table 11.05 and Figures 11.12 and 11.13 illustrate the differences in isotopic composition between these two groups. Although the data overlap considerably, MORB

Table 11.05. Statistical Summary of the Isotopic Composition of Oceanic Basalts

		MORB	OIB
$^{87}Sr/^{86}Sr$			
	Mean	0.70287	0.70370
	Mode	0.70280	0.70319
	Median	0.70279	0.70349
	S. D.	0.00045	0.00089
	S. D. %	0.06%	0.13%
	Skewness	1.76	1.44
	n	2135	3224
ε_{Nd}			
	Mean	8.67	4.96
	Mode	9.98	6.28
	Median	9.22	5.37
	S. D.	2.29	2.69
	S. D. %	26.41%	54.23%
	Skewness	-1.69	-0.7
	n	1678	2580
$^{206}Pb/^{204}Pb$			
	Mean	18.45	18.97
	Mode	18.29	18.87
	Median	18.40	18.89
	S. D.	0.423	0.75
	S. D. %	2.29%	3.95%
	Skewness	0.326	1.22
	n	1495	2581
$^{3}He/^{4}He$ (R/R_A)			
	Mean	8.81	12.24
	Mode	8.1	8.2
	Median	8.1	11.8
	S. D.	2.538	4.88
	S. D. %	28.81%	39.87%
	Skewness	1.053	4.88
	n	573	759

on average have lower $^{87}Sr/^{86}Sr$ and $^{206}Pb/^{204}Pb$ and higher ε_{Nd} than OIB. The difference in mean isotopic composition is only part of the story, however. The isotopic compositions of MORB are also considerably more uniform than those of the OIB, as is apparent from the statistics in Table 11.05. The relative variance, as measured by the standard deviations, is about half as great for MORB as for OIB. This implies that MORB are derived from a more uniform source than are OIB. Another interesting feature is that both the MORB and OIB data are skewed towards higher $^{87}Sr/^{86}Sr$, $^{206}Pb/^{204}Pb$, and $^{3}He/^{4}He$ and lower ε_{Nd}. Statistical tests (Student T-test and F-test) demonstrate that the MORB and OIB means and variances of each isotope ratio differ significantly to a high degree of confidence. Consequently, we can conclude that MORB and OIB represent two distinct populations and are derived from two distinct mantle reservoirs.

There are some inter-oceanic differences in the composition of MORB. The Pacific has the lowest $^{87}Sr/^{86}Sr$ ratios, the Atlantic the highest $^{143}Nd/^{144}Nd$ ratios and the Indian the lowest $^{206}Pb/^{204}Pb$ ratios. Thus the variation is not systematic in the sense of MORB from one ocean being more depleted than those from another. Another difference is that isotopic compositions in Pacific MORB are more uniform than those from other oceans. Some MORB, particularly those from ridge segments near oceanic islands (e.g., the Mid-Atlantic Ridge near the Azores and Iceland; the Galapagos Spreading Center near the Galapagos, etc.), have geochemical characteristics similar to OIB, something first demonstrated by the pioneering work of Jean-Guy Schilling (e.g., Schilling, 1973). If these MORB are excluded, the difference between MORB and OIB is greater. For example, by eliminating the 276 samples in this category, the mean MORB ε_{Nd} increases to 9.23, close to the median of the entire data set. The data also

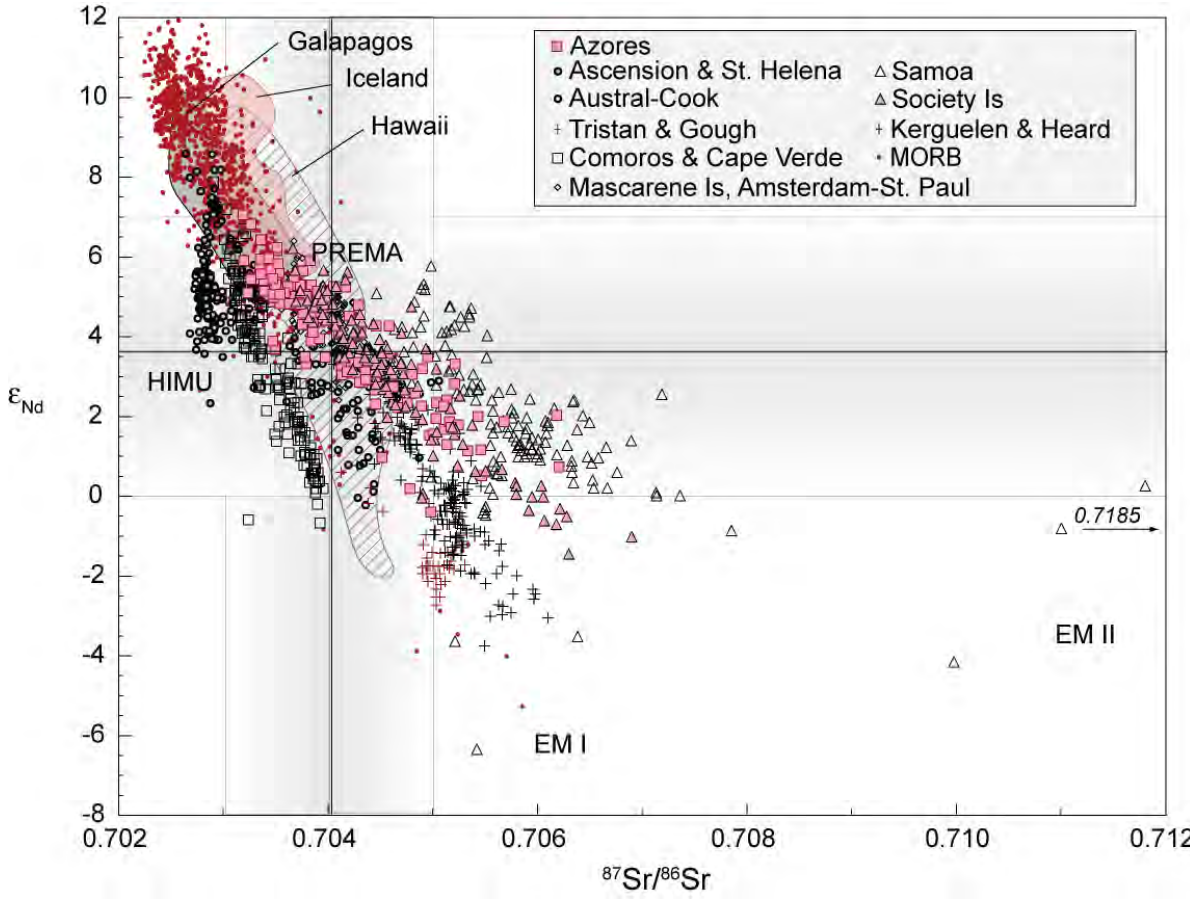

Figure 11.12 ε_{Nd} vs. $^{87}Sr/^{87}Sr$ in MORB and selected OIB. Horizontal and vertical lines indicate Nd and Sr isotopic compositions, respectively, of the bulk silicate Earth estimated in section 11.3.3. Gray background is meant to suggest the uncertainty in these estimates.

show considerably less dispersion, with the standard deviation dropping from 2.3 to 1.7, and are less skewed, the skewness changing from -1.7 to -0.8. This suggests that the mantle supplying melt to oceanic island volcanoes also supplies melt to mid-ocean ridges near these volcanoes.

In Figure 11.12, MORB typically plot at higher ε_{Nd} and lower $^{87}Sr/^{86}Sr$ and than the estimated composition of bulk silicate Earth, while the opposite is true of OIB. These ratios imply that the mantle that gives rise to MORB magmas, the "MORB source" has low time-integrated Rb/Sr and high Sm/Nd ratios. Since Rb and Nd are more incompatible than Sr and Sm, respectively, we infer that the MORB source is relatively depleted in incompatible elements. From this we can conclude that the mantle source of most MORB experienced depletion in incompatible elements while the sources of many OIB have experienced enrichment in incompatible elements. Interestingly, many of the OIB arrays in Figure 11.12 appear to converge near the estimated bulk silicate Earth composition. This may also be true of ε_{Nd} vs $^{206}Pb/^{204}Pb$ in Figure 11.13. There is greater uncertainty about the Pb isotopic composition of the bulk silicate Earth than for the Sr and Nd isotopic composition. However, the concentrations in Table 11.03 suggests the Earth has $^{206}Pb/^{204}Pb$ in the range of 18.25 to 18.45, $^{207}Pb/^{204}Pb$ of 15.51 to 15.62, and $^{208}Pb/^{204}Pb$ of 37.86 to 38.05 assuming the Earth is 4.45 Ga old.

Figure 11.14 shows He isotope ratios (in R/R_A units: see Chapter 8) in OIB plotted against ε_{Nd}. The highest $^3He/^4He$ ratios are associated with ε_{Nd} in the range of +4 to +8. ^4He is, of course, produced by α-day of U and Th. Any part of the mantle undergoing partial melting would likely suffer loss of He. Unlike other incompatible elements, which could be recycled into the mantle, He in partial melts would subsequently be lost to the atmosphere and then from the Earth. Consequently, mantle that has melted in the past should have lower $^3He/^4He$ than primitive mantle. Thus the relationships in Figure 11.14 are consistent with the idea that the most primitive regions of mantle have ε_{Nd} of about +4 to +8.

A number of papers have pointed out the convergence of OIB isotopic arrays around intermediate values and that these OIB have particularly high $^3He/^4He$. This "common" component has variously been called PREMA (Zindler and Hart, 1986, PHEM, Farley et al., 1992, FOZO (Hart et al., 1992), and 'C' Hanan and Graham (1996). Under the old assumption of an Earth that had chondritic abundances of refractory lithophile elements, the ε_{Nd} of this component was too high for this to be primitive mantle.

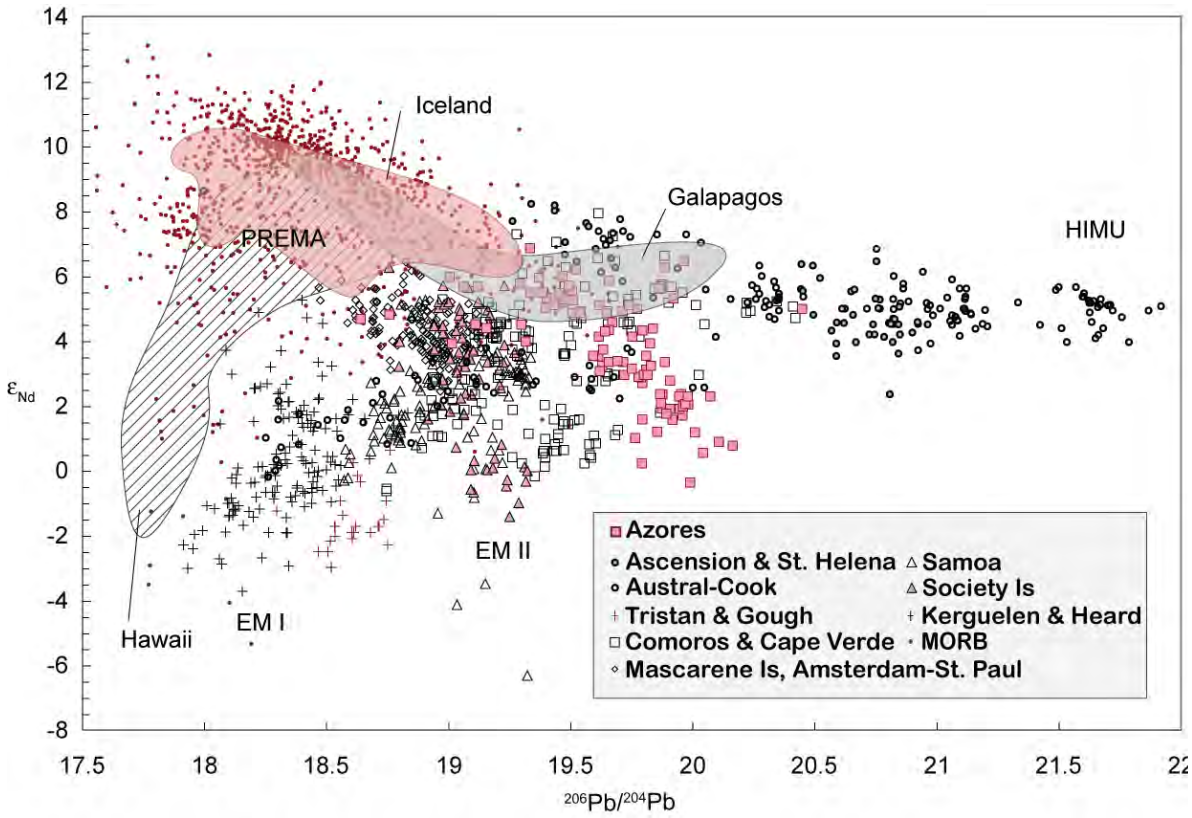

Figure 11.13. ε_{Nd} vs $^{206}Pb/^{204}Pb$ in mid-ocean ridge basalts (MORB) and selected oceanic island basalts (OIB) from the PetDB and GEOROC databases.

However, using the revised bulk silicate Earth composition in Section 11.3.3, it would appear that this component is indeed something close to primitive mantle and, as suggested by Hanan and Graham (1996), may be common to many plumes.

Figure 11.15 illustrates the difference between MORB and OIB in rare earth elements. Relative to chondrites, the light rare earths in MORB are underabundant compared to the heavier rare earths. i.e., MORB are light rare earth-depleted. Part of this reflects the fact that the Earth itself appears to be slightly light rare earth-depleted compared to chondrites (as evidenced by its higher than chondritic $^{142}Nd/^{144}Nd$). However, average MORB are still slightly light rare earth-depleted relative to the bulk Earth composition listed in Table 11.03. The easiest way to produce such depletion in the mantle is to extract a melt from it. The incompatible elements, including the light rare earths, partition preferentially into the melt leaving a residue depleted in LRE. When the mantle melts again, the basalt produced will inherit this light rare earth depletion (though the basalt will not be as light rare earth-depleted as its mantle source). Thus the mantle source of mid-ocean ridge basalts appears to have suffered melt extraction in the past.

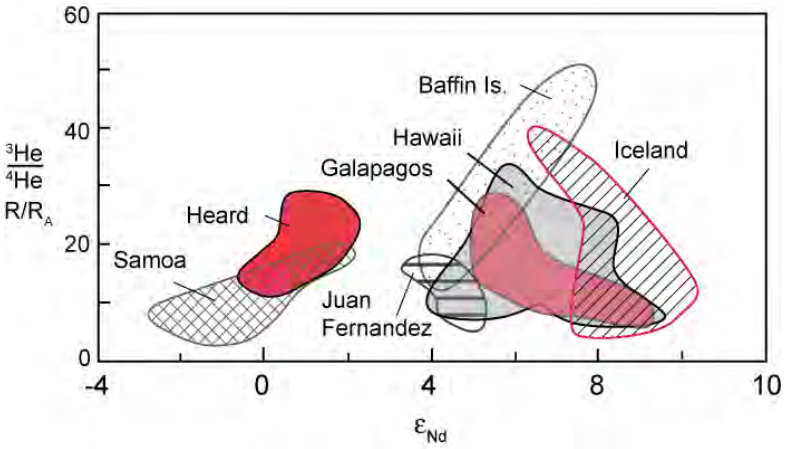

Figure 11.14. $^3He/^4He$ vs. ε_{Nd} in some OIB and Tertiary basalts from Baffin Island in the Canadian Arctic. The latter are thought to be produced by the Iceland mantle plume. Modified from Ellam and Stuart (2004) with data from the GEOROC database.

OIB are light rare earth-enriched to varying degrees. Part of the difference in rare earth patterns of MORB and OIB may be due to the smaller degrees of melting involved in the generation of some, and perhaps most, OIB magma. Many, though by no means all, OIB are alkalic, whereas almost all MORB are tholeiitic. Alkali basalts are produced by smaller degrees of melting than tholeiites. The relatively large extents of melting that generate MORB probably reflect their generation where lithosphere is thin or non-existence. This allows mantle to rise to very shallow depth, allowing high extents of melting (Chapter 7). On the other hand, there is fairly strong evidence, based ultimately on olivine-melt geothermometry (Chapter 4), that mantle plumes are hotter than the mantle beneath mid-ocean ridges, which, of course, favors higher degrees of melting (Herzberg et al, 2007, Putrika et al., 2007). Consequently, not all the differences in rare earth patterns between OIB and MORB

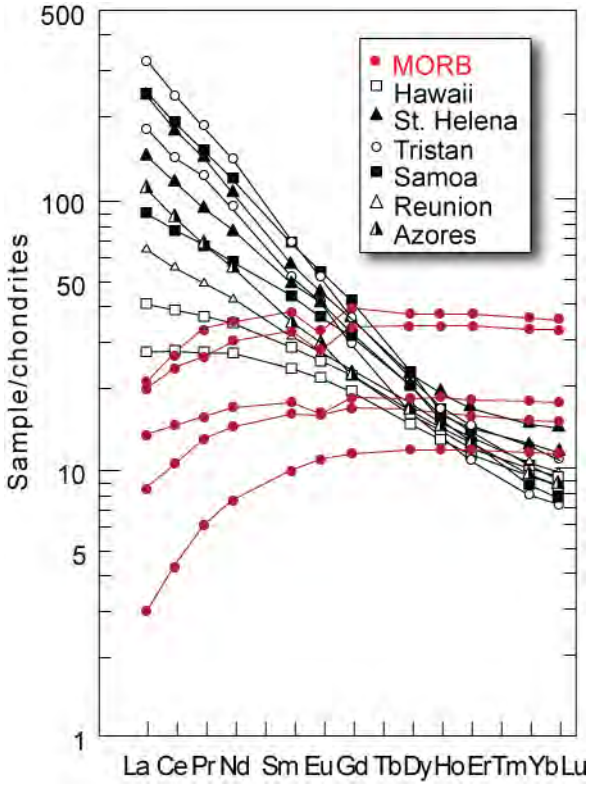

Figure 11.15. Rare earth patterns of mid-ocean ridge basalts and oceanic island basalts.

can be attributed to degree of melting — there must also differences in the rare earth abundances in the mantle sources of these magmas.

We conclude that MORB and OIB are derived from distinct mantle "reservoirs". Deciphering the physical properties of these reservoirs, where they are located, their size, and how they have evolved is more difficult. At one extreme, these two reservoirs might coexist as different lithologies in the same volume of mantle. As we discuss below consensus view, however, is that MORB are derived from the shallow mantle, while oceanic island basalts are derived from deep mantle carried to the surface by rising mantle plumes. This reservoir is often called the "depleted mantle" or the "depleted MORB mantle" (DMM). As explained below, oceanic island basalts are thought to be derived from mantle plumes, which are columns of buoyant mantle that rise from the deep mantle. If this is the case, the OIB produced by melting of these plumes provide insights into the composition of the deep mantle.

11.5.2 Evolution of the Depleted MORB Mantle

MORB is easily the most abundant magma type on Earth — this magma forms the entire oceanic crus, produced at a rate of about 3 km^3/yr. This suggests the source of MORB, DMM, is a major reservoir, if not the major reservoir, in the mantle. This observation immediately inspires several questions. Where it is located? How has it evolved? How big is it? We consider these questions in the following paragraphs.

There are some fairly straightforward reasons for this thinking MORB come from the shallow mantle and OIB from the deep mantle. MORB are by far the most abundant volcanic rocks on the Earth and they are also compositionally the most uniform. This kind of basalt is erupted, with a few exceptions, wherever plates are moving apart. This is most easily explained if the MORB source is relatively close to the surface. Furthermore, the pull of subducting lithospheric slabs has been shown to be the primary force acting on lithospheric plates. Upwelling of mantle beneath mid-ocean ridges appears to be largely a passive response to the plate motion induced by this "slab-pull". Again, this suggests that the DMM is located in shallow mantle, specifically the asthenosphere, the region characterized by relatively low seismic velocities (Figure 11.03) just beneath the lithosphere.

The incompatible element-depletion that we can infer for the DMM from both the trace element and isotopic composition of MORB is most easily explained by extraction of partial melts from it, which carried away the incompatible elements. Where have these melts gone? To form the oceanic and continental crusts, both of which are created by magmatism and are incompatible element-enriched. Of these, the continental crust is by far the more significant reservoir of incompatible elements. The oceanic crust is less enriched in incompatible elements and furthermore is temporary. It survives less than 100 million years on average before being subducted back into the mantle. We can use isotopic compositions to make a simple first order estimate of the volume of the DMM if we assume that it is the only incompatible element-depleted reservoir and that the continental crust is the only complimentary incompatible element-enriched reservoir.

This is essentially a mass balance problem among a number of reservoirs, so, following DePaolo (1980) we begin by writing a series of mass balance equations. The first is mass of the reservoirs:

$$\sum_j M_j = 1 \qquad 11.24$$

where M_j is the mass of reservoir j as a fraction of the total mass of the system, in this case the silicate Earth. We can also write a mass balance equation for any element i as:

$$\sum_j M_j C_j^i = C_0^i \qquad 11.25$$

where C_o is the concentration in the silicate Earth. For an isotope ratio, R, of element i, or for an elemental ratio of which element i is the denominator, the mass balance equation is:

$$\sum_j M_j C_j^i R_j^i = C_0^i R_0^i \qquad 11.26$$

Our problem assumes the existence of 3 reservoirs: the continental crust, the mantle depleted by crust formation, and the undepleted, or primitive, mantle, which constitutes the remainder of the man-

tle (we explicitly ignore oceanic island basalt reservoirs and continental lithosphere in this calculation). These mass balance equations can be combined to solve for the mass ratio of depleted mantle to continental crust.

$$\frac{M_{DM}}{M_{CC}} = \frac{C^i_{CC}}{C^i_0}\frac{\left(R^i_{cc} - R^i_{DM}\right)}{R^i_0 - R^i_{DM}} - 1 \qquad 11.27$$

where the subscripts *DM* and *CC* refer to depleted mantle and continental crust respectively. A number of solutions to the mass balance equations are possible; we want an expression based on values that are relatively well constrained. Isotopic composition of mantle reservoirs are well constrained because the magmas they produce have the same isotopic composition, but this is not true of elemental concentrations. We do have good estimates of concentrations in the crust because great numbers of samples can be taken and an average value computed (section 11.6.2). (Once we have solved for the mass of depleted mantle, however, it would be straightforward to solve for the depleted mantle concentration.)

The Nd isotope system is perhaps best suited for this question since $^{142}Nd/^{144}Nd$ ratios constrain the Nd isotopic composition of the Earth and, being a refractory lithophile element, its concentration in the bulk silicate Earth is also constrained (though not precisely). The Nd concentration and the Sm/Nd ratio of the continental crust are also better constrained than many other elements. The Sm/Nd ratio and $^{143}Nd/^{144}Nd$ of the crust are related through isotopic evolution, specifically:

$$^{143}Nd/^{144}Nd = (^{143}Nd/^{144}Nd)_0 + ^{147}Sm/^{144}Nd(e^{\lambda t} - 1) \qquad 11.28$$

Because the half-life of ^{147}Sm is long compared to the age of the Earth and because we do not need the level of precision necessary for geochronology, we can linearize this equation as:

$$^{143}Nd/^{144}Nd = ^{143}Nd/^{144}Nd_0 + ^{147}Sm/^{144}Nd\lambda t \qquad 11.29$$

The continental crust is certainly not of a single age, i.e., it was not created a at single time *t*. However, because it is linear, this equation remains valid for an average crustal age, *T*. Hence we may write:

$$(^{143}Nd/^{144}Nd)_{CC} = (^{143}Nd/^{144}Nd)^T_{PM} + (^{147}Sm/^{144}Nd)_{CC}\lambda T \qquad 11.30$$

where the superscript *T* denotes the value at time *T*. The $^{143}Nd/^{144}Nd$ value of the primitive mantle can be calculated at any time from the present-day $^{143}Nd/^{144}Nd$ and $^{147}Sm/^{144}Nd$ of primitive mantle. The $^{143}Nd/^{144}Nd$ of the continental crust calculated in 11.30 can then be used in equation 11.27 to calculate the mass fraction of depleted mantle.

Now let's assign some values to these equations. The mass of the continental crust as a fraction of the mass of the silicate Earth, $M_{CC,}$ is about 0.0055. For the $^{143}Nd/^{144}Nd$ value of the depleted mantle, we'll chose 0.51310 (equal to the median value for MORB listed in Table 11.05, $\varepsilon_{Nd} \approx +9$). Based on assessments of the composition of continental crust (section 11.6.2), a good estimate for the $^{147}Sm/^{144}Nd$ ratio of the continental crust is 0.123. We can use these values to calculate the mass of depleted mantle as a fraction of the silicate Earth as a function of the other parameters in equation 11.27, namely the ratio of Nd concentration in the crust to primitive mantle, C_{CC}/C_0 the average age of the continents, *T*, and the $^{143}Nd/^{144}Nd$ of the silicate Earth (expressed in epsilon units). Figure 11.16 shows the results. A good estimate of C_{CC}/C_{PM} is about 19, but there is considerable uncertainly. A good estimate of *T* is about 2 Ga, but there is easily 10% uncertainty in this value. If the Sm/Nd ratio is chondritic, Figure 11.16 suggests that the depleted mantle constitutes 40% or less, and more likely only about 25% of the mantle. However, the $^{142}Nd/^{144}Nd$ of terrestrial materials suggests the Sm/Nd ratio is non chondritic. That result tended to favor 2-layer convention models, and implied only the mantle above the discontinuity was involved in crust production. If the terrestrial Sm/Nd ratio is 3% greater than chondritic, corresponding to the composition listed in Table 11.03, then the ε_{Nd} value of the Earth is +3.6 and the depleted mantle constitutes 40 to 60% of the mantle. If the Sm/Nd ratio of the Earth is 6% greater than chondritic, as Caro and Bourdon (2010) argue, then the ε_{Nd} of the Earth is +6.9, then the mantle depleted by crust extraction constitutes at least 70% of the entire mantle and possibly all of it.

This is quite a different picture of the mantle from the one of 30 years or so ago. Mass balance models based on the assumption that the Earth has chondritic Sm/Nd and therefore $\varepsilon_{Nd} = 0$ suggested the depleted mantle occupied only the mantle above the 660 seismic discontinuity, i.e., the upper mantle (e..g., Jacobsen and Wasserburg, 1979). This suggested this discontinuity was a barrier to mass transport across it and that separate convection systems existed above and below it (so-called two-layer convection). This became difficult to reconcile with subsequent tomographic imagery of the Earth's interior showing subducted oceanic lithosphere penetrating through the discontinuity. In this respect, a non-chondritic Earth is more consistent with seismic evidence and geodynamic models. It implies that nearly the entire mantle convects and participates in continent creation and the plate tectonic cycle.

11.5.2 Evolution of Mantle Plume Reservoirs

Oceanic island volcanism, in contrast to mid-ocean ridge volcanism, appears to be the result of mantle upwelling from great depth. To begin with, as Wilson (1963) pointed out long ago, the locus of active volcanism in oceanic volcanic chains remains approximately fixed for periods as long as 100 million years, indicating that this upwelling rises from depths beneath the convection associated with plate motions. More recently, seismic imaging has shown columns of low seismic velocity, suggesting hot temperatures, that extend, in some cases, to the base of the mantle beneath many oceanic islands (e.g., Montelli et al., 2004). Furthermore, broad topographic swells, suggestive of dynamic mantle upwelling, are associated with some oceanic islands chains, most spectacularly with Hawaii. All this is consistent with Morgan's (1971) idea that oceanic island volcanoes are produced by plumes of hot mantle rising from near the core-mantle boundary. Finally, the volume of oceanic island volcanism is much smaller than mid-ocean ridge volcanism; it would be easier to poke a few plumes though the depleted MORB mantle (the asthenosphere) than to get a lot depleted MORB mantle through an OIB-source upper mantle that only rarely

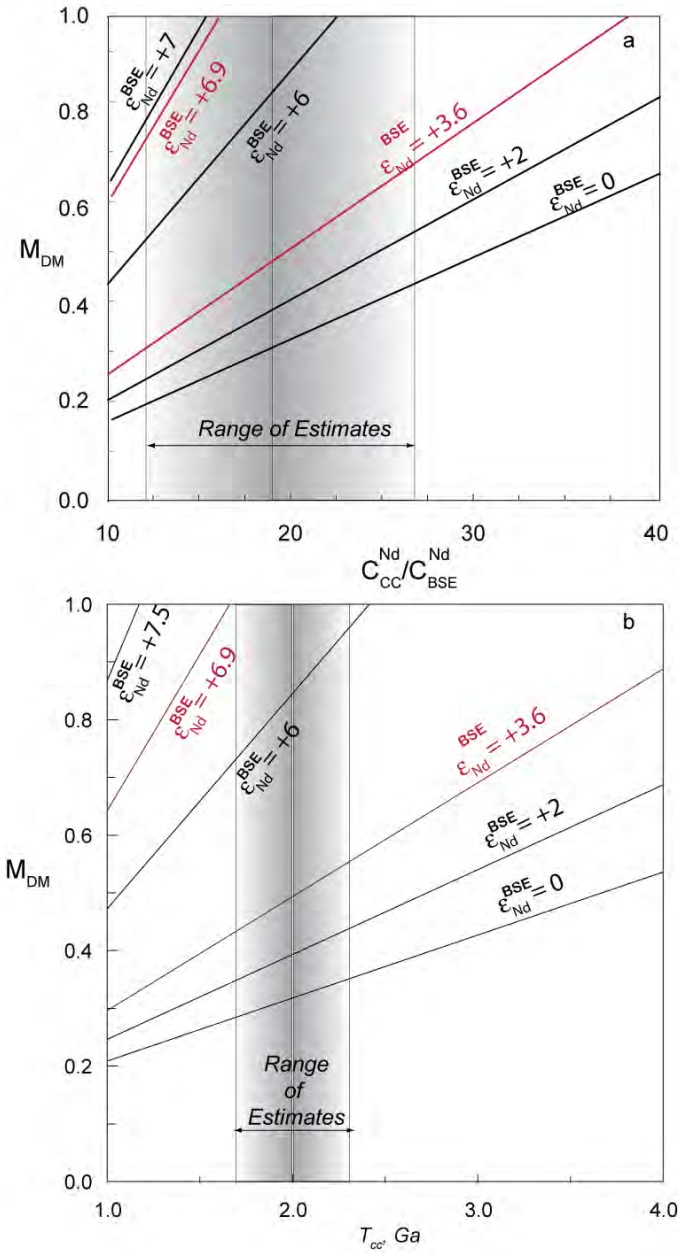

Figure 11.16. Mass fraction of the depleted mantle (DMM) calculated from equation 11.27. Top graph shows this for a variety of values of ε_{Nd} for the silicate Earth and a range of C_{CC}/C_{PM} assuming an average age of the continents of 2 Ga. Lower graph shows the same thing for $C_{CC}/C_{PM} = 19$ and a range for the average age of the continents.

melts. Although alternative models have been proposed, here we adopt the consensus viewpoint that OIB derived from mantle plumes, which rise from the deep mantle.

Let's now consider the evolution of these mantle reservoirs. As the preceding discussion shows, the geochemistry of OIB is more variable than that of MORB. As discussed above, primitive mantle could be a component of many plumes, but the diversity of isotopic compositions in Figures 11.13 and 11.14 clearly requires a variety OIB mantle sources with distinct chemical histories. Although there are many mantle plumes and each is to some degree geochemically unique, there appear to be a much smaller number of geochemical reservoirs from which they are drawn. These groups, named *St. Helena, Kerguelen, Society*, and *Hawaii* for a type island by White (1985) and HIMU (high U/Pb), EM I (Enriched Mantle 1), EM II (enriched mantle 2) and PREMA (prevalent mantle) by Zindler and Hart (1986), show distinctive correlations between isotope ratios or have distinctive isotopic compositions. For example, OIB of the St. Helena group, which encompasses the Austral Islands (Pacific) and Ascension (Atlantic) as well as St. Helena (Atlantic), have Sr and Nd isotope ratios that plot below the main array in Figure 11.13, and their Pb isotopic compositions are very radiogenic (Figure 11.14). Indeed, all basalts with very radiogenic Pb ($^{206}Pb/^{204}Pb > 20$) plot within or close to the St. Helena field on a Sr-Nd isotope diagram. Similarly, islands of the Society group, which include the Azores (Atlantic), the Marquesas (Pacific), and Samoa (Pacific) as well as the Societies (Pacific), define a shallower Sr-Nd isotope correlation than do basalts from Kerguelen group islands, which include Tristan da Cunha (Atlantic), and Juan Fernandez (Pacific) as well as Kerguelen (Indian). The Kerguelen group OIB always have less radiogenic Pb than the Society group. To these groups, an additional one could perhaps be added, those represented by the Comoros and Cape Verde Islands. These islands form a separate array beneath the main one in Figure 11.13. Hart et al. (1986) called this the LOND array (for low-Nd).

Is there some aspect of the chemistry of OIB that might betray their evolutionary histories and parallel the isotopic differences discussed in the preceding paragraph? Figure 11.17 compares the incompatible element abundances in MORB and typical OIB alkali basalt in a *spider diagram*, in which elements are ordered according to their incompatibility and normalized to primitive mantle values. This kind of plot is also sometimes referred to as an *extended rare earth plot*. Melts will be enriched, and residual solids depleted, in elements on the left. The spider diagrams suggest complex histories of enrichment and depletion, but, with some exceptions, most notably Pb, an element's enrichment is related to its compatibility. Melting in the lower mantle, because it would involve minerals with very different structures, would create patterns of enrichment and depletion quite different from those in Figure 11.17 (e.g., Corgne et al., 2005, Kato et al., 1988). Thus while plumes may come from the deep mantle, they carry chemical signatures created in the upper mantle. This is a very important inference indeed.

Weaver (1991) suggested EMI, EMII, and HIMU basalts could be distinguished based on their trace element geochemistry. However, Willbold & Stracke (2006) found that while HIMU basalts can indeed be distinguished from EM basalts, there are no systematic differences between EMI and EMII. They found that HIMU have lower Rb/Sr, Ba/La, K/La, Th/U, Pb/Ce, and higher U/Pb, Lu/Hf, and Nb/Rb than EM basalts. The distinctions identified by Willbold & Stracke (2006) can be seen to some degree in Figure 11.16. Most oceanic basalts display negative Pb anomalies (the continental crust and island arc volcanic typically have positive Pb anomalies), but they are smaller for the EM basalts, and the Samoan example actually has a slightly positive Pb anomaly. HIMU basalts, exemplified in Figure 11.16 by the St. Helena sample, are enriched in Nb and Ta relative to K and Rb, have particularly strong depletion in Pb. The HIMU basalts also show a decrease in normalized abundance with increasing incompatibility for elements more incompatible than Nb.

Determining how these distinct geochemical reservoirs have evolved is among the most vexing problems in mantle geochemistry. The principal observation to be explained is that mantle plumes invariably have less depleted isotopic signatures than MORB, and the isotopic compositions of some indicate net enrichment in incompatible elements. As we discussed in the previous section, the convergence of several OIB arrays around isotopic compositions close to those expected of primitive mantle in Figures 11.13 through 11.15 suggests primitive mantle could indeed be a component of at least some plumes. However, these same arrays indicate that in most cases an incompatible element-enriched component must also be present.

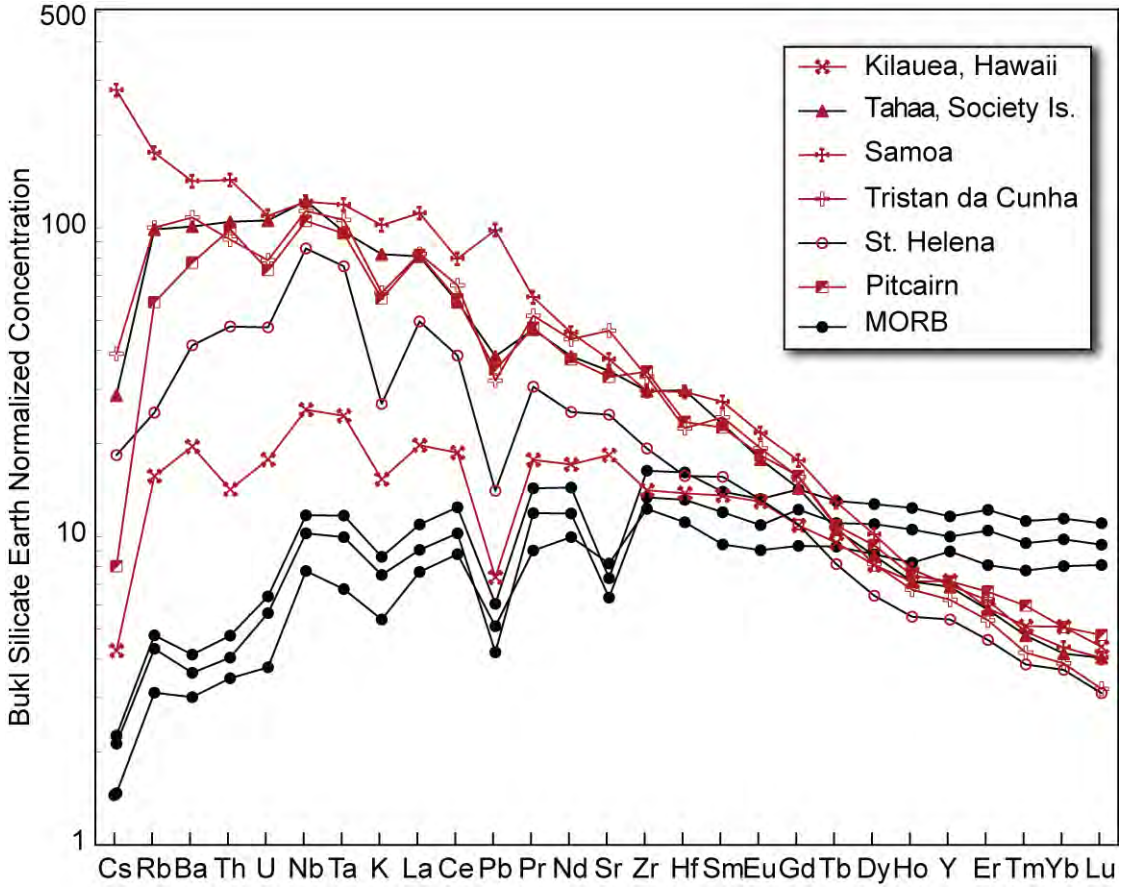

Figure 11.17. "Spider diagram" displaying concentrations of trace elements normalized to the bulk silicate Earth values in Table 11.3 and ordered by increasing compatibility. The plot shows representative patterns for MORB, Hawaii, St. Helena (HIMU), Tristan da Cunha and Pitcairn (EM I) and Samoa and the Society Is. (EM II). Modified from White (2010).

Hofmann and White (1982) suggested mantle plumes obtain their unique geochemical signature through deep recycling of oceanic crust. This idea is illustrated in the cartoon shown in Figure 11.18. Partial melting at mid-ocean ridges creates oceanic crust that is less depleted in incompatible elements than the depleted upper mantle. The oceanic crust is inevitably subducted back into the mantle (we know this because almost no ancient oceanic crust is preserved at the surface). The question is what becomes of it then? Hofmann and White noted that once oceanic crust reaches depths of about 90 km it converts to eclogite that is denser than peridotite. Because it is rich in Fe, and garnet-forming components, it remains denser than peridotite at all depths greater than 90 km (except, perhaps, just at the 660 discontinuity due to the negative Clapeyron slope). Thus it could potentially sink to the base of the mantle. This is indeed what some seismic tomographic images of the mantle appear to show. Hofmann and White originally suggested radioactive heating would ultimately cause it to become buoyant. It now seems more likely that heat conducted from the core may be more important. Indeed, Sleep (1989) and Davies (1989) calculated that mantle plumes carry to the surface roughly the amount of heat expected to be lost from the core. Upon sufficient heating, the subducted material becomes buoyant and rises. As it reaches depths of less than 200 km, decompression melting begins and the resulting magmas form chains of intraplate volcanoes.

An alternative origin for enriched mantle plume reservoirs was proposed by McKenzie and O'Nions (1983). They noted the common evidence for incompatible element enrichment in the subcontinental lithosphere (which we discuss in the next section) and suggested under certain circumstances, such as

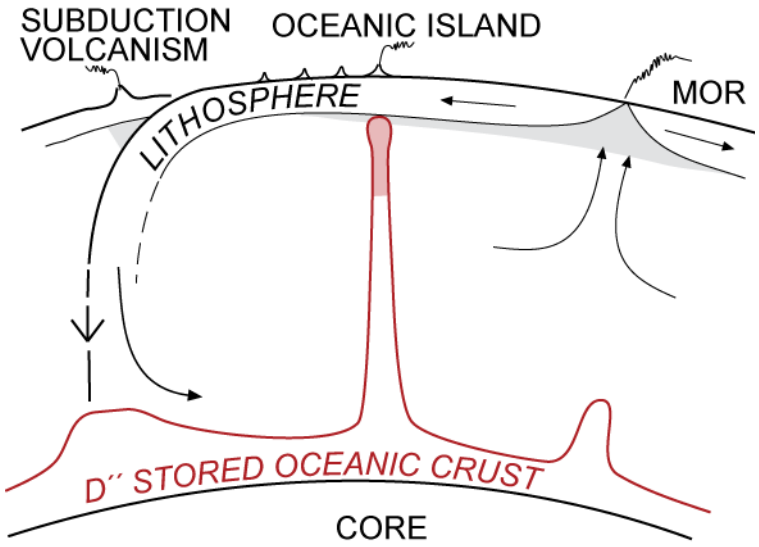

Figure 11.18. Cartoon illustrating the oceanic crustal recycling model of Hofmann and White (1982). Oceanic crust is transformed into eclogite and post-eclogite assemblages upon subduction. It separates from the less dense underlying lithosphere and sinks to the deep mantle where it accumulates. Eventually, it becomes sufficiently hot to form plumes that rise to the surface, producing oceanic island volcanism. After Hofmann and White (1982).

continent-continent collisions, this lithosphere may occasionally detach or "delaminate" from the crust above it. Because it is cold, it would also sink to the deep mantle. As in the case of the Hofmann and White model, it would be stored at the base of the mantle where it is heated by the core, eventually rising to form mantle plumes. Because mantle plumes come in several geochemical varieties, it is possible that both mechanisms operate.

Indeed, other as yet unknown processes may be involved as well. Two other processes that appear to result in the transport of incompatible element-enriched crust into the mantle are subduction erosion (von Huene et al., 1991) and lower crustal floundering, also called, somewhat inaccurately, delamination (Kay and Kay, 1991; Kay et al., 1994). There is considerable geologic evidence that in sediment-starved subduction zones, such as the Peru-Chile margin, the subducting oceanic crust can abrade and ultimately significantly erosion the overriding continental plate from below. There is also some geochemical evidence that this has occurred in Central America (Goss and Kay, 2005). In regions where compression thickens continental crust, there is evidence that the lowermost crust can sink into the mantle. Again, the Peru-Chile margin provides and example where the convergence with the Nazca plate has greatly thickened the South American plate, creating the Andes. The crust here is so thick that the lowermost crust is converted to eclogite, which is denser than mantle peridotite. This eclogitic lower crust can then sink into the mantle, as some seismic imaging appears to show (McGashen et al., 2008).

Workman and Hart (2004) suggested yet another alternative, namely that the enriched component in EM II type OIB was metasomatized oceanic lithosphere. In both the McKenzie and O'Nions and Workman and Hart hypotheses, lithosphere is enriched as small-degree melts percolate into it from below. The volume of melt is small, so it never reaches the surface. Instead it freezes in or reacts with, cold lithosphere. As we will see in the next section, there is indeed some evidence from xenoliths that such *metasomatism* occurs. However, recent studies have shown that the Os isotope composition of the subcontinental lithosphere is quite distinctive, and quite different from that of mantle plumes, as we shall see in the next section. This rather strongly suggests that "delaminated" subcontinental lithosphere does not contribute to mantle plumes.

There is also a geographic pattern to both the distribution of mantle plumes and their isotopic compositions. Mantle plumes appear to be preferentially located within regions of slow lower mantle seismic velocities, as may be seen in Figure 11.19. There are two areas where isotopic compositions are particularly extreme (e.g., high $^{87}Sr/^{86}Sr$), one in the southeastern Indian Ocean and South Atlantic, the other in the central South Pacific (Hart, 1984; Castillo, 1989). The anomaly in the Indian Ocean is called the DUPAL anomaly, while that in the South Pacific is called the SOPITA anomaly. Interestingly enough, both anomalies close to regions where lower mantle seismic velocities are particularly slow

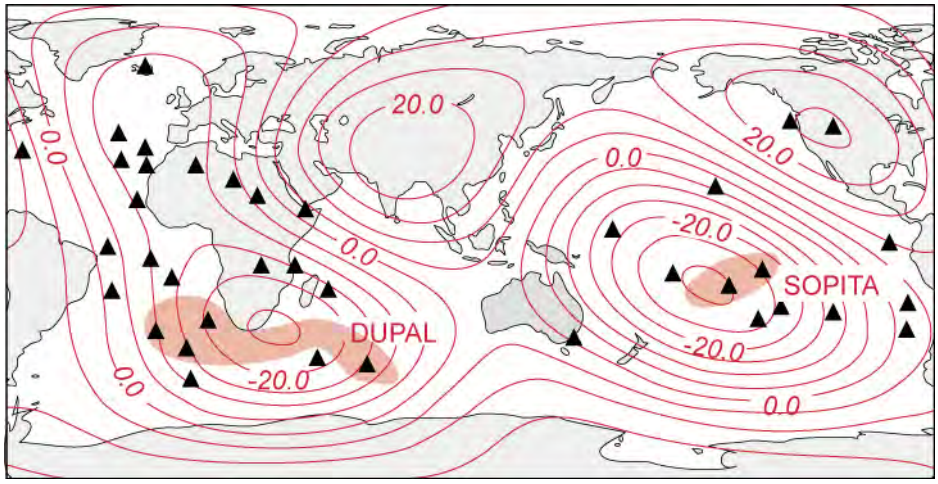

Figure 11.19. Map showing the distribution of mantle plumes (triangles), P-wave velocity anomalies (m/sec) averaged over the whole lower mantle (red lines), and location of the DUPAL and SOPITA isotope anomalies (pale red regions). Mantle plumes are located in regions of slow lower mantle seismic velocities, implying high temperatures. The DUPAL and SOPITA anomalies are located near seismic velocity minima. After Castillo (1989).

(Figure 11.19), which indicate low densities. The low density in turn implies that these are regions of high temperatures in the lower mantle. While the exact significance of this remains unclear, it does establish a connection with oceanic island volcanism and lower mantle properties, strengthening the plume hypothesis, and favoring a lower mantle origin for plumes.

11.5.3 The Subcontinental Mantle Lithosphere

Beneath continents, there are regions of mantle through which heat is conducted rather than convected. These regions tend to have fast seismic velocities, suggesting they are cold compared to the convective mantle. Xenoliths derived from these regions (their depth of origin can be established using the thermobarametric techniques covered in Chapter 4) are often harzburgitic, which is a comparatively low-density peridotite. This subcontinental lithosphere is of quite variable thickness: it is only 10's of km thick under tectonically active areas such as the Great Basin of the Western U.S., but is more than

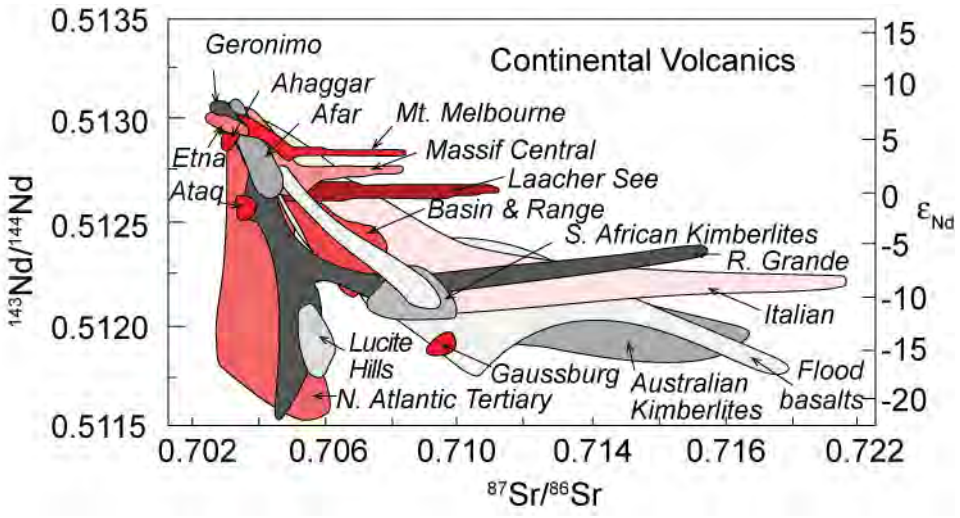

Figure 11.20. Sr and Nd isotope ratios in continental basalts. After Zindler and Hart (1986).

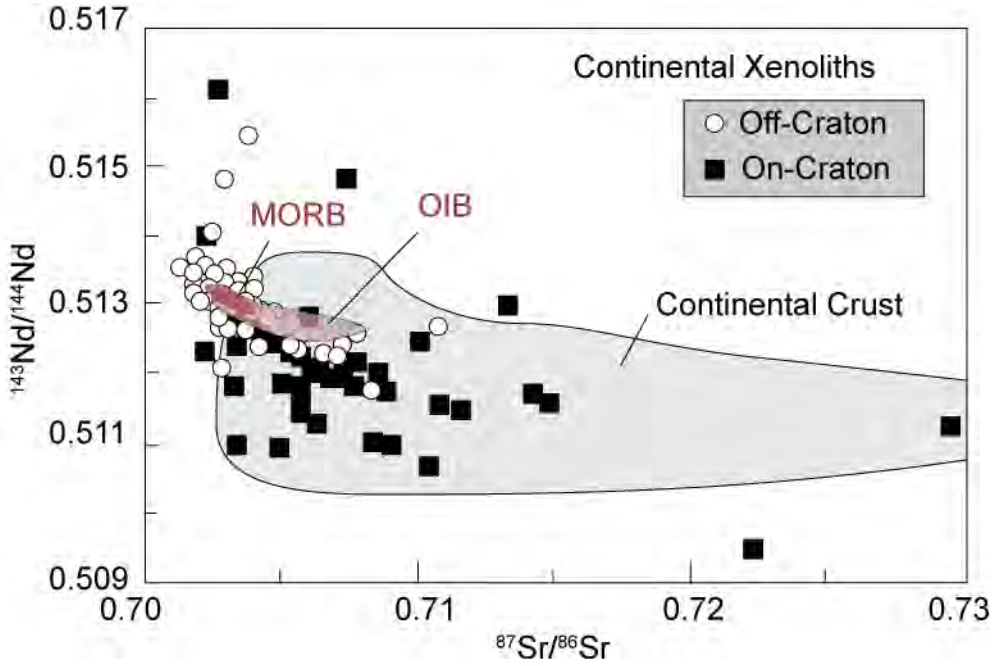

Figure 11.21. Sr and Nd isotope ratios in garnets and clinopyroxenes from peridotite xenoliths from the subcontinental lithospheric mantle. After Pearson et al. (2003).

200 km thick under the South African craton. In addition to seismic properties, basalts and xenoliths derived from this region inform us of its character. Figure 11.20 shows Sr and Nd isotopic variations in continental basalts. The data span a much larger range than oceanic basalts. Some, but not all, of this variation reflects the effects of assimilation of continental crust. Assimilation effects can be avoided by considering peridotite xenoliths in continental basalts, the data for which is shown in Figure 11.21. As may be seen, the range of values is even greater, particularly among xenoliths from outside Precambrian cratons. However, caution is needed when directly comparing the heterogeneity observed in xenoliths to that in basalts because the two represent different scales of sampling of the mantle. Basalts are created by melting of regions that have characteristic scales of at least tens of kilometers. The magma generation process undoubtedly averages out small-scale heterogeneities. Xenoliths, on the other hand, have characteristic dimensions of centimeters. Thus variations in isotope ratios in basalts reflect large-scale heterogeneity in the mantle, while xenoliths reflect small-scale heterogeneity. Despite this, it appears that the subcontinental lithosphere is more heterogeneous, even on relatively large scales, than is the suboceanic mantle.

The subcontinental mantle can be quite old, and often has the same age as the crust it underlies. Geochronological studies of xenoliths and inclusions in diamond from South African kimberlites suggests the mantle is 3 –3.5 Ga old in this region, ages similar to that of the South African craton. The greater isotopic heterogeneity of the subcontinental lithosphere probably reflects it long-term stability: the greater the age of the material, the more variations in parent-daughter ratios will be expressed as variations in radiogenic isotope ratios. Convective mixing in the suboceanic mantle will tend to destroy heterogeneity in the suboceanic mantle.

Though many xenoliths have isotopic compositions indicating incompatible element enrichment, others xenoliths show parts of the subcontinental lithosphere can be extremely incompatible element depleted. ε_{Nd} values of +500 have been recorded in garnets in eclogites from the Roberts Victor mine kimberlite. These eclogites appear to be rafts of subducted oceanic crust stranded in the subcontinental lithosphere over 3 Ga ago, an interpretation supported by highly variable oxygen isotope ratios in the eclogites. They apparently suffered extreme LRE depletion around that time, perhaps by a small de-

gree of melting or dehydration after subduction. Much of the subcontinental lithosphere may consist of mantle from which partial melts have been extracted to form the continental crust. Interesting, when the upper mantle undergoes melting both the melt and residual solid will have a density that is less than the original material. This residue is less dense is because garnet, a very dense phase, is preferentially removed during melting. Thus both the crustal and mantle parts of the continental lithosphere have relatively low density, which may help to explain its stability.

If the subcontinental lithosphere is residual material from which melts have been extracted, why are xenoliths and basalts with "enriched" isotopic signatures so common? What process or processes could have produced this incompatible element enrichment of many parts of the subcontinental lithosphere? One possibility, first suggested by Brooks et al. (1976), is that partial melts from mantle plumes migrate upward into the lithosphere, where they freeze. The extent to which upwelling mantle can melting will depend on the depth to which it rises. Where continental lithosphere prevents plumes from rising above 200 km depth or so, the degree of melting is likely to be quite small, meaning the melts would be quite incompatible element enriched. These melts could then migrate upward into the lithosphere, metasomatizing it, i.e., reacting with it and enriching it in incompatible elements. Yet another possibility is that hydrous fluids released during dehydration of subducting oceanic lithosphere may migrate into the continental lithosphere and react with it (Hawkesworth, 1990). Judging from studies of island arc magmas, such fluids appear to be particularly enriched in soluble incompatible elements, such as the alkalis and alkaline earths. Petrographic studies of some xenoliths clearly reveal features, such as the secondary growth of hydrous minerals such as phlogopite (Mg-rich mica) and richterite (an alkali-rich amphibole) indicative of such metasomatism. Menzies and Hawkesworth (1987) provide a good overview of the topic.

Studies of Os isotope ratios in xenoliths from the subcontinental lithosphere have been particularly enlightening. Most xenoliths derived from below regions of old continental crust have low Os isotope ratios, which imply that low Re/Os ratios were established long ago. The low Re/Os ratios are consistent with the idea that this material undergone partial melting in the past, since Re is moderately incompatible, and would partition into the melt, while Os is highly compatible, and would remain in the solid. Despite their low $^{187}Os/^{188}Os$ ratios, many of these same xenoliths have quite low ε_{Nd} (Figure 11.22). The low ε_{Nd} suggests incompatible element enrichment, and hence would appear to be inconsistent with the high $^{187}Os/^{188}Os$ ratios. The explanation of this paradox appears to be that Os is was not affected by the metasomatism that enriched these regions in incompatible elements and decreased Sm/Nd ratios (e.g., Carlson and Irving, 1994). Apparently, neither Re nor Os are transported effectively by metasomatic fluids. If the fluids are aqueous, this is perhaps not surprising, since these elements have low solubilities under reducing conditions. If the fluids are silicate melts, it is unclear why they do not transport Re. The answer may have to do with dependence of the Re partition coefficient on composition and oxygen fugacity.

11.6 The Crust

We now turn our attention to the crust. Though the crust forms only a small fraction of the mass of the Earth (about 0.5%), it is arguably the most varied and interesting fraction. Further, it's the fraction we can examine directly and therefore know most about. The crust has formed through igneous processes from the mantle over geologic time. There are two fundamental kinds of crust: oceanic and continental. Oceanic crust, created mainly by magmatism at mid-ocean ridges, is basaltic in composition, thin, ephemeral, and relatively uniform. The continental crust is much thicker, essentially permanent, and on average andesitic in composition. The continental crust is also much more varied. Although it too has formed by magmatism, its evolution is far more complex than that of oceanic crust. Though we have an excellent understanding of how oceanic crust forms, our understanding of the processes that have led to the present continental crust is far from complete. Subduction-related, or 'island arc' volcanism appears to play a particularly important role in the formation of the continental crust, so we will pay special attention to processes in islands arcs. We will then consider the problem of interaction of

mantle-derived magma with the crust, then the problems of the composition and evolution and the continental crust, and finally differentiation of the crust through melting and metamorphism.

11.6.1 The Oceanic Crust

In a 1962 paper that he called "an essay in geopoetry," Harry Hess summarized his radical views on seafloor spreading. He speculated that mid-ocean ridges were produced by rising mantle convention currents, and that these convection currents then moved laterally away from the mid-ocean ridges, producing the phenomenon of continental drift. This concept now forms the basis of plate tectonics, the fundamental paradigm of geology. Hess did miss one detail, however. He thought the oceanic crust was hydrated mantle, consisting of "serpentinized peridotite, hydrated by release of water from the mantle over the rising limb of a convention current." However, as we saw in Chapter 7, when hot mantle decompresses as it rises, it melts. This melting generates the basaltic magma that form the oceanic crust. In some respects, though, Hess's mistake is a very minor indeed. Oceanic crust is very ephemeral, and for this reason, it is sometimes better to think of it as part of the mantle reservoir than the crustal one. Nevertheless, igneous processes at mid-ocean ridges have fascinated many geochemists and much has been learned about them in the past several decades.

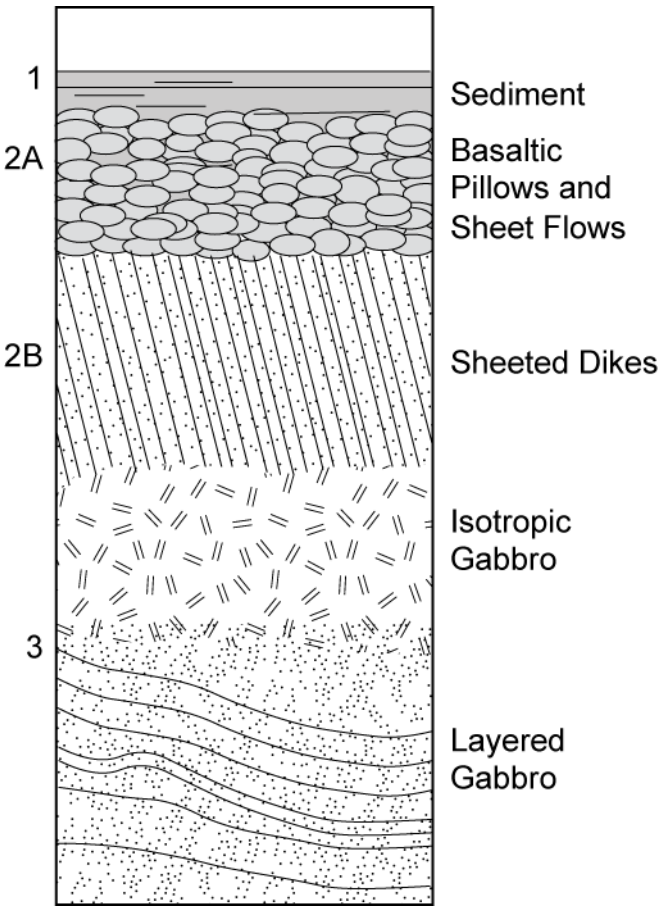

Figure 11.22. Cross-section of typical oceanic crust. Numbers on the left side refer to the layers indentified in seismic velocity profiles.

11.6.1.1 Structure of the Oceanic Crust

Seismic studies show that the oceanic crust has a layered structure (Figure 11.22). Studies of the rare cases where oceanic crust is exposed on land, formations called *ophiolites*, together with drilling into the oceanic crust and examining ocean crustal cross-sections exposed in faulted regions, such as the Hess Deep along the East Pacific Rise have helped in interpreting this seismic structure. The uppermost layer, which is not present at mid-ocean ridges, consists of sediments (Seismic Layer 1). The sediment is underlain by basaltic lava flows and below that by the dikes that fed their eruption; together these constitute seismic layer 2. Seismic layer 3 consists of gabbros formed by basaltic magmas that crystallized in place (isotropic gabbros) and accumulations of minerals that

Table 11.06. Major Element Composition of the Oceanic Crust

	Average MORB[1]	Lower Crust[2] Average	Bulk Crust[1]
SiO_2	50.06	50.6	50.1
TiO_2	1.52	0.78	1.1
Al_2O_3	15.00	16.7	15.7
ΣFeO	10.36	7.50	8.3
MnO	0.19	0.14	0.11
MgO	7.71	9.4	10.3
CaO	11.46	12.5	11.8
Na_2O	2.52	2.35	2.2
K_2O	0.19	0.06	0.11
P_2O_5	0.16	0.02	0.1

[1]From White and Klein (2012)
[2]From Coogan (2012).

crystallized from the basaltic magma in crustal magma chambers (the layered gabbros). Because of the latter, the gabbros are probably somewhat more mafic on average than are the basalts. On average, the lava flows are about 800 m thick; the sheeted dike complex appears to be of roughly similar thickness. The gabbros are roughly 5 km thick on average and thus compose most of the oceanic crust, which is typically 6 to 7 km thick.

The structure of the oceanic crust reflects its construction. Melts rise buoyantly from the mantle because they are less dense than surrounding peridotite. Once they reach the crust, however, they are no longer buoyant and they pond within the crust. Seismic studies show that beneath fast-spreading ridges, such as the East Pacific Rise, a permanent pool of melt exists about 2 km beneath the seafloor. This "melt lens" is only about a kilometer or so wide and 100 meters or so deep. Beneath it is a seismically slow area interpreted as a crystal mush. In some cases, pools of melt also appear to exist in the deeper crust. Magma enters the crust at temperatures of 1200˚C or so, but conductive heat loss at the seafloor, and more importantly circulation of seawater (which emerges to form hydrothermal vents and "black smokers") withdraws heat rapidly from the magma. Consequently it cools and crystallizes. Judging from the thickness of the lower crustal gabbros, most magma crystallizes in place within the lower oceanic crust. As crystallization proceeds, however, the residual magma becomes less dense, so that some of the magma, perhaps 20 to 25%, will rise toward the seafloor. About half of that will erupt to form lava flows and half will freeze in conduits to form the sheeted dike complex. From this we can see that MORB will not be compositionally representative of the whole oceanic crust, rather it will be richer in incompatible elements that remain in the melt during fractional crystallization and poorer in compatible elements that partition into the crystallizing minerals.

Table 11.07. Trace Element Composition of the Oceanic Crust (all concentrations in ppm)

	Bulk Crust*	Ave. MORB*	Lower Crust†
Li	3.52	6.63	
Be	0.31	0.64	
B	0.80	1.80	
K	651	1237	
Sc	36.2	37	37
V	177	299	209
Cr	317	331	308
Co	31.7	44	50
Ni	134	100	138
Cu	43.7	80.8	71
Zn	48.5	86.8	38
Rb	1.74	4.05	
Sr	103	138	115
Y	18.1	32.4	13.9
Zr	44.5	103	28.4
Nb	2.77	6.44	0.93
Cs	0.02	0.05	
Ba	19.4	43.4	
La	2.13	4.87	0.86
Ce	5.81	13.1	2.75
Pr	0.94	2.08	0.52
Nd	4.90	10.4	2.78
Sm	1.70	3.37	1.1
Eu	0.62	1.20	0.58
Gd	2.25	4.42	1.6
Tb	0.43	0.81	0.31
Dy	2.84	5.28	2.09
Ho	0.63	1.14	0.46
Er	1.85	3.30	1.34
Tm	0.28	0.49	
Yb	1.85	3.17	1.27
Lu	0.28	0.48	0.19
Hf	1.21	2.62	
Ta	0.18	0.417	
Pb	0.47	0.657	
Th	0.21	0.491	
U	0.07	0.157	

*From White and Klein (2012)
†From Coogan (2012).

11.6.1.2 Composition of the Oceanic Crust

The basaltic lavas, MORB, that constitute the uppermost oceanic crust are readily sampled by dredging, coring, and submersible sampling at mid-ocean ridges. Their average composition is listed in Tables 11.06 and 11.07, along with the average composition of lower crustal gabbros. While the MORB average is based on thousands of samples, the lower crustal average is based on far fewer samples; there is consequently much more uncertainty about the composition of the lower oceanic crust. The bulk composition of the oceanic crust listed in Table 11.06 was computed by White and Klein (2012) based on the assumption that (1) MORB are the products of fractional crystallization within the oceanic crust and (2) the composition of the magma parental to MORB was in equilibrium with mantle olivine at the just before it entered the oceanic crust.

Mantle olivine is typically 90-92% forsterite, and according to experimental studies such as that of Roedder and Emslie (1970) (see Chapter 4), a melt in equilibrium with it would have an Mg-number (the Mg-number is the atomic $Mg/(Mg+Fe^{2+})$ ratio in percent) of around 72. The average composition listed in Table 11.06 has an Mg# of 59, and therefore could not be in equilibrium

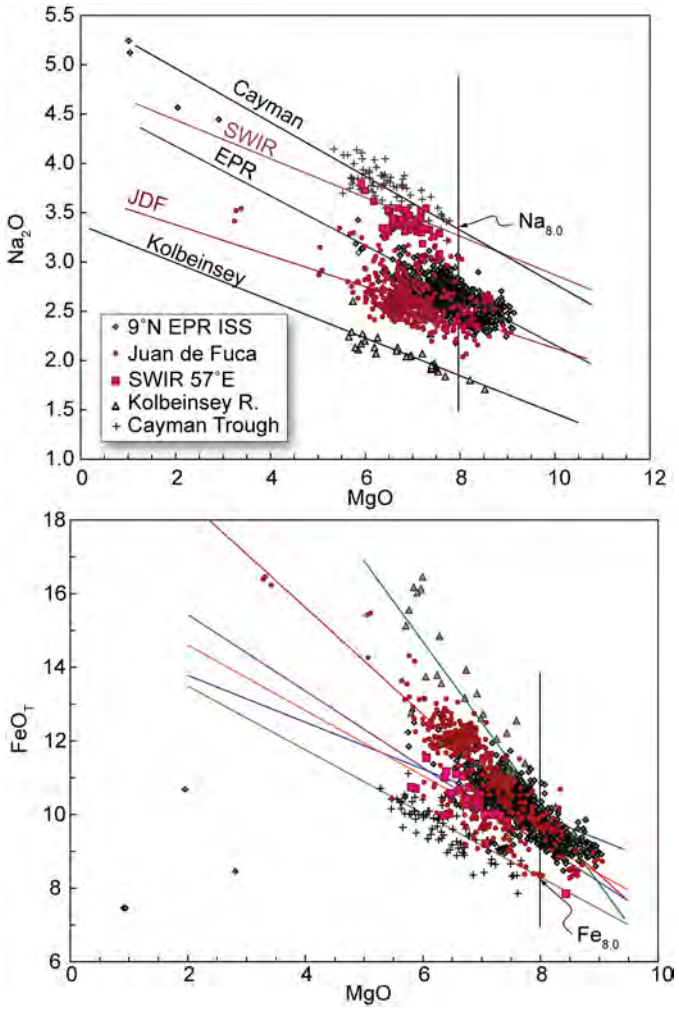

Figure 11.23. Na_2O and FeO vs. MgO in MORB from various regions of the mid-ocean ridge system plot along liquid lines of decent of varying slopes. $Fe_{8.0.}$ and $Na_{8.0}$ are the value of Na_2O and FeO, respectively, of the lines at 8.0% MgO. EPR: the Integrated Study Site (ISS) at 9° N on the East Pacific Rise; JDF: Juan de Fuca Ridge; SWIR: Southwest Indian Ridge; Kolbeinsey Ridge is north of Iceland, and the Cayman Trough is a small spreading center in the Caribbean. After White and Klein (2012).

with mantle olivine. The bulk composition of the oceanic crust was determined by using the MELTS program (Ghiorso and Sack; 1994; see Chapter 4) to determine which minerals would crystallize from average MORB and then adjusting the composition by adding these back. This was continued until olivine of 90% forsterite was in equilibrium with the melt composition. Trace elements are then computed for this parental composition using the fractional crystallization equations in Chapter 7.

The composition of MORB is remarkably uniform throughout the ocean basins and in this respect is unique among igneous rocks. Nevertheless, some systematic regional variations have been identified. Some of this can be related to fractional crystallization. The amount of fractional crystallization is generally greater at fast-spreading ridges. Sinton and Detrick (1992) found that the mean Mg-number decreased from 57.1 for basalts erupted along ridges with full spreading rates less than 5 cm/yr to 52.8 for basalts erupted on fast-spreading ridges (>8 cm/yr). Rubin and Sinton (2007), using a much more extensive data set, demonstrated a more or less linear decrease in Mg-number with spreading rate through the entire range. They found that lavas at the slowest spreading ridges erupt roughly 20° C hotter than at the fastest-spreading ones. The greater extent of crystallization and lower eruption temperatures at fast-spreading ridges is likely a direct consequence of the crystallization occurring primarily at shallower depths at fast-spreading regions.

The other factors that control the major element composition of MORB are the degree and depth of melting, which are in turn controlled by mantle temperature. The 1987 study of Klein and Langmuir elucidated how these factors affected both the thickness and composition of oceanic crust. However, to assess mantle temperature requires first correcting for the effects of fractional crystallization. Klein and Langmuir (1987) found that basalts in each region they consider formed coherent trends in plots of oxides vs. MgO concentrations (Figure 11.23). Klein and Langmuir assumed these trends represented liquid line of descents produced by fractional crystallization within crustal magma chambers To compare compositions from different regions, they defined the parameter $Na_{8.0}$ as the value of Na_2O where the trends crossed 8 wt. % MgO (Figure 11.23). $FeO_{8.0}$ was defined in a similar way.

Corrected for fractional crystallization in this way, major elements correlate in revealing and predictable ways. Most significantly, regions with low mean $Na_{8.0}$ are also characterized by high mean $Fe_{8.0}$. Furthermore, these major element variations correlate with physical characteristics of the ridge axis from which they were recovered. Regional averages of $Na_{8.0}$ and $Fe_{8.0}$, for example, showed a positive and an inverse correlation, respectively, with the average ridge depth from which the lavas were recovered (Figure 11.24). $Na_{8.0}$ correlated inversely with seismically and geologically determined estimates of the crust thickness in each region.

These relationships can be understood as the interplay between the extent of melting and the pressure of melting. Sodium is a moderately incompatible during melting of mantle minerals

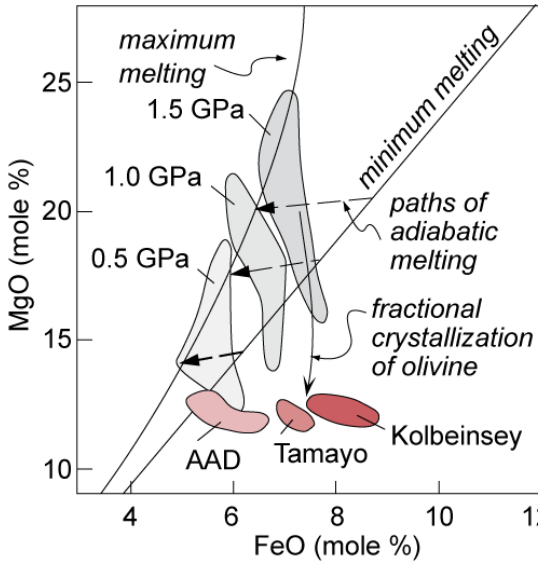

Figure 11.25. Variation of MgO and FeO in partial melts of mantle peridotite. Grayed fields show the compositions of experimental produced partial melts of peridotite at 3 different pressures. Colored fields show compositions of high MgO basalts from the Australian-Antarctic Discordance (AAD), Tamayo Fracture Zone of the East Pacific Rise, and Kolbeinsey regions. Dashed arrows show the path of melt composition produced by melting of adiabatically rising mantle. Curved arrow shows how the compositional a 1.5 GPa melt will evolve due to fractional crystallization of olivine. After Klein and Langmuir (1987).

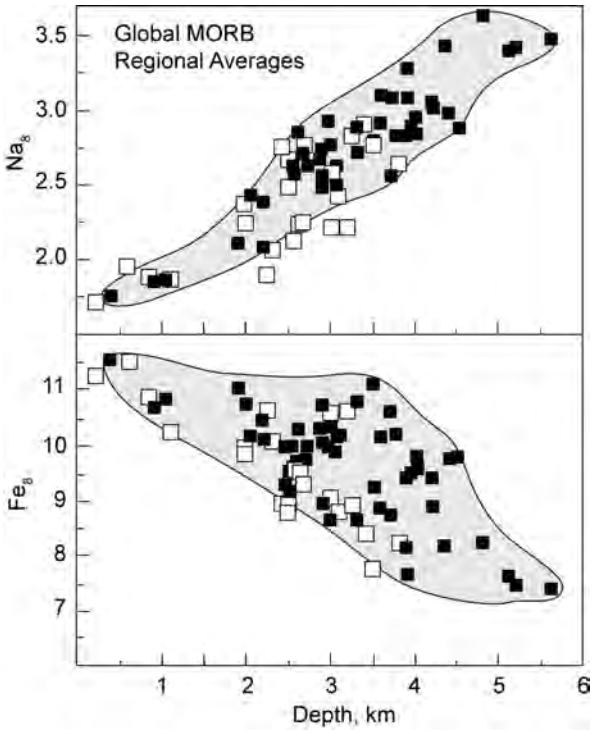

Figure 11.24. Regional average $Fe_{8.0}$ and $Na_{8.0}$ vs. axial depth in the mid-ocean ridge system. Solid squares are MORB from "normal" ridge segments; open squares are from ridges influenced by the Galapagos, Azores, Jan Mayen, Tristan, Iceland, and Bouvet hotspots. Yellow field encompasses normal ridge basalts. After Klein and Langmuir (1987) and White and Klein (2012).

(D~0.02-0.03), and therefore will be concentrated in the melt at small extents of melting. Iron, on the other hand varies in the melt as a function of the pressure of melting (Figure 11.25). Thus, the inverse correlation between mean $Na_{8.0}$ and mean $Fe_{8.0}$ suggests that there is a positive correlation between the mean extent of melting and the mean pressure of melting.

Klein and Langmuir concluded mantle temperature was the key factor in accounting for both depth of the ridge axis and the composition of melts erupted, because mantle temperature affects both degree of melting and the mean depth of melting. Shallow segments of the mid-ocean ridge system overlie relatively hot mantle. The hot mantle intersects the solidus at greater depth and ultimately melts to a greater degree (Figure 11.26). Hotter mantle is less dense and therefore more buoyant, so that ridges overlying hotter

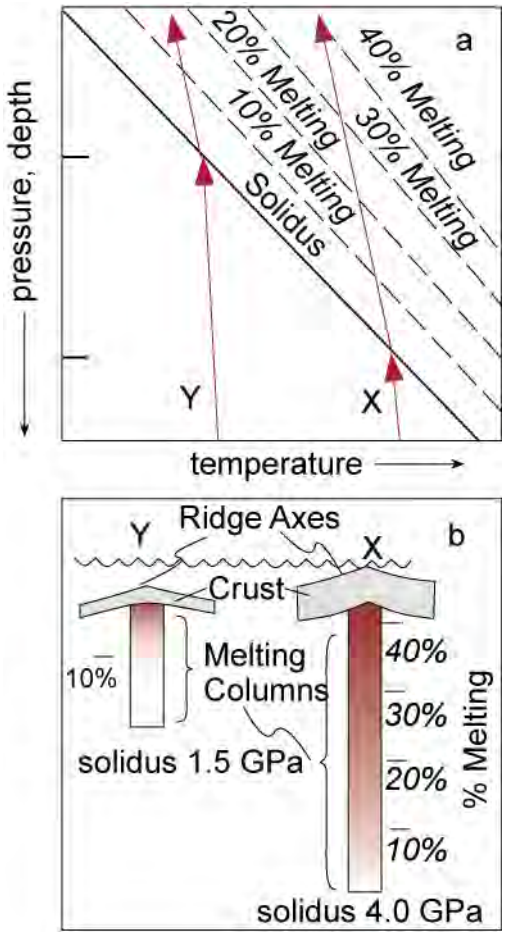

Figure 11.26. a.) Pressure-temperature relationship of adiabatically rising mantle undergoing melting. Hotter mantle (X) intersects the solidus at higher pressure and ultimately melts to a higher degree than cooler mantle (Y). The break in slope occurs because energy is consumed by melting (enthalpy of fusion). b.) Relationship between axial depth, crustal thickness, melting, and mantle temperature. Hotter mantle (X) maintains the ridge at higher elevation because of its buoyancy. It also has a deeper melt column and melts to a greater degree, producing thicker crust than cooler mantle (after Klein and Langmuir, 1989).

mantle will be more elevated. Cooler mantle will not begin to melt until it reaches shallower depth, and total extent of melting will be more limited. Klein and Langmuir concluded that a range in degree of melting of 8-20% and in mean pressure of melting of 0.5 to 1.6 GPa were required to produced the range in compositions observed. The hottest regions of the mantle occur near mantle plumes such Iceland. Some of the coolest mantle is found at the Australian-Antarctic Discordance, a region where the ridge is particularly deep and isotope studies have suggested is a boundary between mantle convection cells. Overall, the data suggested a range in mantle temperature of some 250° C.

11.6.2 The Continental Crust

The continental crust is the part of the Earth that is most readily samples and the part with which we are most familiar. It is, however, very likely the most variable part of the Earth in every respect, including compositionally. It is the part of the Earth where geology reveals the planet's history (albeit, as mentioned in the previous chapter, not the very earliest part of that history). In this respect, the continents are arguably the most interesting part of the planet. We'll first consider the composition of the continental crust, then we'll see what geochemistry can reveal about its creation and evolution.

The continental crust is extremely heterogeneous, thus task of estimating its overall composition is a difficult one. Furthermore, only the upper part of the continental crust is exposed to direct sampling: the deepest scientific borehole, drilled by the Russians in the Kola Peninsula reached only 12 km. The average thickness of the continental crust is about 35 km so we have been able to directly sample only the upper third. Fortunately, however, tectonic and volcanic processes sometimes bring bits of the deep crust to the surface where it can be studied.. Nevertheless, geochemists must rely heavily on inferences made from indirect observations to estimate the composition of the continental crust. Beginning with Clarke (1924) and Goldschmidt (1933), a number of such estimates of the composition of the continental crust have been made. These have become increasingly sophisticated with time. Among the most widely cited works are those of Taylor and McLennan (1985, 1995), Weaver and Tarney (1984), Wedepohl (1995) and Rudnick and Fountain (1995). These estimates are not entirely independent. For example, Weaver and Tarney (1984) and Rudnick and Fountain (1995) both rely in part of versions of Taylor and McLennan's studies. Taylor and McLennan in turn rely on the work of Shaw (1967) for many elements, as does Wedepohl (1995). In the following, we will focus particularly on the

estimates of Taylor and McLennan (1985, 1995), and Wedepohl (1995), and the recent work of Rudnick and Gao (2003).

We can divide the problem of estimating crustal composition into two parts. The first is to estimate the composition of the upper, accessible parts of the crust. This is referred to as the "upper crust." Direct observations provide the most important constraints on the composition of this part of the crust. The second problem is the composition of the deeper, less accessible part of the crust. For this part of the crust, indirect observations, particularly geophysical ones such as seismic velocity and heat flow, provide key constraints on composition. As we shall see, these observations indicate that the continental crust is compositionally stratified, with the lower part being distinctly more mafic, i.e., richer in Mg and Fe and poorer in SiO_2 and incompatible elements. Some workers divide the deep crust into a middle and lower crust, while others consider only a single entity that they refer to as the lower crust. The chemical contrasts between the upper and deep crust are much stronger in continents than in the ocean. We should emphasize, however, that any division of the continental crust into layers is doen for convenience and somewhat arbitrary. The continental crust does not appear to have a systematic layered structure that directly results from it creation in that way that the oceanic crust does. Instead, chemical zonation in the continents has evolved over time through a variety of processes.

11.6.2.1 Composition of The Upper Continental Crust

Historically, two approaches to estimating the composition of the upper continental crust have been used. The first approach, pioneered by F. W. Clarke in 1889, is to average analyses of samples taken over a large area. An alternative is to mix sample powders to form *composites* of various rock types and thus reduce the number of analyses to be made (e.g., Shaw et al., 1986; Wedepohl, 1995, Borodin, 1998, Gao et al., 1998). Studies of these kinds consistently produce an average upper crustal composition similar to that of granodiorite with the concentrations of major oxides agreeing within 20% and most within 10% (Figure 11.27). This is encouraging since granodiorite is the most common igneous rock in the crust. Such estimates also tend to produce relatively similar average concentrations for minor and trace elements. Most modern estimates of upper crustal major element and soluble trace element concentrations are based on this approach.

The second method is to let the Earth make the composites for us. A couple of kinds of such materials are available. Goldschmidt (1933) suggested the use of glacial clays in melt-water lakes adjacent to the Pleistocene ice front. An alternative but similar approach is to use *loess*, which is fine-grained aeolian material of Pleistocene age. The most readily available of this kind of natural composite, however, is simply sediments. One advantage of sediments over glacial material is that whereas most glacial deposits are of Pleistocene age (but there are various glacial deposits of ages ranging up to 2.3 Ga), sediments of all ages are available so that secular variations in crustal composition can be determined.

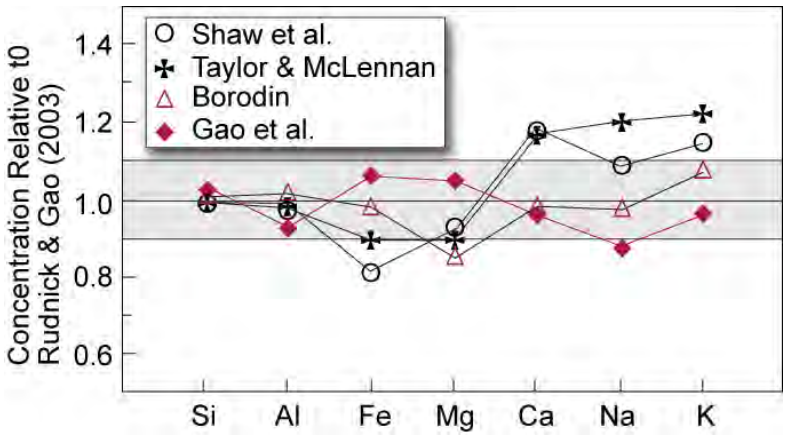

Figure 1127. Estimates of major element concentrations in the upper continental crust by studies mentioned in the text derived from analysis of crustal composites compared to the estimated upper crustal composition of Rudnick and Gao (2003). Modified from Rudnick and Gao (2003).

The advantages of using geologic composites should be obvious, but there are disadvantages as well. The primary problem is that chemical fractionations are involved in producing sediments from their parents. Weathering of rock typically produces three fractions: sands consisting of resistant minerals, clays, and a solution. These products are transported with varying degrees of efficiency away

from the site of production. Since elements tend to be concentrated in one of these three fractions, none of the fractions will have a composition representative of the parent rock. Because it is produced primarily by physical, rather than chemical, action, glacial loess is less susceptible to this kind of chemical fractionation, though some fractionation nevertheless occurs. For example, loess is enriched in SiO_2, Hf, and Zr (Figure 11.28) as a consequence of its enrichment in mechanically and chemically stable minerals, such as quartz and zircon. That in turn results from clays being carried further from their site of origin by wind and water. Loess is also depleted in Na, Mg, and Ca, reflecting loss by leaching.

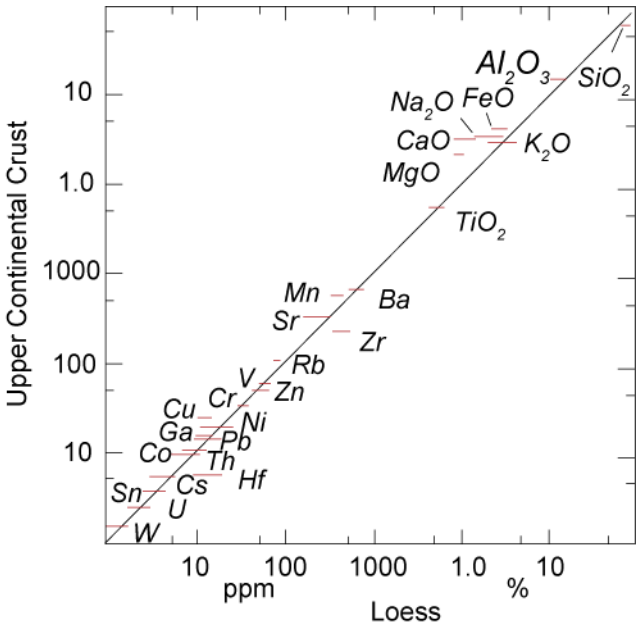

Figure 11.28. Comparison of elemental concentrations in loess with estimated upper crust. After Taylor and McLennan (1985).

Numerous studies have shown that when rock weathers to produce a sediment, the rare earth pattern of the parent is usually preserved in the sediment. This is because the rare earths are concentrated in the clay fraction, which ultimately form shales. Other Group 3 elements (Sc and Y), as well as Th, behave similarly to the rare earths during weathering. Furthermore, rare earth patterns are remarkably similar in different shales, suggesting shales are indeed good averages of crustal composition. This is illustrated in Figure 12.29, which compares three shale composites from three continents. Because of these properties of the rare earths, S. R. Taylor and colleagues at the Australian National University used them as a point of departure for estimating the composition of the upper continental crust.

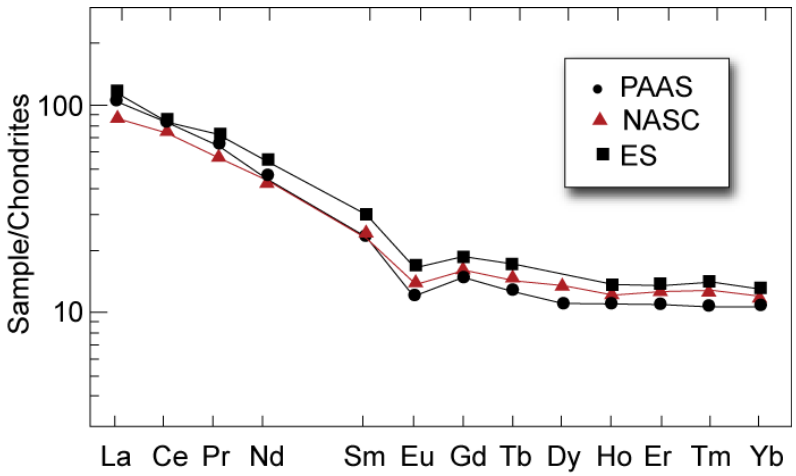

Figure 12.29. Rare earth patterns of Post-Archean Australian Shale (PAAS) composite, the North American Shale Composite (NASC) and the European Shale (EC) composite. After Taylor and McLennan (1985).

Most recent estimates of crustal composition are based on a combination of both approaches, together with assumptions about the ratios between elements. The most recent comprehensive study of crustal composition is that of Rudnick and Gao (2003). Their estimate of upper crustal composition is compared with earlier ones in Table 11.08. The estimates are broadly similar, and indicate an upper crust of "granodioritic" or "tonalitic" composition (although there are few elements, such as Cu, where there is considerable disagreement. One should note, however, that the Rudnick and Gao (2003) relied heavily on the work of Taylor and McLennan and both Taylor and McLennan's and Wedepohl's estimates derive in part from the earlier work of Shaw et al. (1986).

Table 11.08. Composition of the Upper Continental Crust

Oxide (wt %)	T& M	Wedepohl	R&G	Normative Mineralogy (T & M)	
SiO_2	66.0	64.9	66.6	Quartz	15.7
TiO_2	0.5	0.52	0.64	Orthoclase	20.1
Al_2O_3	15.2	14.6	15.4	Albite	13.6
FeO	4.5	3.97	5.04	Diopside	6.1
MnO	0.07	0.07	0.10	Hypersthene	9.9
MgO	2.2	2.24	2.48	Ilmenite	0.95
CaO	4.2	4.12	3.59		
Na_2O	3.9	3.46	3.27		
K_2O	3.4	4.04	2.80		
P_2O_5	0.20	0.15	0.15		

	T & M	Wedepohl	R & G		T & M	Wedepohl	R & G
Li	20	22	21	Sb	0.2	0.31	0.4
Be	3	3.1	2.1	Te			
B	15	17	17	I		1.4	1.4
C		3240		Cs	3.7	5.8	4.1
N		83	83	Ba	550	668	624
F		611	557	La	30	32.3	31
S		953	621	Ce	64	65.7	63
Cl		640	370	Pr	7.1	6.3	7.1
Sc	11	7	14	Nd	26	25.9	27
Ti	3000	3117		Sm	4.5	4.7	4.7
V	60	53	97	Eu	0.88	0.95	1.0
Cr	35	35	92	Gd	3.8	2.8	4.0
Co	10	11.6	17	Tb	0.64	0.5	0.7
Ni	20	18.6	47	Dy	3.5	2.9	3.9
Cu	25	14.3	28	Ho	0.8	0.62	0.83
Zn	71	52	67	Er	2.3		2.3
Ga	17	14	17.5	Tm	0.33		0.30
Ge	1.6	1.4	1.4	Yb	2.2	1.5	2.0
As	1.5	2	4.8	Lu	0.32	0.27	0.31
Se	0.05	0.083	0.09	Hf	5.8	5.8	5.3
Br		1.6	1.6	Ta	2.2	1.5	0.9
Rb	112	110	82	W	2	1.4	2
Sr	350	316	320	Re ppb	0.4		0.20
Y	22	20.7	21	Os ppb	0.05		0.031
Zr	190	237	193	Ir ppb	0.02		0.022
Nb	25	26	12	Pt ppb			0.5
Mo	1.5	1.4	1.1	Au ppb	1.8		1.5
Ru ppb			0.34	Hg ppb		56	50
Pd ppb	0.5		0.52	Tl	0.75	0.75	0.9
Ag ppb	50	55	53	Pb	20	17	17
Cd ppb	98	102	90	Bi	127	123	0.16
In ppb	50	61	56	Th	10.7	10.3	10
Sn	5.5	2.5	2.1	U	2.8	2.5	2.6

Concentrations in ppm except where noted. T&M: Taylor and McLennan (1985,1995), Wedepohl: Wedepohl (1995). R&G: Rudnick and Gao (2003).

11.6.2.2 Composition of the Middle and Lower Continental Crust

Rocks from the middle and lower crust, typically in *amphibolite* and *granulite* metamorphic facies are sometimes exposed at the surface by tectonic processes and hence can provide insights into the nature of this part of crust. Amphibolites are, as their name implies, metamorphic rocks that are relatively rich in amphibole, a mineral that contains water in its structure, but less water than mica-bearing rocks, such as granites and rocks metamorphosed at lower temperature. Granulites on the other hand are anhydrous, with pyroxene replacing amphibole and biotite. Middle crustal cross-sections of amphibolite- to granulite-facies rocks contain a wide variety of lithologies, including metasedimentary rocks, but they are dominated by igneous and metamorphic rocks of the dioritic, granodioritic, and granitic composition.

However, these *granulite terranes* have often been subjected to retrograde metamorphism (metamorphism occurring while temperatures and pressure decrease), which compromises their value. Furthermore, questions have been raised as to how typical they are of lower continental crust. These questions arise because granulite terranes are generally significantly less mafic than xenoliths from the lower crust. Xenoliths perhaps provide a better direct sample of the lower crust, but they are rare. The point is, any estimate of the composition of the middle and lower crust will have to depend on indirect inference and geophysical constraints as well as analysis of middle and lower crustal samples. There are two principal geophysical constraints:

- Heat flow in the continental crust. A portion of the heat flowing out the crust is produced by radioactive decay of K, U, and Th within the crust (other radioactive elements do not contribute significantly to heat generation because of their long half-lives are low abundances). The concentrations of these elements can be related to rock type, as indicated in Table 11.09.
- Seismic velocities in the continental crust. Seismic velocities depend on density, compressibility and the shear modulus (equations 11.01 and 11.02), which can in turn be related to composition.

Both tell us something of first order importance about the nature of the continental crust: it is vertically zoned, becoming more mafic (i.e., richer in Fe and Mg and poorer in Si and incompatible elements, including K, U, and Th) with depth. Let's consider them in greater detail.

The average heat flow of the continents is about 60 mW/m^2. This heat has two components: heat conducted out of the mantle and heat generated by radioactive decay within the continents. The concentrations of K, U, and Th observed at the surface of the crust would produce more heat than is observed to be leaving the continental crust if these concentrations were uniform through the crust. Thus, the concentrations of these elements must decrease. The problem is complicated, however, by variations in the "mantle" heat flow, which averages about 20 mW/m^2. Heat flow varies significantly with tectonic age. If, as we believe, the continental crust is created by magmatism, it will be initially hot and then cool over time. Subsequent episodes of magmatism may also heat the crust. In addition, variation in mantle heat flow can results from different thickness of the lithosphere (Vitorello and Pollack, 1990; Nyblade and Pollack, 1993). The lithosphere is a conductive boundary layer, so that the thicker the lithosphere, the lower the mantle heat flow out the top of it. Nyblade and Pollack (1993) have argued that regions of old Archean crust are underlain by particularly thick mantle lithosphere, an argument supported by geochronological and thermobarometric studies of mantle xenoliths from these regions.

Table 11.09. U, Th, and K Concentrations and Heat Production in Various Rock Types.

Igneous Rock Type	U (ppm)	Th (ppm)	K (%)	Th/U	K/U	Density g/cm^3	Heat Production 10^{-6} W/m^{-3}
Granite/Rhyolite	3.9	16.0	3.6	4.1	0.9×10^4	2.67	2.5
Granodiorite/Dacite	2.3	9.0	2.6	3.9	1.1×10^4	2.72	1.5
Diorite/Andesite	1.7	7.0	1.1	4.1	0.7×10^4	2.82	1.1
Gabbro/Basalt	0.5	1.6	0.4	3.2	0.8×10^4	2.98	0.3
Peridotite	0.02	0.06	0.006	3.0	0.3×10^4	3.28	0.01
Continental Crust	1.25	4.8	1.25	3.8	1.0×10^4	—	0.8

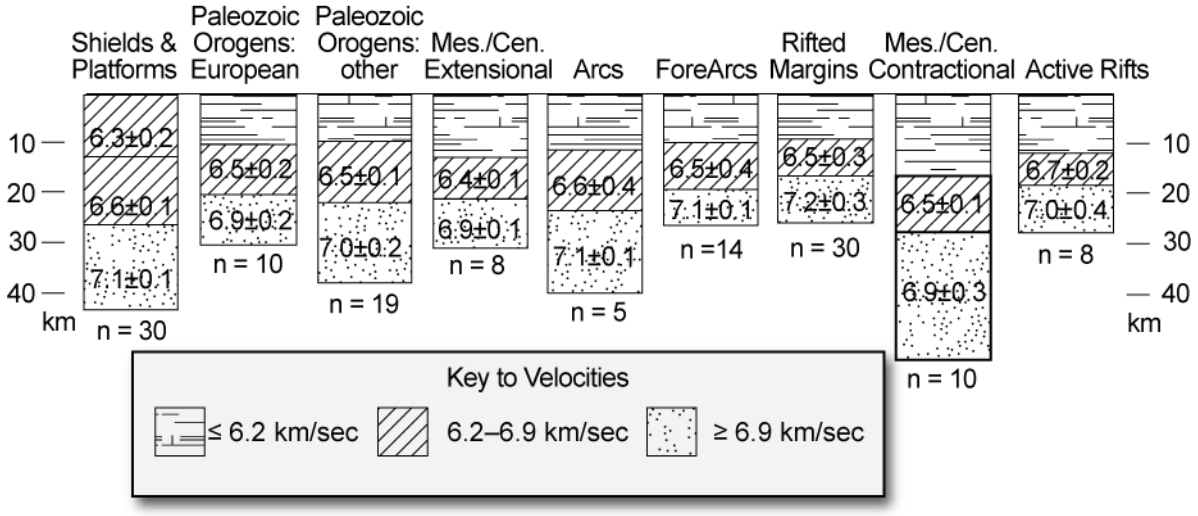

Figure 12.30. Seismic velocity structure of the continental crust, illustrating its 3-layered nature. Velocity structure falls into 9 types. The number of profiles used to construct each type is shown below each type. After Rudnick and Fountain (1995).

Despite these complexities, heat flow in the crust suggests the middle and lower crust contains significantly less K, U, and Th than the upper crust. This in turn suggests the deep continental crust is more mafic than the upper crust.

Seismic velocity profiles vary widely from place to place, as does crustal thickness, but in general p-wave velocities increase with depth in the crust from about 6 km/sec in the upper crust to about 7 km/sec in the lower crust.. Rudnick and Fountain (1995) examined a global database of seismic cross sections and found that they can be divided into 9 classes, which are illustrated in Figure 12.30. One must next relate seismic velocity to composition by making measurements of seismic velocity in the laboratory on samples of known composition. For example, Figure 12.31 shows the relationship between SiO_2 and seismic velocity in a variety of rock types. Recalling that seismic wave speed is inversely related to density (equations 11.01 and 11.02), we might have expected mafic rocks, which poorer in SiO_2 and richer in Mg and Fe and are denser (Table 11.09), to have slower seismic velocities. However, the lower compressibility of mafic rocks results in seismic waves traveling faster through them. Seismic velocities are thus consistent with the heat flow evidence that the middle and lower crust is more mafic than the upper crust.

To produce an estimate of crustal composition, Rudnick and Fountain assigned an average lithology to the seismic sections shown in Figure 12.30. They then assigned a composition to each lithology using a database of the composition of lower crustal xenoliths. Then by estimating the aerial extent of each type of crustal section, and averaging analyses of middle and lower crustal rocks and xenoliths, they produced the compositional estimates. These estimates were subsequently update by Rudnick and Gao (2003) and are listed Table 11.10. This table shows that the composition of the lower crust corresponds to that of tholeiitic basalt; in metamorphic terminology it would be a mafic granulite. The composition of the middle crust corresponds to that of an andesite. At the prevailing

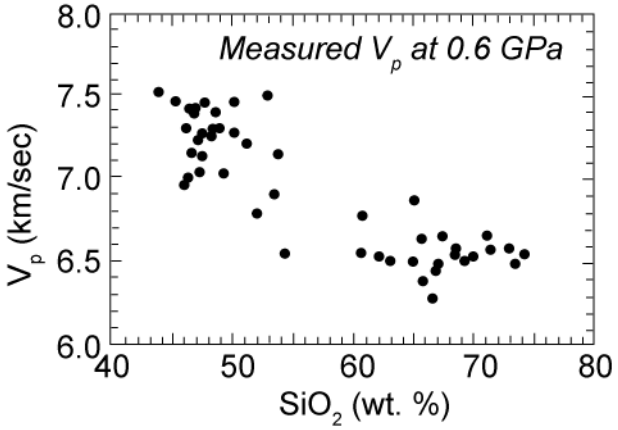

Figure 12.31. Correlation between measured seismic velocity (v_P) and SiO_2 concentration. After Rudnick and Fountain (1995).

pressures and temperatures this rock would be an amphibolite, consisting mainly of amphibole and plagioclase.

Table 11.10. Composition of the Middle and Lower Continental Crust

Major Oxides, %

	R & G Middle	Wedepohl Lower	R & G Lower
SiO_2	63.5	59.0	53.4
TiO_2	069	0.85	0.82
Al_2O_3	15.0	15.8	16.9
FeO	6.0	7.47	8.57
MnO	0.10	0.12	0.10
MgO	3.59	5.32	7.24
CaO	5.25	6.92	9.59
Na_2O	3.39	2.91	2.65
K_2O	2.30	1.61	0.61
P_2O_5	0.15	0.20	0.10

Trace Elements in ppm except as noted

	R & G Middle	Wedepohl Lower	R & G Lower		R& G Middle	Wedepohl Lower	R & G Lower
Li	12	13	13	Sb	0.28	0.3	0.1
Be	2.29	1.7	1.4	I		0.14	0.1
B	17	5	2	Cs	2.2	0.8	0.3
C		588		Ba	532	568	259
N		34	34	La	24	26.8	8
F	524	429	570	Ce	53	53.1	20
S	20	408	345	Pr	5.8	7.4	2.4
Cl	182	278	250	Nd	25	28.1	11
Sc	19	25.3	31	Sm	4.6	6.0	2.8
V	107	149	196	Eu	1.4	1.6	1.1
Cr	76	228	215	Gd	4.0	5.4	3.1
Co	22	38	38	Tb	0.7	0.81	0.5
Ni	33.5	99	88	Dy	3.8	4.7	3.1
Cu	26	37.4	26	Ho	0.82	0.99	0.7
Zn	79.5	79	78	Er	2.3		1.9
Ga	17.5	17	13	Tm	0.32	0.81	0.24
Ge	1.13	1.4	1.3	Yb	2.2	2.5	1.5
As	3.1	1.3	0.2	Lu	0.4	0.43	0.25
Se	0.064	0.17	0.2	Hf	4.4	4.0	1.9
Br		0.28	0.3	Ta	0.6	0.84	0.6
Rb	65	41	11	W	0.60	0.6	0.6
Sr	282	352	348	Re			0.18
Y	20	27.2	16	Os			0.05
Zr	149	165	68	Ir			0.05
Nb	10	11.3	5	Pt	0.85		2.7
Mo	0.60	0.6	0.6	Au	0.66		1.6
Ru			0.75	Hg	0.0079	0.021	0.014
Pd	0.76		2.8	Tl	0.27	0.26	0.32
Ag	48	80	65	Pb	15.2	12.5	4
Cd	0.061	0.101	0.1	Bi	0.17	0.037	0.2
In		0.052	0.05	Th	6.5	6.6	1.2
Sn	1.3	2.1	1.7	U	1.3	0.93	0.2

R & G: Rudnick and Gao (2003), Wedepohl: Wedepohl (1995).

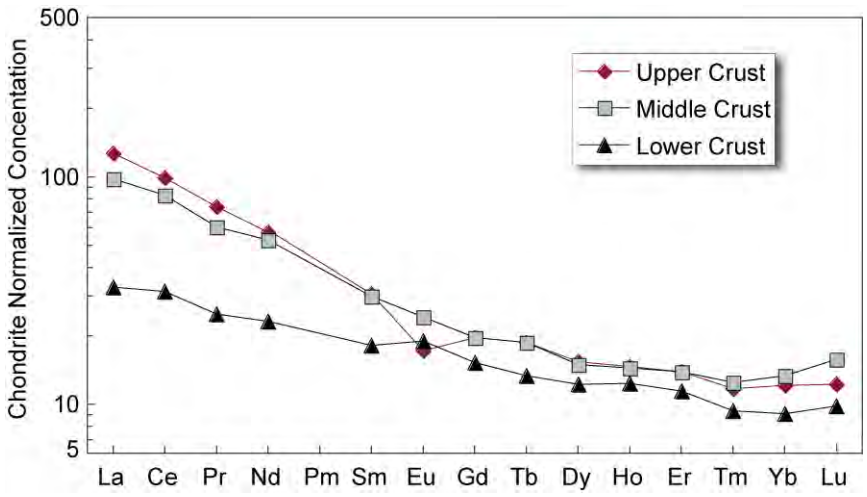

Figure 12.32. Comparison of chondrite-normalized rare earths patterns in upper, middle and lower crust. Data of Rudnick and Gao (2003).

Wedepohl (1995) used the European Geotraverse as a model of the seismic structure of the crust. This seismic cross-section runs from northern Scandinavia to Tunisia and crosses a great variety of tectonic provinces, ranging from the Archean Fennoscandian Shield to the young fold belts to the young Alpine orogen. He assigned 3 lithologies to 3 ranges of seismic velocities: sediments, granites, and gneisses (V_P < 6.5 km/s) corresponding to the upper crust, felsic granulites (6.5 < V_P < 6.9 km/s), and mafic granulites (6.9 < V_P < 7.5 km/s). He used a database of compositions of felsic and mafic granulites from both xenoliths and exposed terranes to calculate an average composition for each of the latter two. He then computed a lower crustal composition by weighting felsic and mafic granulites in the proportions their characteristic seismic velocities were observed in the European Geotraverse. His estimate of the composition of the lower crustal is also listed in Table 11.10.

Rare earth patterns of upper, middle and lower crust as estimated by Rudnick and Gao (2003) are compared in Figure 12.32. The negative Eu anomaly in the upper crust and slight positive anomalies in the middle and lower crust (such positive anomalies are typical of many granulites) are an interesting features of these patterns. Eu is strongly held in plagioclase (Chapter 7). The presence of plagioclase in the melting residue would result in melts having a negative Eu anomaly and the residue having a positive one. Thus these anomalies suggest that crustal has at least partially differentiated to form distinct

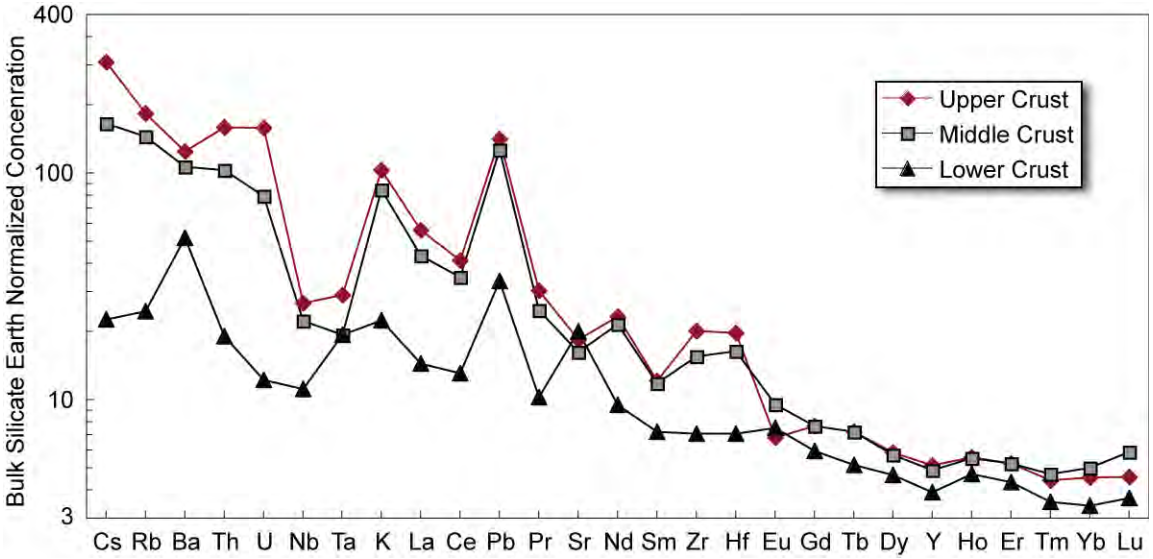

Figure 11.33. Enrichment of incompatible elements relative to bulk silicate Earth (Table 11.03) in the upper, middle, and lower crust. Data from Rudnick and Gao (2003).

layers through partial melting, with granitic melts forming the upper crust and granulitic residues of gabbroic composition forming the lower crust. The actual evolution of the deep crust is undoubtedly more complex, however. Intrusion and ponding of mantle-derived magmas of basaltic composition is likely to be another important reason for the mafic composition of the lower crust.

Figure 12.33 is a "spider diagram" comparing incompatible element abundances in the upper, middle, and lower continental crust. The lower and middle crusts are less enriched in incompatible elements than the upper crust. This is also consistent with the idea that magmatic processes have been important in creating the compositional layering observed in the crust.

11.6.2.3 Composition of the Total Continental Crust

The approach used by most workers to estimate the composition of the total continental crust is simply to calculate an average of the weighted average of crustal layers considered above. This was done, for example, by Rudnick and Fountain (1995) and Weaver and Tarney (1984), both of whom divided the crust into an upper, lower, and middle section. Both Weaver and Tarney (1984) and Rudnick and Fountain (1995) relied on Taylor and McLennan's upper crustal estimate. Weaver and Tarney (1984) used average Lewisian* amphibolite as their middle crust composition and average

Table 11.11. Composition of the Continental Crust

Major Oxides, wt. %

	R & G	T & M	W & T	We	Shaw
SiO_2	60.6	57.3	63.2	61.5	63.2
TiO_2	0.7	0.9	0.6	0.68	0.7
Al_2O_3	15.9	15.9	16.1	15.1	14.8
FeO	6.7	9.1	4.9	5.67	5.60
MnO	0.1	0.18	0.08	0.10	0.09
MgO	4.7	5.3	2.8	3.7	3.15
CaO	6.4	7.4	4.7	5.5	4.66
Na_2O	3.1	3.1	4.2	3.2	3.29
K_2O	1.8	1.1	2.1	2.4	2.34
P_2O_5	0.1		0.19	0.18	0.14

Trace Elements (in ppm unless otherwise noted)

	R & G	T & M	We		R & G	T & M	We
Li	15	13	18	Sb	0.2	0.2	0.3
Be	1.9	1.5	2.4	Te, ppb			5
B	11	10	11	I, ppb	700		800
C			1990	Cs	2	1	3.4
N	56		60	Ba	456	250	584
F	553		525	La	20	16	30
S	404		697	Ce	43	33	60
Cl	244		472	Pr	4.9	3.9	6.7
Sc	21.9	30	16	Nd	20	16	27
V	138	230	98	Sm	3.9	3.5	5.3
Cr	135	185	126	Eu	1.1	1.1	1.3
Co	26.6	29	24	Gd	3.7	3.3	4.0
Ni	59	105	56	Tb	0.6	0.6	.65
Cu	27	75	25	Dy	3.6	3.7	3.8
Zn	72	80	65	Ho	0.77	0.78	0.8
Ga	16	18	15	Er	2.1	2.2	2.1
Ge	1.3	1.6	1.4	Tm	0.28	0.32	0.3
As	2.5	1	1.7	Yb	1.9	2.2	2.0
Se	0.13	0.05	0.12	Lu	0.30	0.3	0.35
Br	0.88		1.0	Hf	3.7	3	4.9
Rb	49	32	78	Ta	0.7	1	1.1
Sr	320	260	333	W	1	1	1.0
Y	19	20	24	Re, ppb	0.188	0.4	0.4
Zr	132	100	203	Os, ppb	0.041	0.005	0.05
Nb	8	11	19	Ir, ppb	0.037	0.1	0.05
Mo	0.8	1	1.1	Pt, ppb	1.5		0.4
Ru, ppb	0.6		0.1	Au, ppb	1.3	3	2.5
Rh, ppb			0.06	Hg, ppb	30		40
Pd, ppb	1.5	1	0.4	Tl, ppb	500	360	520
Ag, ppb	56	80	70	Pb	11	8	14.8
Cd, ppb	80	98	100	Bi, ppb	180	60	85
In, ppb	52	50	50	Th	5.6	3.5	8.5
Sn	1.7	2.5	2.3	U	1.3	0.91	1.7

R & G: Rudnick and Gao (2003), T & M: Taylor and McLennan (1985, 1995), We: Wedepohl (1995), Shaw: Shaw et al. (1986), W & T: Weaver and Tarney (1984).

* The Lewisian, which outcrops in Northwest Scotland, is perhaps the classic exposure of lower crust.

Lewisian granulite as their lower crust composition. Shaw et al. (1986) and Wedepohl (1995) used a similar approach, but divided the crust only into upper and lower parts. An important step in this approach is estimating the thickness of the various sections. Here seismological constraints again come into play.

Taylor and McLennan (1985, 1995) used an entirely different approach to estimating total crustal composition, one based on the "andesite model" of Taylor (1967). Taylor (1967) noted the role played by subduction-related volcanism in creation of the continental crust and assumed that on average the crust consisted of island arc andesite. Thus average island arc andesite was used as the estimated composition of the continental crust. This approach was modified in subsequent work, as Taylor concluded that while post-Archean crust was created at subduction zones, Archean crust was not and is compositionally different. Taylor and McLennan (1985) essentially modify the Taylor (1967) andesite model for their estimate of Archean crustal composition.

Estimates of the major element composition of the continental crust by Weaver and Tarney (1984), Shaw et al. (1986), Taylor and McLennan (1995), Wedepohl (1995), and Rudnick and Gao (2003) are given in Table 11.11. Also listed are estimates of trace element concentrations by Taylor and McLennan (1995), Rudnick and Gao (2003), and Wedepohl (1995). The ranges of estimates for SiO_2 and Al_2O_3 in Table 11.11 are about 10% and 8% respectively; the range in Mg# (52 to 57) is similarly only about 10%. Interestingly, earlier estimates of crustal SiO_2 and Al_2O_3, going back to Goldschmidt (1933) also fall within this range. Thus we can conclude with some confidence that the continental crust on the whole is similar to that of diorite (or andesite).

The details of the composition of the crust are less certain, however. Ranges for the other oxides are substantially larger: 75% for FeO, 68% for MgO, and 100% for MnO. Of these estimates, the composition of Taylor and McLennan is the most mafic, and that of Weaver and Tarney the least mafic (ranges for FeO and MnO decrease to 30% and 21% respectively if the estimates of Taylor and McLennan are excluded). Wedepohl's (1995) estimated crustal composition is significantly more enriched in incompatible elements than that of Taylor and McLennan (1985, 1995); Rudnick and Gao's (2003) estimated concentrations of incompatible elements generally fall between the two.

Figure 11.34 compares the rare earth element patterns in the total continental and oceanic crusts. Both are enriched in all rare earths relative to bulk silicate Earth as well as chondrites, but whereas the continental crust is enriched in the light rare earths relative to the heavy rare earths, the opposite is true of the oceanic crust. The light rare earth enrichment of the continental crust is clear evidence that it, like the oceanic crust, originated as a partial melt of the mantle. The oceanic crust is produced through comparatively large extents of melting of mantle that has already been depleted in incompatible elements through previous episodes of melting. The evolution of the continental crust has been more complex. The strong light rare earth

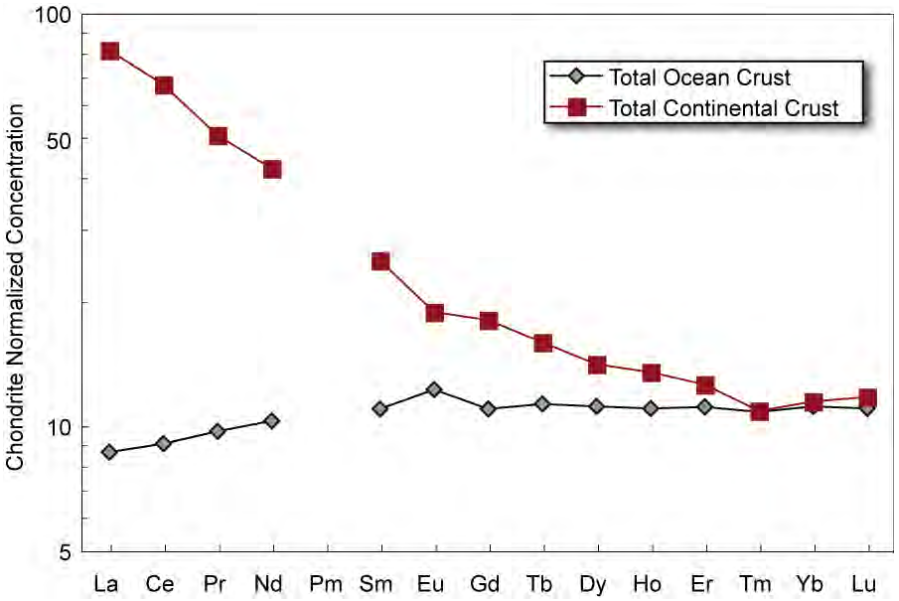

Figure 11.34. Comparison of rare earth patterns of the total oceanic (estimate of White and Klein listed in Table 11.07) and continental crust (estimate of Rudnick & Gao listed in Table 11.11).

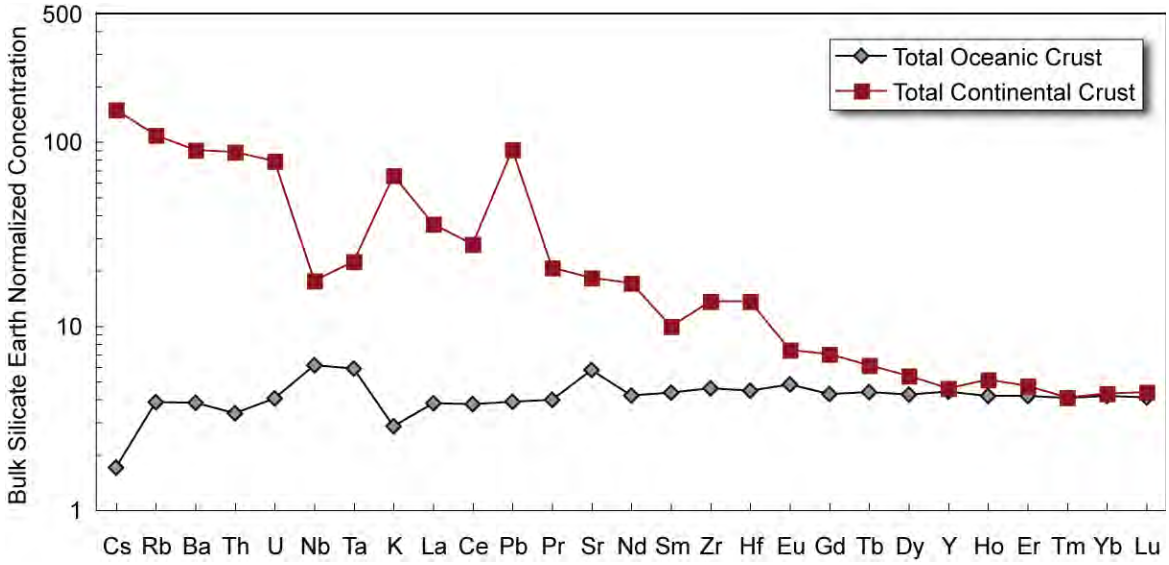

Figure 11.35. Comparison of the incompatible element enrichments of the continental (estimate of Rudnick & Gao listed in Table 11.11) and oceanic crusts (estimate of White and Klein listed in Table 11.07). Negative Nb-Ta and positive Pb anomalies, as well as the overall incompatible element enrichment are significant characteristics of continental crust.

enrichment, however, suggests that relatively small degree melts have been important in its evolution. Figure 11.35 compares the incompatible enrichment of the oceanic and continental crusts. Although the continental crust is enriched in incompatible elements overall, it is significantly less enriched in Nb and Ta and elements of similar incompatibility such as U and K; the oceanic crust exhibits a slight excess enrichment in these elements. It is also much more strongly enriched in Pb than either Ce or Sr, which are similarly incompatible. This negative Nb-Ta 'anomaly' and positive Pb anomaly are characteristics of continental crust. They provide important hints as to the mechanism(s) by which continental crust has been created, a topic we consider in the next section.

11.6.3 Growth of the Continental Crust

The oceanic crust is ephemeral; its mean age is 60 Ma and, with the exception of possible Permian age crust preserved in the Eastern Mediterranean, it is nowhere older than about 167 Ma. In contrast, the continental crust is much older. The oldest crustal rocks, Acasta gneisses in Canada's Northwest Territory, give Sm-Nd ages of 3.98 Ga. Individual zircons separated from a sandstone metamorphosed about ~3 Ga ago into quartzite in the Jack Hills of western Australia have U-Pb ages of 4.0 to 4.4 Ga. The chemical and O isotopic compositions of these grains clearly show they were once part of 'continental"-type rocks such as granites or granodiorites. There are also hints, based on $^{142}Nd/^{144}Nd$† – Sm/Nd correlations) that rocks from the Nuvvagittuq Belt of northwestern Labrador are remnants of continental crust formed at 4.28 Ga (O'Neil et al., 2008). Conventional Sm-Nd dating of these rocks, however, gives an age of 3.84 Ga, which records a subsequent metamorphism. Clearly, then, some continental crust was present very early in Earth's history. More may have been present but has not survived. Most surviving continental crust is, however, much younger.

The question of the age of the continents (very definitely a geochemical question because radiometric dating is a geochemical technique) is a complex one. Because metamorphism, remelting, etc. can reset radiometric ages, the radiometric age of a rock does not necessarily correspond to the time the material that makes up that rock first became part of the continental crust. Indeed, early efforts to system-

† Recall that ^{142}Nd is the daughter of the extinct radionuclide ^{146}Sm whose half-life is 103 Ma.

atically determine the ages of continents and rates of continental growth, such as that of Hurley and Rand (1969) substantially underestimated continental ages because they relied heavily on Rb-Sr ages, which are readily reset during metamorphism. This problem is now widely recognized and modern efforts to determine "crystallization ages" rely primarily on U-Pb dating of zircons.

Zircons are, in a sense, the ultimate natural clock/time capsule. There are several reasons for this. First, U substitutes readily in for Zr in the zircon ($ZrSiO_4$) structure, but Pb is excluded (just as we might expect from our consideration of trace element behavior in Chapter 7 since Zr and U have the same charge, +4, and similar size, Zr = 72 pm; U = 89 pm, whereas Pb has a +2 charge and 119 pm radius). Second, the two U isotopes have short half-lives compared to most other radioactive nuclides used in geochronology. The short half-lives and high U concentrations result in rapid build-up of radiogenic Pb in zircon, allowing for more precise age determinations than other methods can provide. Third, zircon is a chemically robust mineral that resists weathering and chemical breakdown. Fourth, it is a mechanically robust mineral (Mohs hardness of 7.5) and readily survives transport in rivers and streams. Finally, because U has two isotopes that decay to isotopes of Pb at different rates (see Chapter 8), it is possible to determine whether or not the system has been disturbed by subsequent events such as metamorphism. When ^{236}U-^{207}Pb and ^{238}U-^{206}Pb ages agree the age is said to be *concordant*. The systematics of U-Pb often allow the original crystallization age to be determined even when ages are discordant. Finally, it is also possible, using approaches that include mechanical and chemical abrasion and *in situ* analysis, to analyze only the least disturbed parts of zircon crystals*. Thus zircon dating has become 'the gold standard' for determining rates of continental growth. The most recent compilation of ages, that of Condie and Aster (2010), is shown in Figure 11.36.

We can draw several important inferences from Figure 11.36. First, continent production has been episodic. Pulses occurred at approximately 750, 850, 1760, 1870, 2100, 2650, 2700, and 2930 Ma. Other studies have found similar episodicity, which is widely thought to be related to supercontinent cycles. Second, only a small fraction of the surviving continental crust is older than 2.8 Ga (about 6%, according to Condie and Aster). Third, after the large pulse in crust production at 2.6 to .8 Ga, each succeeding pulse has been smaller. Condie and Aster (2010) conclude that only 14% of the continental crust is younger than 600 Ma.

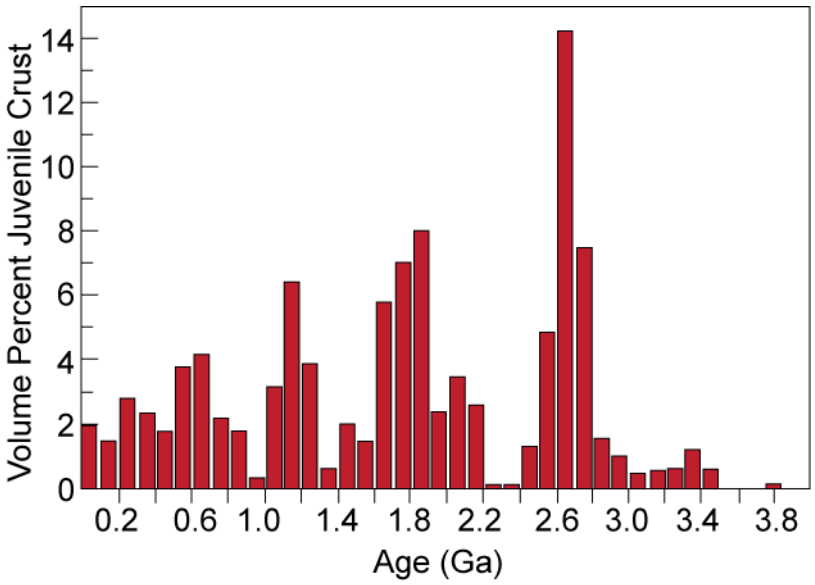

Figure 11.36. Estimated volume of juvenile (i.e., new) crustal additions as a function of geologic age estimated from a database of 40,000 U-Pb ages of granitoid and detrital zircons. After Condie and Aster (2010).

Zircons, however, are an imperfect recorder of crustal growth. One of the problems is that zircons do not crystallize from mafic melts. As we noted above, $^{142}Nd/^{144}Nd$ – Sm/Nd correlations suggest that rocks from the Nuvvagittuq Belt of Labrador may have first formed 4.28 Ga ago but their ^{147}Sm-^{143}Nd age are much younger (O'Neil et al., 2008). The ^{147}Sm-^{143}Nd age was probably reset during a metamorphic event. The rocks themselves, which might have originally been

* Radiation damage is a major cause of discordance in zircon ages. U concentrations that are too high are a curse, since this leads to severe radiation damage and discordant ages. Damaged zircon crystals or parts of the crystals are said to be *metamict*. These can be seen under the microscope and avoided in *in situ* analysis.

basaltic dikes, are mafic amphibolites and contain no zircons. Since mantle melts are almost always mafic in nature, their lack of zircons greatly complicates identifying new additions to the continents from the mantle. Furthermore, remelting of crustal rocks, undoubtedly an important process, may destroy any original zircons with younger ones crystallizing in their place.

Sm-Nd model ages, or crustal residence times, introduced in Chapter 8, provide one way of discriminating between mere reprocessing of pre-existing crust and production of new crust from the mantle. The study of the western U. S. by Bennett and DePaolo (1987) provides an example of the insights Sm-Nd model ages can provide into crustal evolution. Figure 11.37 is a map of the Western U. S. showing contours of Nd crustal residence times (τ_{DM}). The data define 3 distinct provinces and suggest the existence of several others. Ages deduced in this manner are significantly older than those Hurley and Rand (1969) determined using Rb-Sr dating. Figure 11.38 shows the initial ε_{Nd} values of granites from the three numbered provinces of Figure 11.37 plotted as a function of their crystallization age. Although the crystallization ages are often much younger, crustal residence times indicate Provinces 1-3 all formed between 1.65 and 1.8 Ga. Only in province 3 do we find rocks, tholeiitic and calc-alkaline greenstones, whose Sm-Nd crustal residence age is equal to their crystallization ages. From this we can conclude that only Province 3 was a completely new addition to the crustal mass at that time. In the other regions, the oldest rocks have initial ε_{Nd} values that plot below the depleted mantle evolution curve. This suggests that mantle melts mixed with pre-existing crust, perhaps

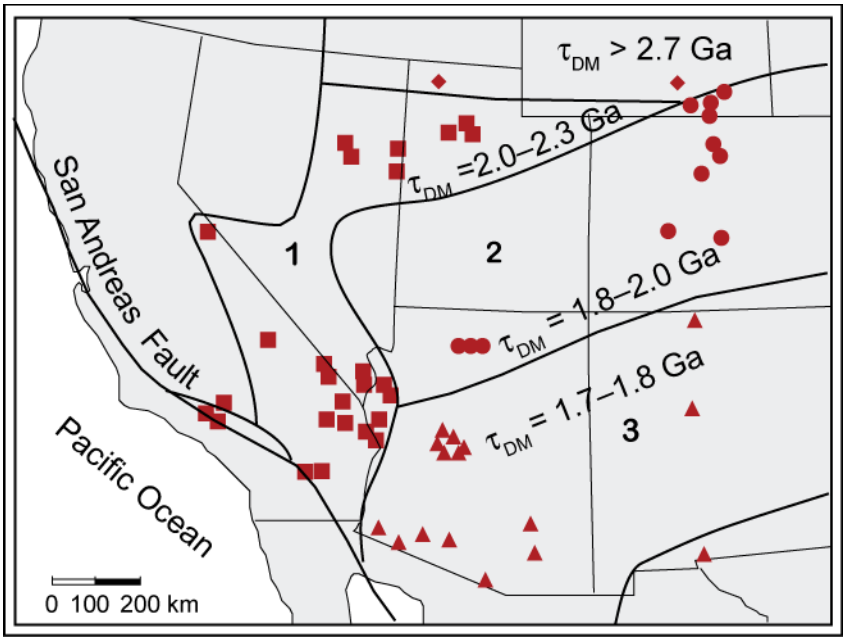

Figure 11.37. Isotopic provinces, based on crustal residence times (τ_{DM}) of the Western U.S. After Bennett and DePaolo (1987).

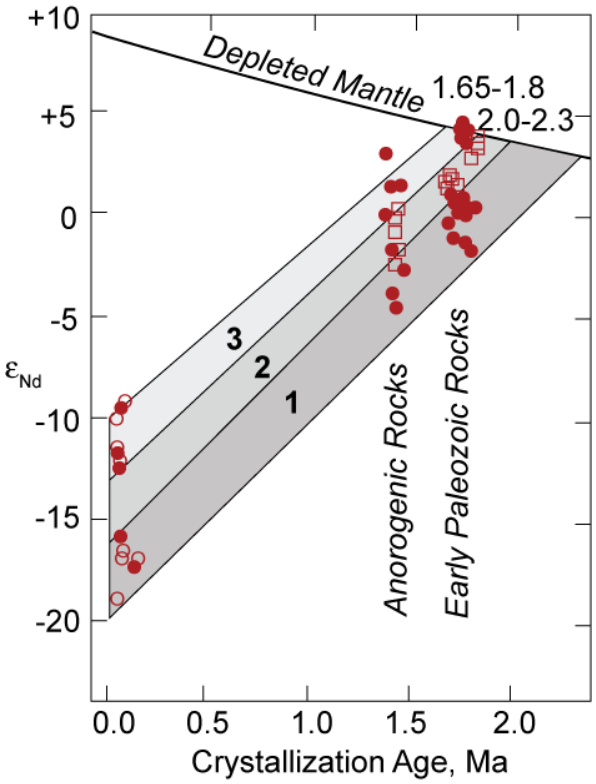

Figure 11.38. Initial ε_{Nd} as a function of crystallization age for igneous rocks of the western U.S. Groupings 1 2, and 3 refer to provinces shown in Figure 11.36. After Bennett and DePaolo (1987).

by assimilating crust (which would have a lower melting temperature) as they ascended through it. Alternatively, pre-existing continental crust might have been carried into the mantle by sediment subduction or subduction erosion (topics we consider below) and mixed with mantle before melting.

Throughout the region there were subsequent episodes of magmatism, including one in the Tertiary. However, the initial ε_{Nd} lie along the same growth trajectory as the older rocks. This suggests that these subsequent igneous events involved remelting of existing crust with little or no new material from the mantle.

The Lu-Hf model ages can also discriminate between reprocessing existing crust and new additions to crust in an analogous manner. This system has the advantage that Hf is strongly concentrated in zircons (not surprisingly, given the similar chemical behavior of Hf and Zr) while Lu is not. Consequently, initial Hf isotopic compositions of zircons are readily determined. These can be compared with models of Hf isotopic evolution in the mantle and, hence, whether or not a zircon, and the rock containing it, was a crustal- or mantle-derived melt. Combined with U-Pb age determinations in the same zircons, this provides a powerful tool that will likely see more common use in the future. A drawback of the Lu-Hf system is that Lu and Hf are readily fractionated within the crust, particularly by weathering and sedimentary processes, whereas Sm and Nd are not.

Figure 11.36 and Sm-Nd and Lu-Hf model ages inform us only about continental crust that has survived to the present day. As we'll discuss below, continental crust can be destroyed. This could bias the inferences we draw from Figure 11.36. However, this should produce a bias for younger crust; thus declining crustal production is unlikely be an artifact. Declining rates of magmatism and tectonism should, in any case, come as no surprise since radioactive decay and original heat provide the energy for those processes. It is also difficult to see how the apparent episodicity in Figure 11.36 could be an artifact of crustal destruction, unless the destruction were also pulsed in tandem with crustal production, which is exactly what Hawkesworth et al. (2010) have proposed.

Nevertheless, one of the most enduring debates in geology is the question of how crustal mass has changed over time and what the *net* rate of crustal growth has been. Armstrong (1968, 1981) argued that despite evidence of new additions to crust throughout geologic time, the mass or volume of continents has remained essentially unchanged since 4.0 Ga because the rate of destruction of continental crust has matched the rate of production. Others, for example, Hurley and Rand (1969) and Vezier and Jansen (1979) argued that there was little crust present before 2.0 Ga. There are at least 3 mechanisms by which continental crust can be destroyed: (1) erosion and transport of sediment to the ocean where it is subsequently subducted into the mantle, (2) subduction erosion, the process by which a subducting plate abrades and removes material from the overriding plate and carries it into the mantle, and (3) lower crustal floundering or delamination, where by during plate convergence, crust becomes over-thickened, resulting in the lower crust being converted to dense eclogite and sinking into the mantle. There is good evidence that all three mechanisms operate and some have argued that the rates of the first two processes are sufficient to balance rates of new crustal addition and, therefore, produce a steady-state crustal volume, just as Armstrong proposed. However, now consensus has formed around these views and the question of the net change in crust mass is still debated.

In summary, we can say that continental crust has been produced over much, if not the entire history of the Earth, but crustal production has been very much episodic. The rate of new crust production has been declining over the last 2.5 Ga. Rates of crustal destruction and *net* continental growth remain controversial.

11.6.4 Subduction Zone Processes and the Origin of Continents

As we have often stated, the crust has growth through magmatism. In the modern Earth and throughout the Phanerozoic, nearly all magmatism occurs and has occurred in one of three tectonic environments: (1) along divergent plate boundaries, such as the Mid-Atlantic Ridge, or intraplate rifts, such as the Great African Rift or the Rio Grande Rift; (2) above mantle plumes, Hawaii for example; and (3) above subduction zones at convergent plate boundaries such as the Andes. While magmatism in all three environments has undoubtedly contributed to continental growth, geochemical evidence suggests that the latter has been the dominant process by which the continents have grown. Figure 11.39 compares incompatible element abundances in the continental crust with examples of magmas

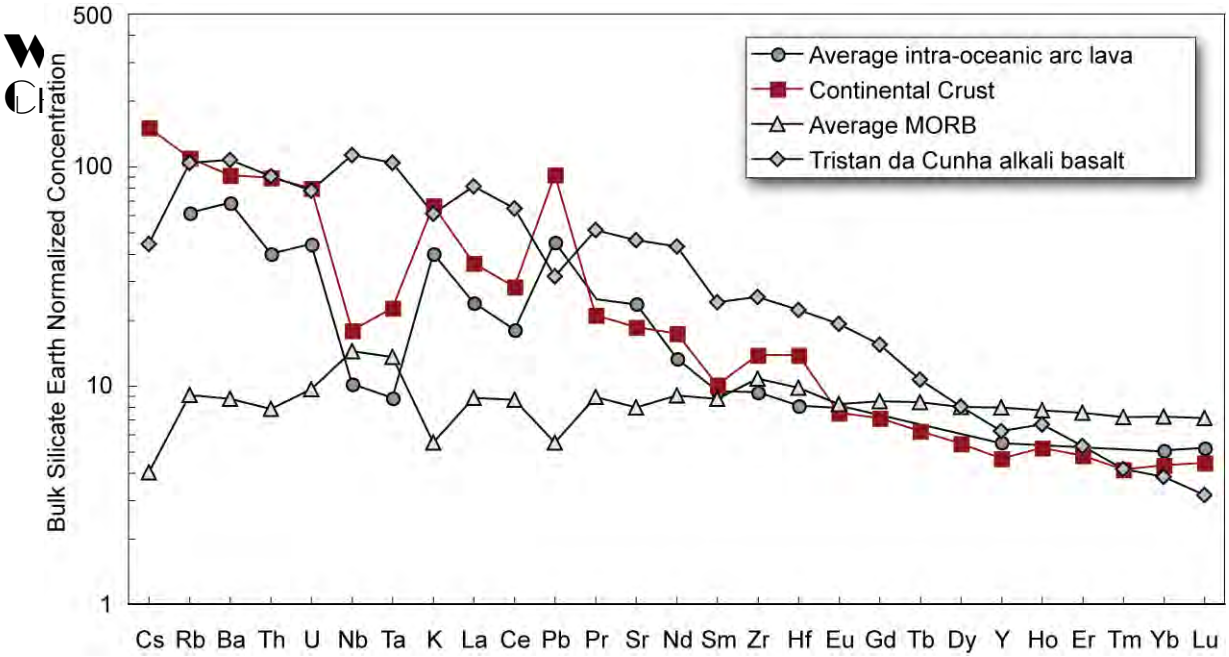

Figure 11.39. Normalized incompatible enrichments of average MORB (Table 11.07), average composition of lavas from 8 intra-oceanic island arcs studied by Porter and White (2009), and an alkali basalt from Tristan da Cunha compared with incompatible element enrichment of the total continental crust (Table 11.11). Only the pattern of island arc lavas matches that of the continental crust.

produced in these three environments: average MORB for convergent boundary settings, an alkali basalt from the South Atlantic volcanic island of Tristan da Cunha, and average intra-oceanic island arc lava. There are clear similarities between the continental crust and the island arc lava: both exhibit incompatible element enrichment, negative Nb-Ta anomalies, and positive Pb anomalies. MORB and the Tristan da Cunha exhibit slight positive Nb-Ta anomalies and negative Pb anomalies. It is also true that at present, most new additions to crust occur in subduction zones, for example, the volcanoes of the Andes and Alaskan Peninsula. Let's consider the geochemistry of subduction zone volcanism in a bit more detail.

11.6.4.1 Major Element Composition

Magmas found in island arcs (we'll use the term *island arc* for all subduction zone magmatism, including continental margin type) appear to be predominantly andesitic. It seems unlikely that andesite is the principle magma produced in arcs, however. Generally, we don't see the lower parts of arc volcanic edifices, which may be basaltic. There is also considerable doubt whether an andesite can be produced by partial melting of the mantle, particularly at depth. Most arcs sit about 100 km above the Benioff zone, and magmas may be generated close to this depth. A safer bet is that the primary magma is actually basaltic, of which andesites are fractional crystallization products. In any case, basalt is not uncommon in intra-oceanic arcs.

In major element composition, island-arc volcanics (IAV) are not much different from other volcanic rocks. Compared to MORB, the major difference is perhaps simply that siliceous compositions are much more common among the island-arc volcanics. Most IAV are silica saturated or oversaturated; silica undersaturated magmas (alkali basalts) are rare. In that sense, we might call them *tholeiitic*. However, in the context of island arc magmas, the term *tholeiite* has a more restrictive meaning. Two principal magma series are recognized, one called *tholeiitic*, the other called *calc-alkaline*. There are two principal differences between these rock series.

First, tholeiites differentiate initially toward higher Fe and tend to maintain higher Fe/Mg than the calc-alkaline lavas (Figure 11.40). The lower Fe content of the calc-alkaline series reflects results from the suppression of plagioclase crystallization as a result of (1) higher pressure and (2) higher water content of the magma (Grove and Baker, 1984). In the tholeiitic series, the crystallization sequence is typically olivine, plagioclase, followed by clinopyroxene. At higher pressure or higher water content, clinopyroxene supplants plagioclase as the second crystallizing phase, which buffers the iron concentration. As we shall see, another characteristic of subduction zone magmas is that they can have much

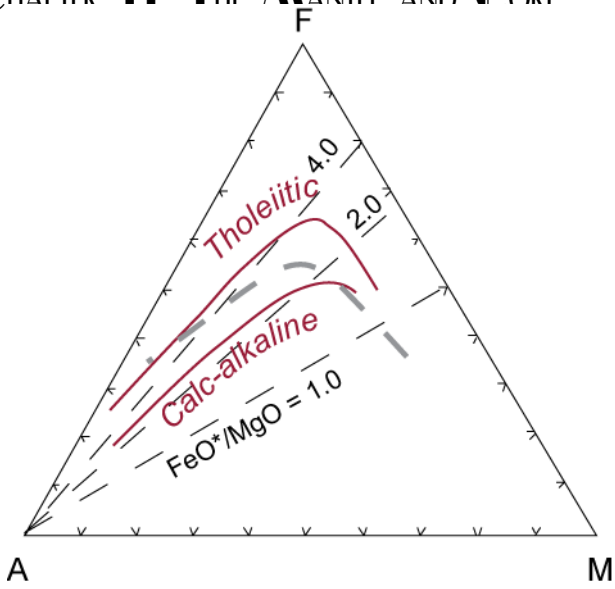

Figure 11.40. AFM (A=K_2O+Na_2O, F=FeO+MnO, M=MgO) diagram illustrating the difference between tholeiitic and calc-alkaline lava series of island arcs. Calc-alkaline rocks plot below the heavy gray line, tholeiites above.

higher water content than magmas found in other tectonic settings. Kay et al. (1983) found that, in least for the Aleutians at least, occurrence of these two phases could be related to tectonic environment. Tholeiites occur in extensional environments within the arc where magma can ascend relatively rapidly into the upper crust where they undergo fractional crystallization at low pressure. Calc-alkaline lavas tend to occur in compressional environments within the arc where they cannot so readily ascent to shallow depths and hence undergo crystallization at greater depth.

The second difference is that calc-alkaline magmas are richer in alkalis (K_2O and Na_2O) than tholeiites. Indeed, the calc-alkaline magmas are defined as those that have $Na_2O+K_2O \approx CaO$, whereas tholeiites have $Na_2O+K_2O < CaO$, and alkaline rocks have $Na_2O+K_2O > CaO$. IAV also tend to be somewhat poorer in Ti than MORB and OIB.

Perfit et al. (1980) argued that the difference in Ti content is due to early crystallization of oxides, illmenite ($FeTiO_3$) in IAV, which buffers the Ti concentration. That in turn, they argued, reflected higher oxygen fugacities. Kelley et al (2009) have confirmed higher fugacities in IAV by measuring the Fe^{2+}/Fe^{3} ratio in glass inclusions in phenocrysts using synchrotron-based near-edge structure (μ-XANES) spectroscopy. The technique makes use of small differences in the X-ray adsorption spectra of Fe^{2+} and Fe^{3+}. A synchrotron produces a sufficiently high intensity X-ray beam for this analysis to be performed on the micron scale. The fount that while MORB had $Fe^{3=}/\Sigma Fe$ of 0.13 to 0.17, IAV had $Fe^{3=}/\Sigma Fe$ of 0.18 to 0.32. They also found that $Fe^{3=}/\Sigma Fe$ correlated directly with water content.

Plank and Langmuir (1988) investigated the factors that control the variation in major element composition of island arc basalts. They treated the data in a manner analogous to Klein and Langmuir (1987), correcting regional data sets to a common MgO content, but they used 6% MgO rather than the 8% used by Klein and Langmuir. They found that $Na_{6.0}$ and $Ca_{6.0}$ (i.e., Na_2O and CaO concentrations corrected to 6% MgO) correlated well with crustal thickness (Figure 11.41). They argued that crustal thickness determines the height of the mantle column available for melting. Most island arc volcanoes are located above the point where the subducting lithosphere reaches a depth of 100-120 km. This suggests that melting begins at a relatively constant depth in all island arcs. If this is so, then the distance over which mantle can rise and undergo decompressional melting will be less if the arc crust is thick, leading to smaller extents of melting beneath arcs with thick crust, and higher $Na_{6.0}$ and $Ca_{6.0}$ in the parental magmas.

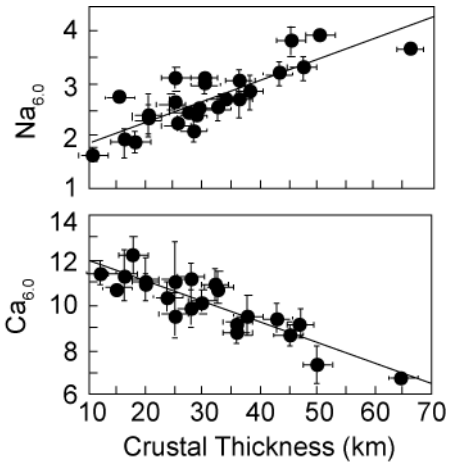

Figure 11.41. Correlation of $Ca_{6.0}$ and $Na_{6.0}$ with crustal thickness in island arc basalts. $Ca_{6.0}$ and $Na_{6.0}$ are the CaO and Na_2O concentrations after correction for fractional crystallization to 6.0 MgO. After Plank and Langmuir (1988).

11.6.4.2 Trace Element Composition

The differences in trace elements between island arc volcanics and those from other tectonic environments are more significant than the differences in major elements. Rare earths, however, are not particularly distinctive. There is a very considerable range in rare earth patterns: from LRE depleted to LRE enriched (Figure 11.42). IAV are virtually never as LRE depleted as MORB, but absolute REE concentrations are often low, and it is not unusual for the middle and heavy rare earths to be present at lower concentrations than in MORB. One other aspect is of interest. Ce anomalies occur in some IAV, whereas they are never seen in MORB or OIB, though they have been observed in continental carbonatites and kimberlites. Ce anomalies occur in sediment, so there is suspicion that the anomalies in IAV are inherited from subducted sediment.

An important and ubiquitous feature of island-arc volcanics is a relative depletion in Nb and Ta, which can be seen in Figure 11.38. Island-arc volcanics are also richer in the incompatible alkalis and alkaline earths (K, Rb, Cs, Sr, and Ba) relative to other incompatible elements when compared with MORB or OIB. This is illustrated in Figure 11.43, using the Ba/La ratio. Though both IAV and oceanic basalts can have a large range in rare earth patterns, as illustrated by the range in La/Sm ratios, the Ba/La ratios of IAV are generally higher.

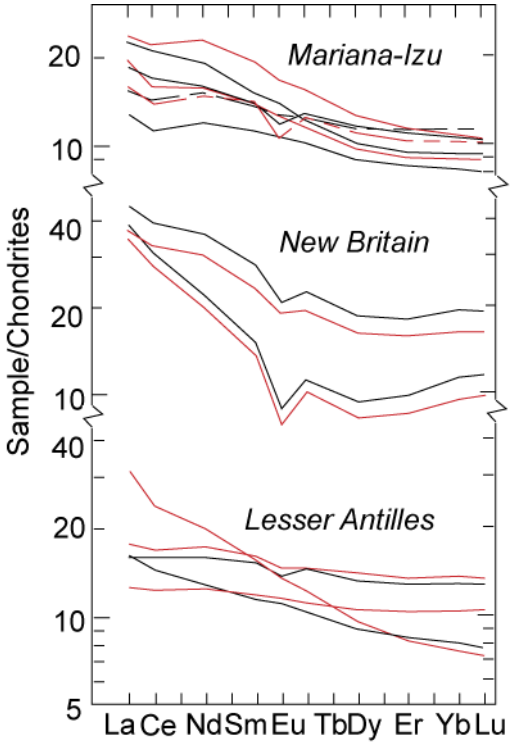

Figure 11.42. Rare earth patterns of some typical island arc volcanics. After White and Patchett (1984).

11.6.4.3 Isotopic Composition and Sediment Subduction

Island arcs overlie subduction zones, which raises the obvious question of the degree to which subducting lithosphere, including oceanic crust, overlying sediment and underlying mantle lithosphere, might contribute to island arc magmas. These questions have been most successfully addressed through isotope geochemistry. Sr isotope ratios are generally higher, and Nd isotope ratios generally lower than in MORB, with $^{87}Sr/^{86}Sr$ ratios around 0.7033-0.7037 and ε_{Nd} of +6 to +8 being fairly typical of intra-oceanic IAV. This range overlaps considerably with MORB and OIB, there is, however, a tendency for IAV to have slightly higher Sr isotope ratios for a given Nd isotope ratio and hence plot to the right of the oceanic basalt array on a Nd–Sr isotope ratio plot such as Figure 11.12. This shift to higher Sr isotope ratios is thought to reflect a contribution of sub-

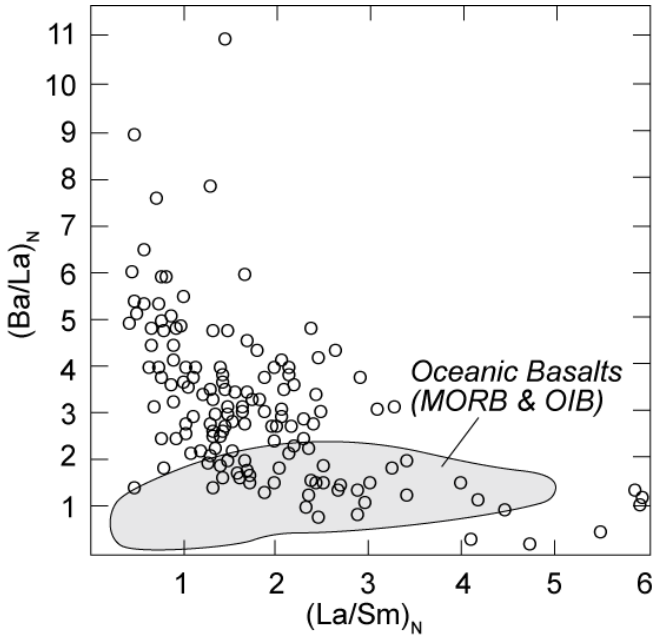

Figure 11.43. Relative alkali-alkaline earth enrichment of IAV illustrated by plotting the $(Ba/La)_N$ ratio vs. the $(La/Sm)_N$ ratio. The subscript N denotes normalization to chondritic values. After Perfit et al. (1980).

ducted oceanic crust to IAV magma sources. Weathering and hydrothermal alteration of the oceanic crust shifts Sr isotope ratios of the oceanic crust toward seawater (higher) values, but does not affect Nd isotope ratios because of the extremely low concentration of Nd in seawater.

Clear evidence of sediment involvement comes from Pb isotope studies of island arc volcanics, beginning with the work of Armstrong and Cooper (1971). As Figure 11.44 shows, $^{206}Pb/^{204}Pb$ isotope ratios overlap MORB values, but $^{207}Pb/^{204}Pb$ ratios are typically higher IAV than most oceanic basalts. They tend to form steeper arrays on $^{207}Pb/^{204}Pb$–$^{206}Pb/^{204}Pb$ plots, and overlap the field of marine sediments. For most island arcs, Pb isotope ratios in the arc volcanics lie between sediment local to the arc and the MORB field (Karig and Kay, 1980). On the whole then, Pb in island arc magmas appears to be a mixture Pb from local sediment and local upper mantle.

Finally, ^{10}Be provides unequivocal evidence of sediment involvement in IAV magma sources. As we found in Chapter 8, ^{10}Be is a cosmogenic isotope produced in the atmosphere by cosmic ray spallation of ^{14}N. It has a half-life of only 1.5 million years, so we would not expect to find significant amounts of ^{10}Be in the Earth's interior; any present when the Earth formed has long since decayed away. ^{10}Be created in the atmosphere is purged by rainfall and is strongly absorbed by clays of sediment and soil. Tera et al. (1986) found measurable quantities (>10^6 atoms per gram) of ^{10}Be in some arc lavas, while ^{10}Be was completely absent non-arc lavas. The interpretation is that the ^{10}Be originates from sediment subducted to the magma genesis zone.

Subducted sediment appears to influence the trace element compositions of arc lavas as well. Plank and Langmuir (1993) carried out careful study of the composition of volcanics from 8 arcs and the sediments being subducted beneath them. By analyzing representative samples from the sediments and considering the proportions of sediment types being carried beneath the arc, they estimated the flux of elements being carried by sediment beneath the arc. They found they could relate the degree of enrichment of most incompatible elements to the sediment flux of that element. For example, the

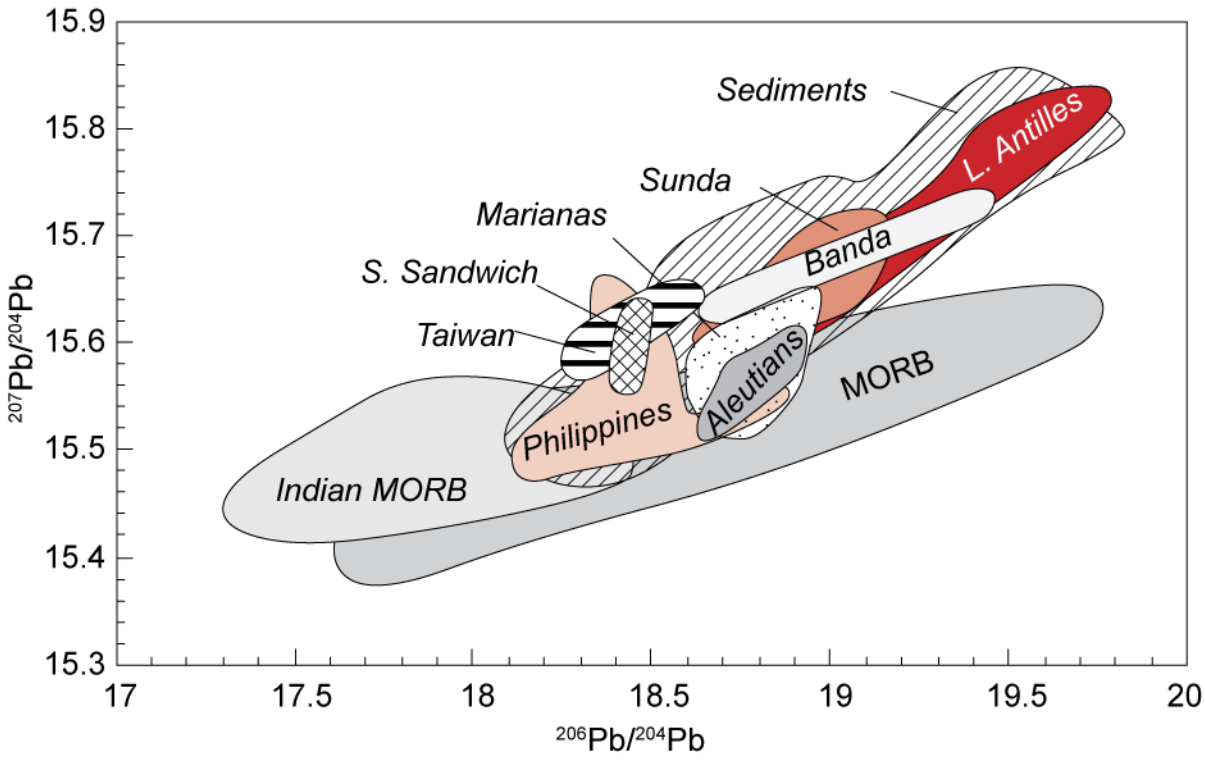

Figure 11.44. Pb isotope ratios in island arc volcanics. Fields for the South Sandwich, Lesser Antilles, Aleutians, Marianas, Philippines, Taiwan, Banda and Sunda arcs are compared with fields for Atlantic and Pacific MORB (field labeled MORB) and Indian Ocean MORB, and modern marine sediments.

Ba/Na and Th/Na ratio (after correction for fractional crystallization to 6% MgO) correlate strongly with the Ba and Th sediment fluxes (Figure 11.45). Different arcs are enriched to different degrees in these elements: for example, the Lesser Antilles arc has moderate Th/Na ratios but low Ba/Na ratios. The difference appears to be due to the difference in the sediment flux.

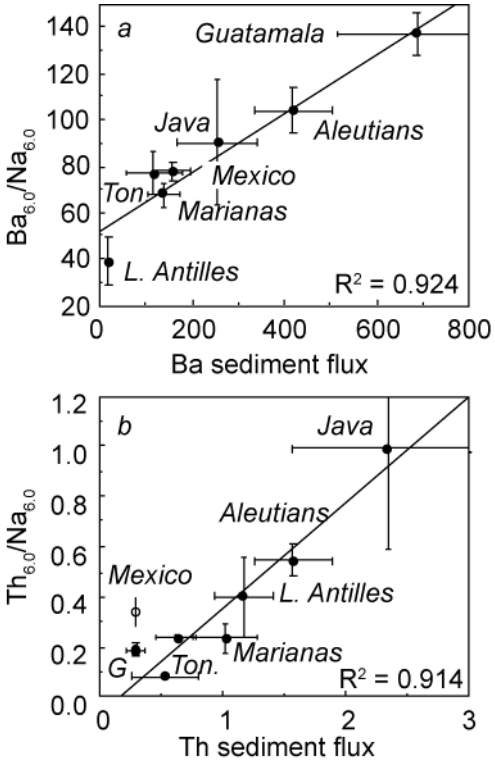

Figure 11.45. Relationship between $Ba/Na_{6.0}$ and $Th/Na_{6.0}$ in volcanics from 8 arcs and Ba and Th sediment flux beneath those arcs. Horizontal bars represent uncertainty in the amount of sediment subducted; vertical bars reflect the variance of the ratio in the arc volcanics. G is Guatemala, M: Mexico, J: Java, T: Tonga, Mar: Marianas, Al: Aleutians, Ant: Lesser Antilles. From Plank and Langmuir (1993).

11.6.4.4 Magma Genesis in Subduction Zones

Now that we have an overview of the composition of arc magmas, let's consider in more detail the processes that lead to the unique geochemistry of island arc magmas. Most geochemists and petrologists believe that arc magmas are produced primarily within the mantle wedge, the part triangular region of mantle overlying the subducting slab. The evidence for this is: (1) Primary arc magmas differ only slightly in their major element chemistry from oceanic basalts, which are definitely mantle-derived; the andesitic nature of many arc magmas probably results from fractionation crystallization in a crustal or subcrustal magma chamber. It is therefore most likely IAV are partial melts of peridotite rather than subducted basalt or sediment. (2) Radiogenic isotopic and trace element systematics generally allow only small fraction of sediment (generally a few percent or less) to be present in arc magma sources. Relatively high $^3He/^4He$ ratios in arc lavas confirm a mantle source. (3) Rare earth patterns of island arc magmas are consistent with these magmas being generated by partial melting of peridotite, but not by partial melting of eclogite, which would be the stable form of subducted basalt at 100 km depth (the subducting lithosphere is typically located at about 100 to 120 km depth beneath island arc volcanoes). Because the heavy rare earths partition strongly into garnet (e.g., Figure 7.16), melts of eclogite should show steep rare earth patterns, with low concentrations of the heavy rare earths. This is not generally the case. Rare high magnesium andesites, sometimes called "adakites" (after a well documented occurrence on Adak Island in the Aleutians) with steep rare earths patterns may represent exceptions to this rule and may indeed by generated by small extents of melting of subducted oceanic crust (Kay, 1978; Defant and Drummond, 1990). It is possible that such "slab melts" were more common several billion years ago.

If IAV magmas are not melts of the slab, how do they acquire the geochemical signature or "flavor" of subducting oceanic crust and sediment? Dehydration and migration of the evolved hydrous fluid has long been suspected as the primary means by which the subducting slab influences the composition of IAV magmas. For example, White and Dupré (1986) modeled the observed enrichment of Lesser Antilles low-K basalts in incompatible elements assuming the source was a mixture of depleted mantle and sediment using Nd isotope ratios to calculate the fraction of sediment. This simple model predicted the concentrations of the rare earths and Th reasonably well, but the enrichment of Pb, Cs, Rb, U, K, Ba, and Sr was greater than predicted. These are the elements expected to partition into hydrous fluid, suggesting their enrichment was due to preferential partitioning into and transport by aqueous fluids. The elemental fractionation that must occur during transported from the subducting slab into the mantle wedge is further illustrated in Figure 11.46. Ba/La ratios in Marianas arc lavas plot systematically above a mixing line between MORB and sediment subducting beneath the arc (sampled in ODP

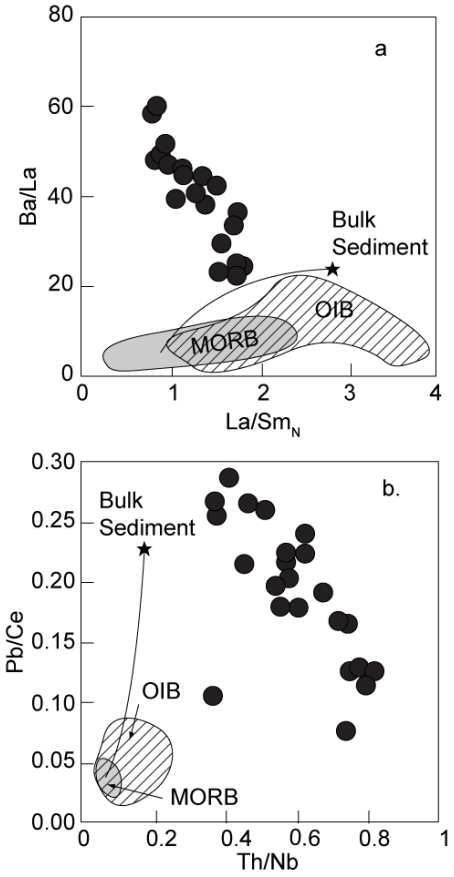

Figure 11.46. a. Ba/La vs La/Sm$_N$ (subscripted N denotes the chondrite-normalized ratio) in Marianas arc lavas compared with those in MORB, OIB, and bulk sediment from ODP Hole 801b, located on the Pacific plate outboard of the Marianas arc. Line connecting MORB and sediment is a mixing curve. Ba enrichment in the arc cannot be explained only by mixing of MORB and sediment. B. Pb/Ce vs. Th/Nb is Marianas arc lavas. Th is enriched more than can be explained by sediment-MORB mixing alone. Elliott et al. (1997) suggested sediment melting is responsible. Modified from Elliott et al. (1997).

Hole 801) on a plot of Ba/La vs. La/Sm. The same is true of Th/Nb ratios (Figure 11.46b), which are systematically higher than predicted from simple MORB-sediment mixing. Elliott et al. (1997) concluded from these relationships and $^{230}Th/^{232}Th$ isotope ratios (recall that ^{230}Th is the intermediate daughter of ^{238}U), that both a hydrous fluid and a silicate melt were involved in transport of sediment. They proposed that the melt was a result of hydrous partial melting of the subducted sediments. Melting is necessary to account for the fractionation between Th and Nb, neither of which is particularly soluble in aqueous fluids. Furthermore lavas with the highest Th/Nb also show the greatest light rare earth enrichment. Subsequent dehydration and melting experiments by Johnson and Plank (1999) confirmed the need for melting to transport elements such as Th into the magma genesis zone of the subarc wedge.

This brings us to what is perhaps the most fundamental question: why does melting occur at all in an area where cold lithosphere is descending? The answer is water. Water lowers the solidus of rock and leads to enhanced melting at any given temperature compared to dry conditions; water released by the subducting slab migrates into the overlying hotter mantle wedge where it induces melting. The extent of this effect had been somewhat uncertain, in large part due to experimental difficulties. This has now been largely resolved and it is clear that the effect is a large one. Figure 11.47 is a P-T phase diagram (Chapters 3 and 4) based on the work of Grove et al. (2006) and shows that under water-saturated conditions, the peridotite solidus is depressed by hundreds of degrees C compared to the "dry solidus". At 1.5 GPa (corresponding roughly to 50 km depth in the Earth), peridotite begins to melt at over 400°C lower temperature than under "dry" conditions. The effect is even larger at higher pressure.

Figure 11.47 also shows that at pressures above about 2 GPa, ilmenite along with chlorite would be stable at and above the solidus. The stability of ilmenite is particularly significant because Nb and Ta strongly partition into it. Thus the characteristic Nb-Ta depletion of island arc lavas, and indeed the entire continental crust (Figure 11.38) may be due to residual ilmenite being present during the initial states of melting deep within the arc.

Figure 11.48 summarizes magma generation at subduction zones. Sediment and hydrothermally altered oceanic crust carry water and incompatible elements into the mantle as oceanic lithosphere is subducted. Where the sediment pile is thick, such as in the Lesser Antilles and Sunda arcs, some or most of the sediment is scraped off creating *accretionary prisms*, but both seismic and geochemical evidence indicates that some, 100 m or more, is subducted. Compression during the early phases of subduction drives off much of the unbound water occupying pores and veins in the subduction lithosphere. This water sometimes emerges as "seeps" in accretionary prisms and supports chemosynthetic

communities. In other cases, it hydrates and serpentinizes the overlying shallow mantle. Some much water is liberated that the serpentine is mobilized and can emerge as serpentine mud volcanoes, such as those found in the Marianas forearc.

As the subducting lithosphere encounters increasing temperature and pressure it is metamorphosed with water-rich minerals progressively replaced by water-poor ones and ultimately by anhydrous minerals. The water released in these reactions rises into the overlying mantle wedge. The wedge immediately above the subducting slab has an inverted thermal gradient: temperature decreases with depth because the cold subducting slab acts as a heat sink. Immediately above the slab, the mantle is too cold to melt, even though it is water saturated. However, 10 km above the slab, temperatures approach 1000° C, above the dry solidus, but well above the wet solidus. Consequently, melting begins. These initial melts may contain as much as 28% water (Grove et al., 2006), but as they rise, continued melting progressively dilutes the water content.

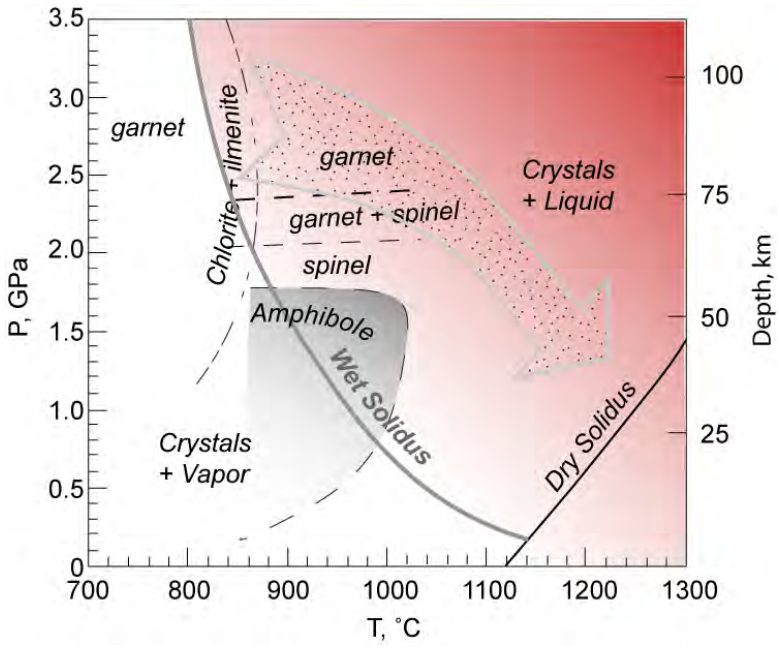

Figure 11.47. Experimentally based phase diagram for the system peridotite+water. The peridotite dry solidus is from Hirschmann (1999). Under 'wet' conditions, meaning vapor present, peridotite begins to melt along the curve labeled "wet solidus" at temperatures hundreds of degrees lower. Curved dashed lines are the chlorite+ilmenite- and amphibole-out curves. Straight dashing lines illustrate the progressive replacement of spinel with garnet Broad stippled arrow shows the path the melts take in T-P space as they rise through the mantle wedge (Figure 11.47). Modified from Grove et al. (2006).

Work over the past couple of decades has produced directly evidence relating water content to melting in subduction zones has. Stolper and Newman (1994) showed that water concentrations correlated inversely with the concentrations of moderately incompatible elements, such as Ti, Zr, and Na in lavas from the Marianas back-arc spreading center. Since water, or H, effectively behaves as an incompatible element itself, this requires explanation. Stolper and Newman (1994) proposed that extent of melting varied inversely with the amount of H_2O-rich component in the source mixture. The smallest extents of melting (about 5%) occur in H_2O-poor sources and give rise to incompatible element-rich basalts, while the highest extents (over 20%) give rise to H_2O-rich and incompatible element-poor basalts. Stolper and Newman (1994) focused on back-arc basalts because they erupted at under several km of water, where pressure prevents degassing of water. Degassing typically results in the loss of all volatiles in subareally erupted lavas, so 11measuring their water contents is generally meaningless. Kelley et al. (2010) got around this problem by measuring the water content of melt inclusions, microscopic pockets of melt trapped in olivine crystals, in the lavas of Marianas arc volcanoes by using Fourier Transform Infrared Spectrometry (FTIR), which measures water content by measuring the absorption of infrared radiation by the O-H bond, and by ion probe. That study confirmed the results of Stolper and Newman (1994), again revealing an anti-correlation between water content and concentrations of moderately incompatible elements.

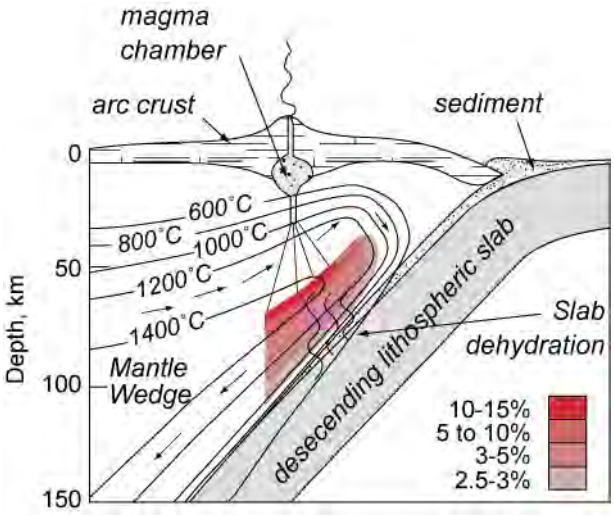

Figure 11.48. Cross-section of a subduction zone illustrating island-arc magma genesis. Arrows show the direction of mantle flow. Color shading indicates the predicted extent of partial melting in the mantle wedge resulting from the addition of water. Modified from Grove et al. (2006).

In summary, much of the continental crust has been produced through subduction zone magmatism. (This is certainly a bit ironic, since subduction zones are where oceanic crust and lithosphere destroyed along with smaller amounts of continental crust. The graveyard of continental crust is also its nursery.) Magmatism in subduction zones results from *flux melting*, i.e., the lowering of the solidus by the addition of water. Virtually everywhere else on Earth melting results from decompression (see discussion in Chapter 7). Water also transfers the incompatible element and isotopic 'flavor' of subducting oceanic crust and sediment to the melting region in the mantle wedge melting generation zone, and from there into the crust formed by this magmatism. Partial melts of the oceanic crust and sediment can also carry this flavor into the magma genesis zone. These processes ultimately account for enrichment of continental crust in incompatible elements and its anomalous enrichment in fluid-mobile elements such as Pb. The distinctive negative Nb-Ta anomalies of continental crust and island arc lavas result from retention of these elements in residual ilmenite stabilized by hydrous melting conditions.

Although subduction-related volcanism seems to have been the dominant mode of crustal growth at least through the Proterozoic and Phanerozoic, other mechanisms have played a role. The Wrangalia Terrane in NW British Columbia and Alaska, is widely considered to consist in part of oceanic plateaus. The plateaus were produced over a mantle plume in Paleozoic time and later accreted to the North American continent by plate tectonic processes. The Coast Ranges of Oregon represent another example of accreted oceanic crust. Mantle plumes surfacing beneath continents also produce magmas that add mass to the continents. The most voluminous eruptions occur in the initial stages of the plume, when the large buoyant plume head approaches the surface. Under these circumstances, enormous volumes of basalt erupt. Examples of such flood basalts include the Siberian Traps, the Karoo of South Africa, the Deccan of India, the Parana of Brazil, and the Columbia River of the NW U. S. Gravity anomalies suggest even greater volumes of basaltic magma were trapped at deep crustal levels. This process, whereby dense basaltic magma crystallizes at near the base of the crust, is sometimes called underplating. This may be an important mechanism of crustal growth, but with few samples from this region, the overall importance of this process is difficult to evaluate.

Continental rifts can also be sites of voluminous eruption of basaltic magma. A well-documented example is the Proterozoic Keweenawan or Mid-Continent Rift of the U. S., which formed some 1 to 1.2 Ga ago. Though now mostly covered by Phanerozoic sediments, where it is exposed the rift consists of a trough 150 km wide and 1500 km long filled with up to 15 km of volcanics, primarily basalt, and clastic sediments derived from them. Modern examples of continental rifts include the Rio Grande Rift of New Mexico and the East African Rift. Rift volcanism could also produce significant underplating.

11.6.5 Refining the Continental Crust

Regardless of tectonic environment, nearly all mantle-derived magmas are mafic in composition: typically they are basaltic, but perhaps under circumstances of low pressure and high water continent, mantle melting can yield basaltic or high-magnesian andesites. Even these rare mantle-derived andesites are notably poorer in SiO_2 and generally richer in MgO and FeO than the continental crustal compositions listed in Table 11.11. While andesites do predominate among subduction zone magmas, they

are products of fractional crystallization of basaltic parents. If the continental crust has been produced by partial melting of the mantle, why then is it not basaltic in composition, as is the oceanic crust? Rudnick and Gao (2003) consider 4 possibilities:

1) Magmas have already evolved to andesitic composition by the time the cross the crust-mantle boundary (the Moho). The complementary mafic cumulates are left behind in the upper mantle. However, peridotite xenoliths from the upper mantle are predominantly restitic peridotite, not cumulates; hence this idea is not supported by observation.
2) Lower crustal floundering, or delamination, may occur when continental crust is thickened in compressional environments, such as convergent plate boundaries. The mafic lower crust is transformed in eclogite, which is denser than the underlying mantle. This process would preferentially remove the mafic part of the crust, leaving a residual crust that consequently becomes more silicic. A related process, not considered by Rudnick and Gao (2005) is subduction erosion. Lower crust is also somewhat more likely to be removed by subduction erosion than upper crust, but not to the extent of crustal floundering.
3) Preferential loss of Mg and Ca from continents by weathering and erosion. Mg is then taken up by the oceanic crust during hydrothermal alteration; Ca is precipitated and carbonate sediment. Both are returned to the mantle by subduction.
4) Under hotter conditions of the Archean, melting of subducting oceanic crust may have been much more common, giving rise to silicic melting, particularly the trondhjemite, tonalite, granodiorite suites common to the Archean. However, Taylor and McLennan's (1985) estimate of Archean crustal composition is slightly more mafic that their estimate of present composition, which is inconsistent with this idea.

At present, the question of how the continental crust has evolved to obtain its present composition is still unresolved. This is thus clearly a fruitful area for future research.

References and Suggestions for Further Reading

Ahrens, T. J. and R. Jeanloz. 1987. Pyrite: shock compression, isentropic release, and composition of the Earth's core. *J. Geophys. Res.* 92: 10363-10375.

Albarède, F. 1995. *Introduction to Geochemical Modeling*. Cambridge: Cambridge Univ. Press.

Allègre, C. J., J. P. Poirier, E. Humler and A. W. Hofmann. 1995. The chemical composition of the Earth. *Earth Planet Sci. Lett.* 134: 515-526.

Anderson, D. L. 1989. *Theory of the Earth*. Boston: Blackwell Scientific Publishers.

Anderson, O. L. and D. G. Issak, Another look at the core density deficit in the Earth's outer core, *Phys. Earth Planet. Interiors*, 131: 19-27, 2002.

Andreasen, R. and M. Sharma, Solar nebula heterogeneity in p-process samarium and neodymium isotopes, *Science*, 314: 806-809, doi: 2006.

Armstrong, R. L., 1968. A model for the evolution of strontium and lead isotopes in a dynamic Earth, *Rev. Geophys.*, 6, 175-199.

Armstrong, R. L., 1981. Radiogenic isotopes: the case for crustal recycling on a near-steady-state no-continental-growth Earth. in *The Origin and Evolution of the Earth's Continental Crust*, ed. S. M. and B. F. Windley. 259-287. London: The Royal Society.

Armstrong, R. L. and J. A. Cooper. 1971. Lead isotopes in island arcs. *Earth Planet. Sci. Lett.* 35: 27-37.

Bennett, V. C. and D. J. DePaolo, Proterozoic crustal history of the western United States as determined by neodymium isotope mapping. *Bull Geol. Soc. Amer.*, 99: 674-685, 1987.

Borodin, L. S., Estimated chemical composition and petrochemical evolution of the upper continental crust, *Geochem. Int.*, 37: 723-734, 1998.

Boyet, M. and R. L. Carlson, ^{142}Nd evidence for early (>4.3 Ga) global differentiation of the silicate Earth, *Science*, 309: 576-581, 2005.

Boyet, M. and R. W. Carlson, A highly depleted moon or a non-magma ocean origin for the lunar crust? *Earth Planet. Sci. Lett.*, 262: 505-516, 2007.

Boyet, M., J. Blichert-Toft, M. Rosing, M. Storey, P. Telouk and F. Albarede, ^{142}Nd evidence for early Earth differentiation, Earth Planet. Sci. Lett., 214:427-442, 2003.

Brooks, C., D. E. James and S. R. Hart, Ancient lithosphere: its role in young continental volcanism, *Science*, 193, 1086-1094, 1976.

Carlson, R. W. and A. J. Irving. 1994. Depletion and enrichment history of subcontinental lithospheric mantle; an. *Earth and Planetary Science Letters*. 126: 457-472.

Caro, G., B. Bourdon, A. N. Halliday and G. Quitte, Super-chondritic Sm/Nd ratios in Mars, the Earth, and the Moon, Nature, 336-339, 2008.

Caro, G., B. Bourdon, J.-L. Birck and S. Moorbath, ^{146}Sm-^{142}Nd evidence from Isua metamorphosed sediments for early differentiation of the Earth's mantle, *Nature*, 423: 428-432, 2003.

Castillo, P. 1989. The Dupal anomaly as a trace of the upwelling lower mantle. *Nature*. 336: 667-670.

Chabot, N. and M. J. Drake, Potassium solubility in metal: the effeccts of composition at 15 kbar and 1900˚C on partitioning between iron alloys and silicate melts, *Earth Planet. Sci. Lett.*, 172:323-335, 1999.

Chopelas, A., R. Beohler and K. T. 1994. Thermodynamics and behavior of γ-Mg_2SiO_4 at high pressure: implications for Mg_2SiO_4 phase equilibrium. *Phys. Chem. Mineral.* 21: 351-359.

Clarke, F. W. 1924. The Data of Geochemistry. *U. S. Geol. Surv. Bull*. 770.

Coogan, L. A.,The lower oceanic crust, in in R. L. Rudnick (ed.), *Treatise on Geochemistry Volume 3: The Crust*, Elsevier, Amsterdam 2012.

Condie, K. C. and R. C. Aster, Episodic zircon age spectra of orogenic granitoids: The supercontinent connection and continental growth, Precam. Res., 180: 227-236, doi: 10.1016/j.precamres.2010.03.008, 2010.

Corgne, A., C. Liebske, B. J. Wood, D. C. Rubie and D. J. Frost, Silicate perovskite-melt partitioning of trace elements and geochemical signature of a deep perovskitic reservoir, *Geochim Cosmochim Acta*, 69:485-496, 2005.

Davies G. F. 2009. Effect of plate bending on the Urey ratio and the thermal evolution of the mantle. *Earth Planet. Sci. Lett.* 287: 513-8.

Defant, M. J. and M. S. Drummond. 1990. Derivation of some modern arc magmas by melting of young subducted lithosphere. *Nature*. 347: 662-665.

DePaolo, D. J., 1980. Crustal growth and mantle evolution: inferences from models of element transport and Nd and Sr isotopes, *Geochim Cosmochim Acta*, 44, 1185-1196.

Dickin, A. 1995. *Radiogenic Isotope Geochemistry*. Cambridge: Cambridge University Press.

Ellam, R. M. and C. J. Hawkesworth. 1988. Is average continental crust generated at subduction zones? *Geology*. 16: 314-317.

Ellam, R. M. and F. M. Stuart, Coherent He-Nd-Sr isotope trends in high 3He/4He basalts: implications for a common reservoir, mantle heterogeneity and convection, Earth and Planetary Science Letters, 228: 511-523, 2004.

Elliott, T., T. Plank, A. Zindler, W. White and B. Bourdon, Element transport from subducted slab to juvenile crust at the Mariana arc, J. Geophys. Res., 102: 14,991-915,019, doi: 10.1029/97JB00788, 1997.

Farley, K. A., J. H. Natland and H. Craig. 1992. Binary mixing of enriched and undegassed (primitive ?) mantle components (He, Sr, Nd, Pb) in Samoan lavas. *Earth Planet. Sci. Lett.* 111: 183-199.

Gannoun, A., M. Boyet, H. Rizo and A. El Goresy, ^{146}Sm–^{142}Nd systematics measured in enstatite chondrites reveals a heterogeneous distribution of ^{142}Nd in the solar nebula, *Proc. Nat. Acad. Sci.*, 108: 7693-7697, doi: 10.1073/pnas.1017332108, 2011.

Gao, S., Luo, T.-C., Zhang, B.-R., Zhang, H.-F., Han, Y.-W., Hu, Y.-K., Zhao, Z.-D., 1988. Chemical composition of the continental crust as revealed by studies in East China. *Geochim. Cosmochim. Acta* 62.

Gessmann, C. K. and B. J. Wood, Potassium in the Earth's core? *Earth Planet. Sci. Lett.*, 200: 63-78, 2002.

Ghiorso, M. S. and R. O. Sack, Chemical mass transfer in magmatic processes IV. A revised and internally consistent thermodynamic model for the interpolation and extrapolation of liquid-solid equilibra in magmatic systems at elevated temperatures and pressures, *Contrib. Mineral. Petrol.*, 119: 197-212,: 1995.

Gill, J. B. 1981. *Orogenic Andesites and Plate Tectonics*. Berlin: Springer Verlag.

Goldschmidt, V. M. 1933. Grundlagen der quantitativen Geochemie. *Fortschr. Mineral. Kristall. Petrolgr.* 17: 112-156.

Grove, T. L. and M. B. Baker, Phase equilibrium controls on the tholeiitic versus calc-alkaline differentiation trends, *J. Geophys. Res.*, 89: 3253-3274, doi: 10.1029/JB089iB05p03253, 1984.

Grove, T. L., N. Chatterjee, S. W. Parman and E. Médard, The influence of H2O on mantle wedge melting, *Earth Planet. Sci. Lett.*, 249: 74-89, doi: 10.1016/j.epsl.2006.06.043, 2006.

Hanan BB, Graham DW. 1996. Lead and helium isotope evidence from oceanic basalts for a common deep source of mantle plumes. *Science,* 272: 991-5

Hart, S. R. 1984. The DUPAL anomaly: A large-scale isotopic mantle anomaly in the Southern Hemisphere. *Nature*. 309: 753-757.

Hart, S. R. and A. Zindler, 1986. In search of a bulk-earth composition. *Chem. Geol.*, 57: 247-267.

Hart, S. R., E. H. Hauri, L. A. Oschmann and J. A. Whitehead, 1992. Mantle Plumes and entrainment: isotopic evidence, *Science*, 256, 517-520.

Hart, S.R., Gerlach, D.C. and White, W.M., 1986. A possible new Sr-Nd-Pb mantle array and consequences for mantle mixing. *Geochim. Cosmochim. Acta*, 50: 1551-1557.

Hawkesworth, C. J., B. Dhuime, A. B. Pietranik, P. A. Cawood, A. I. S. Kemp and C. D. Storey, The generation and evolution of the continental crust, *J. of the Geol. Soc. London*, 167: 229-248, doi: 10.1144/0016-76492009-072, 2010.

Hawkesworth, C. J., P. D. Kempton, N. W. Rogers, R. M. Ellam and P. W. van Calsteren. 1990. Continental mantle lithosphere, and shallow level enrichment processes in the Earth's mantle. *Earth Planet Sci. Lett.* 96: 256-268.

Hedge, C. E., Variations in radiogenic strontium found in volcanic rocks, *J. Geophys. Res.*, 71: 6119-6126, doi: 1966.

Herzberg, C., P. D. Asimow, N. Arndt, Y. Niu, C. M. Lesher, J. G. Fitton, M. J. Cheadle and A. D. Saunders, Temperatures in ambient mantle and plumes: Constraints from basalts, picrites, and komatiites, *Geochem. Geophys. Geosyst.*, 8: doi:10.1029/2006gc001390, 2007.

Hess, H. H., History of ocean basins, in A. E. J. Engel, et al. (ed.), *Petrologic Studies: A Volume In Honor Of A. F. Buddington*, 599–620, Geological Society of America, Boulder, CO 1962.

Hirschmann, M. M., Mantle solidus: Experimental constraints and the effects of peridotite composition, *Geochem. Geophys. Geosyst.*, 1: doi: 10.1029/2000gc000070, 2000.

Hofmann, A. W. and W. M. White, 1982. Mantle Plumes from ancient oceanic crust, *Earth Planet. Sci. Lett.*, 57, 421-436.

Hurley, P. M., and J. R. Rand, Pre-drift continental nuclei, *Science*, 164, 1229-1242, 1969.

Jackson, M. G., S. R. Hart, A. A. P. Koppers, H. Staudigel, J. Konter, J. Blusztajn, M. Kurz and J. A. Russell, The return of subducted continental crust in Samoan lavas, Nature, 448: 684-687, 2007.

Jacobsen, S. B. and G. J. Wasserburg, A two-reservoir recycling model for mantle-crust evolution., Proc. Nat. Acad. Sci., 77: 6298-6302, 1980.

Karig, D. E. and R. W. Kay, Fate of sediments on the descending plate at convergent margins, *Phil. Trans. R. Soc. Lond. Ser. A*, 301, 233-251, 1981.

Kato, T., A. E. Ringwood and T. Irifune, 1988. Constraints on element partition coefficients between $MgSiO_3$ perovskite and liquid determined by direct measurements, *Earth Plan. Sci. Lett.*, 90, 65-68.

Kay, R. W. 1978. Aleutian magnesian andesites: metls from subducted Pacific Ocean crust. *J. Volcanol. Geotherm. Res.* 4: 117-132.

Kay, S. M., R. W. Kay, and G. P. Citron. 1983. Tectonic controls on tholeiitic and calc-alkaline magmatism. *J. Geophys. Res.* 87: 4051-4072.

Kay, R. W. and S. M. Kay. 1991. Creation and destruction of lower continental crust. *Geol. Rund.* 80: 259-278.

Kay, S. M., B. Coira and J. Viramonte, Young mafic back arc volcanic rocks as indicators of continental lithospheric delamination beneath the Argentine Puna plateau, central Andes, *J. Geophys. Res.*, 99: 24323-24339, doi: 10.1029/94jb00896, 1994.

Kelley, K. A. and E. Cottrell, Water and the Oxidation State of Subduction Zone Magmas, *Science*, 325: 605-607, doi: 10.1126/science.1174156, 2009.

Kelley, K. A., T. Plank, S. Newman, E. M. Stolper, T. L. Grove, S. Parman and E. H. Hauri, Mantle Melting as a Function of Water Content beneath the Mariana Arc, *J. Petrol.*, 51: 1711-1738, doi: 10.1093/petrology/egq036, 2010.

Kesson, S. E., J. D. Fitz Gerald and J. M. G. Shelley. 1994. Mineral chemistry and density of subducted basaltic crust at lower mantle pressures. *Nature*. 372: 767-769.

Kimura, K., R. S. Lewis and E. Anders, Distribution of gold and rhenium between nickel-iron and silicate melts: implications for the abundances of siderophile elements on the Earth and Moon, *Geochim. Cosmochim. Acta*, 38: 638-701, 1974.

Klein, E. M. and C. H. Langmuir. 1987. Ocean ridge basalt chemistry, axial depth, crustal thickness and temperature variations in the mantle. *J. Geophys. Res.* 92, 8089-8115.

Lee, K. K. M., B. O'Neill, W. R. Panero, S.-H. Shim, L. R. Benedetti and R. Jeanloz, Equations of state of the high-pressure phases of a natural peridotite and implications for the Earth's lower mantle, *Earth Planet. Sci. Lett.*, 223:381-393, 2004.

Li, J. and C. Agee, Geochemistry of mantle-core differentiation at high pressure, *Nature*, 381: 686-689, 1996.

Lodders, K., Solar system abundances and condensation temperatures of the elements, *Astrophys. J.*, 591: 1220-1247, 2003.

Lyubetskaya, T. and J. Korenaga, Chemical composition of Earth's primitive mantle and its variance: 1. Method and results, *J. Geophys. Res.*, 112: B03211, doi: 10.1029/2005jb004223, 2007.

Mattern, E., J. Matas, Y. Ricard and J. Bass, Lower mantle composition and temperature from mineral physics and thermodynamic modelling, *Geophys. J. Int.*, 160:973-990, 2005.

McDonough, W. F. and S.-S. Sun. 1995. The composition of the Earth. *Chem. Geol.* 120: 223-253.

McDonough, W. F., Compositional Model for the Earth's Core, in R. L. Carlson (ed.), *The Mantle and Core Treatise on Geochemistry*, 2: 547-568, Elsevier, Amsterdam 2003.

McGlashan, N., L. Brown and S. Kay, Crustal thickness in the central Andes from teleseismically recorded depth phase precursors, *Geophys. J. Intern.*, 175: 1013-1022, doi: 10.1111/j.1365-246X.2008.03897.x, 2008.

McKenzie, D. P. and R. K. O'Nions, 1983. Mantle reservoirs and ocean island basalts, *Nature*, 301, 229-231.

Menzies, M. A. and C. J. Hawkesworth (ed.), 1987, *Mantle Metasomatism*, London: Academic Press.

Montelli, R., Nolet, G., Dahlen, F.A., Masters, G., Engdahl, R., Hung, S.-H., 2004. Finite-frequency tomography reveals a variety of plumes in the mantle. Science 303, 338-343.

Morgan, W.J., 1971. Convection plumes in the lower mantle. Nature 230, 42-43.

Murakami, M., K. Hirose, K. Kawamura, N. Sata and Y. Ohishi, Post-perovskite phase transition in $MgSiO_3$, *Science*, 304:855-858, 2004.

Nyblade, A. A. and H. N. Pollack. 1993. A global analysis of heat flow from Precambrian terrains: implications for the thermal structure of Archean and Proterozoic lithosphere. *J. Geophys. Res.* 98: 12207-12218.

O'Neil, J., R. L. Carlson, D. Francis and R. K. Stevenson, Neodymium-142 evidence for Hadean mafic crust, *Science*, 321: 1828-1831, 2008.

O'Neill, H. S. C. and H. Palme, Collisional erosion and the non-chondritic composition of the terrestrial planets, *Phil. Trans. R. Soc. London A*, 366: 4205-4238, doi: 10.1098/rsta.2008.0111, 2008.

Oganov, A. R. and S. Ono, Theoretical and experimental evidence for a post-perovskite phase of $MgSiO_3$ in Earth's D'' layer, *Nature*, 430:455-448, 2004.

Palme, H. and H. S. C. O'Neill, Cosmochemical Estimates of Mantle Composition, in D. H. Heinrich and Karl, K. T. (ed.), Treatise on Geochemistry: The Mantle and Core, 1-38, Pergamon, Oxford 2003.

Pearson, D. G., D. Canil and S. B. Shirey, Mantle samples included in volcanic rocks: xenoliths and diamonds, in R. L. Carlson (ed.), *Treatise on Geochemistry v.2 The Mantle and Core*, 171-275, Elsevier, Amsterdam 2003.

Perfit, M. R., D. A. Gust, A. E. Bence, R. J. Arculus and S. R. Taylor. 1980. Chemical characteristics of island-arc basalts: implications for mantle sources. *Chem. Geol.* 30: 227-256.

Plank, T. and C. H. Langmuir. 1988. An evaluation of the global variations in the major element chemistry of arc basalts. *Earth Planet. Sci. Lett.* 90, 349-370.

Plank, T. and C. H. Langmuir. 1993. Tracing trace elements from sediment input to volcanic output at subduction zones. *Nature*. 362: 739-742.

Porter, K. A. and W. M. White, Deep mantle subduction flux, *Geochem. Geophys. Geosyst.*, 10: Q12016, doi: 10.1029/2009gc002656, 2009.

Putirka, K. D., M. Perfit, R. F. J. and M. G. Jackson, Ambient and excess mantle temperatures, olivine thermometry, and active vs. passive upwelling, *Chem. Geol.*, 241: 177-206, doi: 10.1016/j.chemgeo.2007.01.014, 2007.

Qin, L., R. L. Carlson and C. Alexander, Correlated nucleosynthetic isotopic variability in Cr, Sr, Ba, Sm, Nd and Hf in Murchison and QUE 97008, *Geochim. Cosmochim. Acta*, in press.

Righter, K. and M. J. Drake, Metal/silicate equilibrium in the early Earth - new constraints from the volatile moderately volatile siderophile elements Ga, Cu, P, and Sn, *Geochim. Cosmochim. Acta*, 64: 3581-3597, 2000.

Righter, K., M. J. Drake and G. Yaxley, Prediction of siderophile element metal-silicate partition coefficients to 20 GPa and 2800°C: the effects of pressure, temperature, oxygen fugacity, and silicate and metallic melt compositions, *Physics of the Earth and Planet Interiors*, 100: 115-134, 1997.

Ringwood, A. E. and W. Hibberson. 1990. The system Fe—FeO revisited. *Phys. Chem. Mineral.* 17: 313-319.

Ringwood, A. E., 1991. Phase transformation and their bearing on the constitution and dynamics of the mantle, *Geochim. Cosmochim. Acta*, 55, 2083-2110.

Ringwood, A. E., *Composition and Petrology of the Earth's mantle*, New York, McGraw-Hill, 618, 1975.

Rudnick, R. L. and D. M. Fountain. 1995. Nature and composition of the continental crust: a lower crustal perspective. *Rev. Geophys.* 33: 267-309.

Roeder, P. L. and R. F. Emslie, Olivine-liquid equilibrium, *Contrib. Mineral. Petrol.*, 29: 275-289, 1970.

Rubin, K.H., Sinton, J.M., 2007. Inferences on mid-ocean ridge thermal and magmatic structure from MORB compositions. *Earth Planet. Sci. Lett.*, 260, 257-276.

Rudnick, R. L. and D. M. Fountain. 1995. Nature and composition of the continental crust: a lower crustal perspective. *Rev. Geophys.* 33: 267-309.

Rudnick, R. L. and S. Gao, Composition of the Continental Crust, in R. L. Rudnick (ed.), *Treatise on Geochemistry: Volume 3 The Crust*, 1-64, Elsevier, Oxford 2003.

Schilling, J.-G., 1973. Iceland mantle plume: geochemical study of the Reykjanes Ridge, *Nature*, 242, 565-571.

Shaw, D. M., J. J. Gramer, M. D. Higgins and M. G. Truscott. 1986. Composition of the Candadian Precambrian shield and the continental crust of the earth. **In** *The Nature of the Lower Continental Crust, Vol.* J. B. Dawson, C. D. A., J. Hall and K. H. Wedepohl. ed., pp. 275-282. Oxford: Blackwell Scientific Publ.

Sinton, J.M., Detrick, R., 1992. Mid-ocean ridge magma chambers. *J. Geophys. Res.* 97, 197-216.

Sleep, N. H. 1990. Hotspots and Mantle Plumes: some phenomenology, *J. Geophys. Res.*, 95, 6715-6736.

Stolper, E. and S. Newman. 1994. the role of water in the petrogenesis of Mariana trough basalts. *Earth Planet. Sci. Lett.* 121: 293-325.

Taylor, S. R. 1967. The origin and growth of continents, *Tectonophysics*. 4, 17-34.

Taylor, S. R. and S. M. McLennan. 1985. *The Continental Crust: its composition and evolution*. Oxford: Blackwell Scientific Publishers.

Taylor, S. R. and S. M. McLennan. 1995. The geochemical evolution of the continental crust. *Rev. Geophys.* 33: 241-265.

Tera, F., L. Brown, J. Morris, I. S. Sacks, J. Klein, R. Klein and R. Middleton. 1986. Sediment incorporation in island-arc magmas: inferences from ^{10}Be, *Geochim. Cosmochim. Acta.* 50: 535-550.

Touboul, M., T. Kleine, B. Bourdon, H. Palme and R. Wieler, Tungsten isotopes in ferroan anorthosites: Implications for the age of the Moon and lifetime of its magma ocean, Icarus, 199: 245-249, doi: 2009.

Veizer, J. and S. L. Jansen. 1979. Basement and sedimentary recycling and continental evolution. *J. Geol.* 87: 341-370.

Vitorello, I. and H. N. Pollack, On the variation of continental heat flow with age and the thermal evolution of continents, *J. Geophys. Res.*, 85, 983-995, 1980.

von Huene, R. and D. W. Scholl, Observations at convergent margins concerning sediment subduction, subduction erosion, and the growth of continental crust, Reviews of Geophysics, 29: 279-316, doi: 1991.

Wade, J. and B. J. Wood, The Earth's 'missing' niobium may be in the core, *Nature*, 409: 75-78, 2001.

Weaver, B. L. and J. Tarney. 1984. Major and trace element composition of the continental lithosphere. **In** *Structure and Evolution of the Continental Lithosphere, Physics and Chemistry of the Earth, vol 15, Vol.* H. N. Pollack and V. R. Murthy. ed., pp. 39-68. Oxford: Pergamon Press.

Weaver, B. L., 1991. Trace element evidence for the origin of oceanic basalts, *Geology*, 19, 123-126.

Wedepohl, K. H. 1995. The composition of the continental crust. *Geochim. Cosmochim. Acta*. 59: 1217-1232.

Weichert, E., Über die Massenverteilung im Innern der Erde, *Königliche Gesellschaft der Wissenschaften zu Göttingen Nachrichten, Mathematisch-physikalische Klasse*, 3: 221-243, 1897.

White, W. M., 1985. Sources of oceanic basalts: radiogenic isotope evidence, *Geology*, 13: 115-118.

White, W. M., Oceanic Island Basalts and Mantle Plumes: The Geochemical Perspective, *Annual Review of Earth and Planetary Sciences*, 38: 133-160, doi: 10.1146/annurev-earth-040809-152450, 2010.

White, W. M. and B. Dupré, Sediment subduction and magma genesis in the Lesser Antilles: Isotopic and trace element constraints, *J. Geophys. Res.*, 91, 5927-5941, 1986.

White, W. M. and E. Klein, Composition of the Oceanic Crust, in R. L. Rudnick (ed.), *Treatise on Geochemistry Volume 3: The Crust*, Elsevier, Amsterdam 2012.

White, W. M. and P. J. Patchett, 1984, Hf-Nd-Sr isotopes and incompatible element abundances in island arcs: implications for magma origins and crust-mantle evolution, *Earth Planet. Sci. Lett.*, 67: 167-185.

Willbold, M. and A. Stracke, Trace element composition of mantle end-members: Implications for recycling of oceanic and upper and lower continental crust, *Geochem. Geophys. Geosyst.*, 7: Q04004, doi: 10.1029/2005gc001005, 2006.

Workman, R. and S. R. Hart, Major and trace element composition of the depleted MORB mantle (DMM), Earth Planet. Sci. Lett., 231: 53-72, doi: 10.1016/j.epsl.2004.12.005, 2005.

Workman, R., S. R. Hart, M. Jackson, M. Regelous, K. A. Farley, J. Blusztajn, M. Kurz and H. Staudigel, Recycled metasomatized lithosphre as the origin of the Enriched Mantle II (EM2) end member: Evidence from the Samoan Volcanic Chain, *Geochem. Geophys. Geosyst.*, 5, doi: 10.1029/2003GC000623, 2004.

Zindler, A. and S. R. Hart, 1986. Chemical Geodynamics, *Ann. Rev. Earth Planet. Sci.*, 14: 493-571.

Problems

1. Assuming the Earth has a CI chondritic composition (Table 10.02), and using the values for the mass of the core and the mass of the mantle in Table 11.01, calculate what the concentrations of Re, Ir, Mo, and Ag should be in the bulk silicate Earth if the core formed by an equilibrium process if the silicate/metal partition coefficients are 5×10^{-4} , 5×10^{-5}, 8×10^{-4}, and 0.01, respectively. Compare you results with the primitive mantle and core values in Table 11.03 and 11.04.

2. Calculate new bulk silicate Earth concentrations of Re, Ir, Mo, and Ag by adding 1% CI chondritic material to your results from Problem 1. Again compare these results with primitive mantle values of Table 11.03.

3. Assume that the bulk silicate Earth has a $^{87}Sr/^{86}Sr$ ratio of 0.7035, and an age of 4.45 Ga. Calculate the bulk silicate Earth $^{87}Rb/^{86}Sr$ ratio.

4. Suppose a rising mantle plume is 220° hotter than surrounding mantle and that the γ-olivine–Mg-perovskite transition occurs at 660 km depth in the surrounding mantle. Assume a homogeneous mantle density of 3.5 g/cc at 660 km and above and the Clapeyron slope mentioned in section 11.2.4.2. At what depth does the γ-olivine–Mg-perovskite transition occur within the mantle plume?

5. Whether the γ-olivine–Mg-perovskite transition is endothermic or exothermic will affect mantle convection (i.e., sinking of lithospheric slabs, rise of mantle plumes). Discuss why this is so, explaining the effects of both endothermic and exothermic phase transitions on rising mantle plumes and sinking lithospheric slabs.

6. Use a mass balance approach and equations 11.24 through 11.29 to calculate the Nd concentration of the mantle depleted by continent formation (DMM). Take the ε_{Nd} of the Earth to be +3.1, ε_{Nd} of the depleted mantle to be +9, the $^{147}Sm/^{144}Nd$ ratio of the continental crust to be 0.123, and the average age of the continents (T) to be 2.0 Ga. Use the Nd concentrations of the silicate Earth and the continental crust given in Tables 11.04 and 11.11.